1996

Analytical and finite element modeling of a machining system to minimize inaccuracy in milling and using rapid prototyping for die manufacturing

Parag Gupta
Iowa State University

INFORMATION TO USERS

This manuscript has been reproduced from the microfilm master. UMI films the text directly from the original or copy submitted. Thus, some thesis and dissertation copies are in typewriter face, while others may be from any type of computer printer.

The quality of this reproduction is dependent upon the quality of the copy submitted. Broken or indistinct print, colored or poor quality illustrations and photographs, print bleedthrough, substandard margins, and improper alignment can adversely affect reproduction.

In the unlikely event that the author did not send UMI a complete manuscript and there are missing pages, these will be noted. Also, if unauthorized copyright material had to be removed, a note will indicate the deletion.

Oversize materials (e.g., maps, drawings, charts) are reproduced by sectioning the original, beginning at the upper left-hand corner and continuing from left to right in equal sections with small overlaps. Each original is also photographed in one exposure and is included in reduced form at the back of the book.

Photographs included in the original manuscript have been reproduced xerographically in this copy. Higher quality 6" x 9" black and white photographic prints are available for any photographs or illustrations appearing in this copy for an additional charge. Contact UMI directly to order.

UMI

A Bell & Howell Information Company
300 North Zeeb Road, Ann Arbor MI 48106-1346 USA
313/761-4700 800/521-0600

Analytical and finite element modeling of a machining system to minimize inaccuracy in milling and using rapid prototyping for die manufacturing

by

Parag Gupta

A Dissertation Submitted to the

Graduate Faculty in Partial Fulfillment of the

Requirements for the Degree of

DOCTOR OF PHILOSOPHY

Department: Mechanical Engineering
Major: Mechanical Engineering

Approved:

Signature was redacted for privacy.

In Charge of Major Work

Signature was redacted for privacy.

For the Major Department

Signature was redacted for privacy.

For the Graduate College

Members of the Committee:

Signature was redacted for privacy.

Signature was redacted for privacy.

Signature was redacted for privacy.

Signature was redacted for privacy.

Iowa State University
Ames, Iowa
1996

TABLE OF CONTENTS

LIST OF TABLES

LIST OF FIGURES

ACKNOWLEDGEMENTS

The author takes this opportunity to express his sincere thanks towards Professor Jerry Lee Hall whose esteemed guidance and valuable suggestions at every stage of the research work made this project a success.

The author would also like to acknowledge the valuable suggestions of other committee members especially Prof. Ralph F. Scrutton which led to successful completion of the project.

The author is also thankful to the Iowa Center for Emerging Manufacturing Technology for selecting him as a Carver fellow and providing research funding during the first year of the research.

The greatest thanks go to the author's wife Ritu, parents and brother for their support and encouragement which made this work successful.

CHAPTER 1. INTRODUCTION

Background

The term, "milling", as applied to certain kinds of machining operations is based on the action of a multiple-toothed wheel on the workpiece in the same manner as the old "mill stone" acted on the grain in early days. The basic process is that of chip removal due to cutting forces imposed on workpiece by the cutter. The mechanics of chip formation is essentially the same for all machining operations and is depicted in Fig.1.1 (Kalpakjian, 1991). In this model a tool moves along the workpiece with a velocity V and a depth of cut t. A chip is produced in front of the tool by shearing the material continuously along the shear plane. Milling machines employ multi-edged rotating tools called milling cutters. There are a variety of milling operations, end milling being commonly used in CNC machining centers.

The end milling process is used extensively in a gamut of manufacturing areas. Its use accounts for up to 40% of the cost of fabrication of non-electrical parts for a high performance aircraft (Sagherian, 1990). This fact is used to justify the effort spent in improving accuracy and productivity. The milling process is also used extensively in the automotive industry for finishing and roughing cuts of dies which are made solely by the use of end mills. Conventional die manufacturing processes require large amounts of time in Computer Numerically Controlled (CNC) programming and

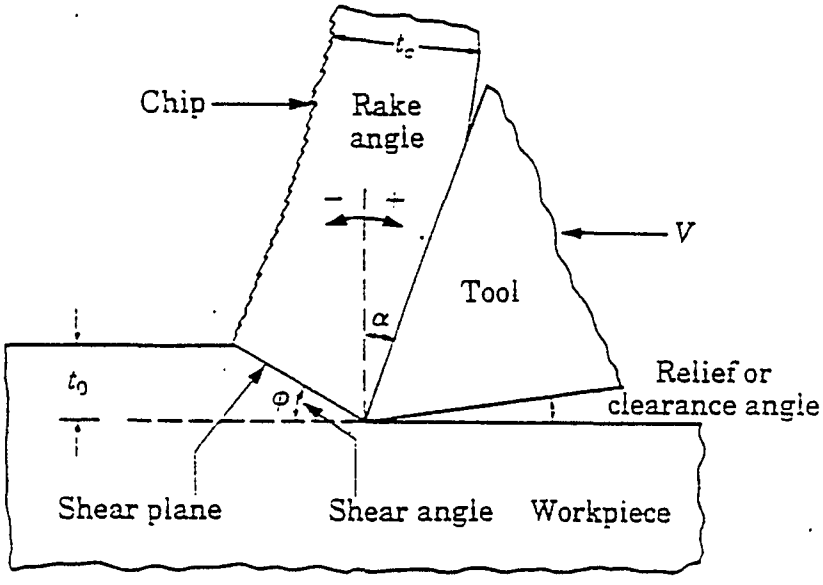

Figure 1.1: Chip Formation

end milling (Gupta, 1994). The skilled labor required for CNC programming accounts for the high cost of the dies. Therefore it would seem that some new technique needs to be developed which would eliminate CNC programming and possibly reduce usage of the milling process, thus reducing cost and time to produce parts.

The goals of the thesis is to minimize the inaccuracy produced in parts which have been end milled and to develop techniques to reduce the cost and time taken to perform conventional CNC milling to produce dies for mass production.

Machining Inaccuracy

In the past decade, the concept of "near net shape manufacturing" has led to greater emphasis being given to finish machining (Arzt, 1980; Brooks, 1980). due to the smaller amount of material wasted in the form of chips. Components are forged or cast to their approximate final shape or "near net shape" which allows them to be finish machined in one pass. However this leads to heavier finishing cuts (typically 2.5-5 mm) which causes greater workpiece and cutter deflection which in turn results in surface taper and error on the finished parts as well as an inferior surface roughness.

Inaccuraccies in machining are caused by a variety of factors such as

(a) Built-up-edge: A built-up-edge (BUE) may form at the tip of the tool during cutting. This edge consists of layers of materials from the workpiece that are gradually deposited on the tool, and is commonly observed in practice. It is one of the factors that most adversely affects surface finish. A built up edge, in effect, changes the geometry of cutting (Kalpakjian, 1991)

(b) Chatter: Machine tools can vibrate due to the dynamic cutting process under certain particular conditions. This types of vibration is self-induced and commonly lend to machine tool chatter which may affect the machining accuracy.

(c) Tool wear

(d) Spindle error: Ideally the spindle should rotate about the longitudinal axis of the milling cutter. However, there may be radial offset between the actual axis of spindle rotation and the axis of the milling cutter which may affect machining accuracy.

(e) Workpiece deflection: The workpiece may deflect under the action of the fixturing forces.

(f) Tool deflection: A milling cutter can be subjected to cantilever deflection.

(g) Thermal expansion of tool and workpiece: The heat generated during metal cutting increases the temperature of the workpiece and the tool which results in thermal expansion. This in turn may affect machining accuracy.

At present the technology is available to minimize built-up-edge and chatter by selecting appropriate cutting tools and cutting parameters. The inaccuracy caused by tool wear and spindle error an also be almost eliminated by present technology. The inaccuracy caused by workpiece deflection, fixture deflection, tool deflection and thermal expansion can be minimized but can not be eliminated. Presently industries use trial and error methods to minimize inaccuracy caused by these factors. For example, the air pressure in the pneumatic chuck of a lathe can be adjusted by trial and error to achieve a desired flatness tolerance and rigidity of the part. A final finishing cut is used to bring the machined surface within tolerance, or else alternatively low speeds and feeds may be used. However, these techniques result in lower productivity.

It is therefore necessary to be able to predict the possible errors of the machined surface in order to optimize cutting parameters, to increase metal removal rates, and at the same time perform precision machining.

Precision machining demands that the workpiece be rigidly fixed, which in turn requires relativelyhigh clamping forces. The clamping forces as well as cutting forces, cause deformation of the workpiece. This deformation of the workpiece hinders and may prevent the final goal of the machinist, which is to achieve low dimensional and geometric tolerance band widths.

Goals and Organization of the Dissertation

The goals of the thesis are to determine ways to (a) minimize inaccuracy in prismatic parts and (b) to reduce the cost and time required to produce these parts. The inaccuracy can be minimized by minimizing the deflection of the workpiece and the tool in the milling process, or by employing a process that will keep the usage of the milling process to a minimum. Other processes could possibly eliminate costly and time consuming CNC programming. Chapters 2, 3 and 4 are papers addressing minimization of inaccuracies in milling processes. In chapter 5 are proposed three new processes developed to reduce the cost and time taken to produce dies by the conventional CNC milling process. The research performed in previous chapters is discussed in chapter 6 and concluding remarks are made concerning the impact of this research in the field of manufacturing.

In the second chapter an analytical non-linear optimization model is developed which will determine the maximum inaccuracy and the optimal clamping forces that will keep the work piece deflection to a minimum while ensuring that the workpiece will not slip during machining. This model assumes rigid fixturing elements and is mainly suitable for simple workpiece shapes.

The third chapter is a finite element model and has the same objective as the analytical non-linear optimization model. This model can be used for any complex workpiece shape. The model takes into account the flexibility of fixtures.

Inaccuracy in machining is partially caused by deflection of the tool. The fourth chapter is a study of the cutting force-induced deflection in a milling cutter. An analytical equation is developed to determine the deflection of an end mill under a given cutting force. A solid model of the complex shape of the milling cutter is

made and finite element analysis is performed to verify the developed equation. This analysis provides an estimate of the error caused by deflection of the milling cutter. Previous researchers have modeled the milling cutter as a simple cylinder.

Chapter five proposes three unique techniques developed to produce dies. They are a casting prototype process, an EDM milling process and a copy milling process. The casting prototype process does not use milling whereas the EDM milling process uses milling for rough cutting purposes. The EDM process is used for finish machining in EDM milling. These two processes minimize inaccuracy in parts by eliminating milling or using milling to remove the rough stock. However, the copy milling process uses milling but the concepts developed in previous chapters can be used to minimize error in this process.

References

Sagherian. R and Elbestawi M. A., 1990, "A simulation system for improving machining accuracy in milling,"Computers in Industry, 14, pp. 293-305

Gupta P. and Hall J. L., 1994, "Rapid Prototyping in Die Manufacturing", Rapid Prototyping Systems-fast track to product realization, SME, pp. 3-17

P.Arzt, 1980, "Methods to determine drive characteristics from cutting data: End milling of titanium", Machine Tool Task Force Report, Vol. 3, Lawrence Livermore Lab., P 8.2-1

R. Brooks, Nov 1980, " Finish machining research emerging as key ingredient for productivity",Met. Work. News

Kalpakjian S., 1991, "Manufacturing Processes for Engineering Materials", Addison-Wesley, New York.

Bhattacharya, A, 1984, "Principles of Metal Cutting", Central Book Publishers. Calcutta, India.

CHAPTER 2. USING AN OPTIMIZATION MODEL TO CONTROL WORKPIECE RIGIDITY AND DEFORMATION IN WORKHOLDING TO ACHIEVE PRECISION MACHINING

A paper[1] published in the book "Operation Research in Production Planning and Control", Springer Verlag, Berlin, pp. 138-150 and presented at Joint German/US Conference on Recent Developments and New Perspectives of Operation Research in the Area of Production Planning and Control, June 25-26, 1992, Hagen, Germany.

Amy J. C. Trappey[2], Parag Gupta[2] and C. Richard Liu[3]

Abstract

The basic criterion in precision machining is to machine a workpiece that satisfies dimensional accuracies and low tolerance variations. Precise machining demands the work-piece to be rigidly fixed, which in turn requires high clamping forces. The clamping forces, as well as cutting forces, result in deformation of the workpiece.

[1]This research is partially supported by the Society of Manufacturing Engineering Education Foundation and the Iowa Center for Emerging Manufacturing Technology

[2]Department of Industrial and Manufacturing Systems Engineering, Iowa State University, Ames, Iowa 50011, USA

[3]School of Industrial Engineering, Purdue University, West Lafayette, Indiana 47907, USA

This deformation of the work-piece hinders the final goal of the machinist, which is to machine within low dimensional and geometric tolerance band-widths. In this paper an analytical, yet practical, nonlinear optimization model is developed which ensures the rigidity of work-holding and guarantees the precision and accuracy of machining results by proper fixturing. Principles of statics, kinematics, stress-strain, and geometric constraints are applied in developing the model. The model consists of constraints in order to (1) minimize the deformation of the workpiece, (2) compute the fixturing and cutting forces under which there is no slippage, and (3) ensure the applicability of Coulomb's law of friction. A computer program is developed to demonstrate the capability of this model. A given workholding configuration for a specific part geometry is verified when a solution of the model is found.

Background

Several verification approaches have been developed in the past. A brief literature review of each approach is described as are some issues that were not addressed and will be discussed in this paper. First, the kinematic modeling approach is developed by Asada and By (1985). In this model, the characteristics of the workholding, such as the deterministic position, accessibility, detach-ability, and complete restriction, are formulated as geometric constraints. The constraints are structured in terms of the boundary Jacobian matrix and the fixture displacement vector. Asada and By consider only the relationship between the workpiece boundary and the fixture elements, the possible force impact of the machining process is not included in the workholding analysis. Furthermore, due to the need of the boundary Jacobian matrix, the workpiece boundary domains are restricted to differentiable equations.

Screw theory (Ohwovoriol and Roth, 1981) is applied by Chou, Chandru, and Barash (1987) to model the fixturing equilibrium problem for a prismatic workpiece. A linear programming model is used to solve the optimal clamping force magnitudes given fixturing and cutting forces. There are some issues that were not emphasized by Chou et al (1987).First, it is presumed that all of the unit clamping and locating forces are under a friction free condition. In contrast, the locating forces only occur dynamically to counter balance the clamping forces with respect to the clamping force magnitudes and directions as well as the friction coefficient. However, most of the previous research does not consider the frictional effect. Due to the simplified fixturing force direction definition, only prismatic workpiece fixturing can be verified. The kinematic approach (1985, Shoham) is applied by Mani and Wilson (1988) to construct the constraints and to ensure the validity of the fixture configuration. The counter clockwise and the clockwise rotational triangles are used to model and prevent the rotational movement. Although this approach is rather easy to implement in a knowledge based expert system, the application domain is limited to a 2 1/2 dimensional prismatic workpiece. The friction factor between the workpiece and the fixture is not considered, i.e., a friction free surface is assumed. Further, the counter acting concept is not modeled in the analysis so the system may be too restrictive in some situations. The force magnitude is not defined for each force. Therefore, the allowable fixturing force limits are not considered. In the next section the theory of the workholding verification model is presented. The mechanical and geometrical constraints of the workholding configuration are discussed in detail.

Theory of Workholding Verification

This research treats the analytical model as the combination of several constraints which cannot be violated by any workholding element. These mechanical and geometrical constraints are the theoretical bases of the workholding verification.

Equilibrium

The effective force and moment resultants that occur on the workpiece have to be zero (Malvern, 1976) to ensure the stability of the workpiece. A free body diagram is applied to represent all possible forces acting on the workpiece from time to time. Either during the workholding process along (without any effective outside force) or during the machining process (with outside effective force), it is necessary to maintain the equilibrium of the 3-D non-coplanar, non-concurrent, and non-parallel force system. The three force equilibrium equations with respect to X, Y, and Z directions are

$$\sum F_x = 0,\ \sum F_y = 0,\ \sum F_z = 0 \tag{2.1}$$

and the three moment equilibrium equations about X, Y, and Z axes are

$$\sum M_x = 0,\ \sum M_y = 0,\ \sum M_z = 0 \tag{2.2}$$

The equations can be applied to verify the workpiece stability for the most general case. If the equilibrium system is a parallel force system, e.g., along the Z axis, only forces in the Z direction and moments about the X and Y axes need to be considered:

$$\sum F_z = 0,\ \sum M_x = 0,\ \sum M_y = 0 \tag{2.3}$$

If the equilibrium system is a 2-D coplanar force system, e.g., on the X_p-Y_p plane (the fixturing plane of the base plate in fixture design), only forces in the X and Y directions and moments about Z axis need to be considered (Higdon and Stiles, 1968):

$$\sum F_x = 0,\ \sum F_y = 0,\ \sum M_z = 0 \tag{2.4}$$

Force Directions and Limits

For the completeness of the system, the geometrical constraint for the force directions have to be modeled as a verification condition. Assuming the workholding operation is a grasping (not magnetic pulling) action, the force vector-($F_{x,i}$, $F_{y,i}$, $F_{z,i}$) has to be directed toward the workpiece. For instance, the workpiece boundary face has a surface normal with direction cosines l_x, m_y, and n_z. Then the force vector constraint is

$$F_{x,i}l_x + F_{y,i}m_y + F_{z,i}n_z < 0 \tag{2.5}$$

This constraint is even applicable to the machining force direction, when the machining process creates the force impact toward the workpiece.

Frictional Force vs. Normal Force

According to the coefficient of the static friction (μ) between the workpiece surface and the contacting holding element, the magnitude of the frictional force element ($|F_f|$) has to be less than the fractional normal force magnitude, i.e., $\mu|F_n|$

(Malvern, 1976). Therefore, if there is no (or little) friction between the workpiece and the holding element, the fixturing force direction is nearly perpendicular to the boundary face (this is implicitly assumed by most of the previous research as shown in the examples of the previous section). If friction exists as it does in most machining cases, the fixturing force has to be analyzed as the components of the force, the frictional force and the normal force. The proportional constraint of the frictional force and the normal force is formulated in terms of the frictional coefficient. The fixturing force (F) acting on a workpiece at any point can be divided into a normal force component (Fn) and a frictional force component (F_f), i.e., $|F|^2 = |F_n|^2 + |F_f|^2$. Fn is merely but a dot product of the fixturing force and the unit surface normal vector (N) or Fn = $|F.N|$. The ratio of the magnitudes of the frictional force ($|F_f|$) and normal force ($|Fn|$) should be less than the coefficient of friction to avoid slippage. This can be expressed mathematically as

$$\mu > \sqrt{\frac{|F|^2 - |F \cdot N|^2}{|F_n|^2}} \tag{2.6}$$

Further, the system allows for frictional (μ >0) as well as frictionless (μ=0) conditions.

Center of Gravity

The weight of a workpiece has to be considered as one of the force elements in the workholding force system. Vertical supports can be applied to hold the workpiece against the gravitational attraction of the earth (Hoffman, 1985) and create the counter acting forces to balance the weight of the workpiece. The vertical supports (usually three supports) have to be located in such a way that the center of gravity

of a workpiece must be inside the supporting polygonal region defined by the vertical supporting points.

Stress and Strain in Workpiece

It is essential to know the stress and strain developed in the workpiece due to the fixturing and the cutting forces in order to know the deformation in the workpiece. If $F_{x.i}$, $F_{y.i}$, and $F_{z.i}$ are the force components in the x, y, and z directions and A_x, A_y, and A_z are the normalized equivalent areas in the x, y, and z directions, by using the spatial occupancy enumeration approach the workpiece can be discretely represented and, then, the normalized equivalent areas in the x, y, and z directions can be computed as follows.

$$A_x = \frac{r^2 \sum_{\forall j} \sum_{\forall k} (x_{max.jk} - x_{min.jk})}{(x_{max} - x_{min})} \tag{2.7}$$

$$A_y = \frac{r^2 \sum_{\forall j} \sum_{\forall k} (y_{max.jk} - y_{min.jk})}{(y_{max} - y_{min})} \tag{2.8}$$

$$A_z = \frac{r^2 \sum_{\forall j} \sum_{\forall k} (z_{max.jk} - z_{min.jk})}{(z_{max} - z_{min})} \tag{2.9}$$

where $x_{max.jk}$ and $x_{min.jk}$ are the maximum and minimum x values at cell address jk while x_{max} and x_{min} are the overall maximum and minimum x values of the workpiece. The y and z notations are interpreted in the same way as the x's. Thus, the compression stresses in the x, y, and z directions are derived as

$$\sigma_{x.i} = \frac{F_{x.i}}{A_x}, \sigma_{y.i} = \frac{F_{y.i}}{A_y}, \sigma_{z.i} = \frac{F_{z.i}}{A_z} \tag{2.10}$$

If ν is the Poisson's ratio and E is the elastic modulus, the strains in the x, y, and z directions are

$$\epsilon_x = -\frac{\sum_{i=1}^{n}\sigma_{x.i}}{E} + \nu\frac{\sum_{i=1}^{n}\sigma_{y.i}}{E} + \nu\frac{\sum_{i=1}^{n}\sigma_{z.i}}{E} \tag{2.11}$$

$$\epsilon_x = \nu\frac{\sum_{i=1}^{n}\sigma_{x.i}}{E} - \frac{\sum_{i=1}^{n}\sigma_{y.i}}{E} + \nu\frac{\sum_{i=1}^{n}\sigma_{z.i}}{E} \tag{2.12}$$

$$\epsilon_x = \nu\frac{\sum_{i=1}^{n}\sigma_{x.i}}{E} + \nu\frac{\sum_{i=1}^{n}\sigma_{y.i}}{E} - \frac{\sum_{i=1}^{n}\sigma_{z.i}}{E} \tag{2.13}$$

Nonlinear Optimization Model

Following this discussion of fixturing criteria, we can generally represent the fixturing procedure by a nonlinear optimization model. The fixturing configuration, the allowable maximum holding force limits, and the machining force are given through a user interface. If a configuration is valid, the nonlinear model computes the unknown fixturing forces that produce minimum workpiece deformation and ensure workholding rigidity. The model is summarized as follows.

The objective function is to minimize the deformation (described in the section entitled Stress and Strain in Workpiece) caused by all the forces, which is mathematically expressed as

$$Min.\ \ [(\epsilon_x(x_{max} - x_{min}))^2 + (\epsilon_y(y_{max} - y_{min}))^2 + (\epsilon_z(z_{max} - z_{min}))^2]^{1/2} \tag{2.14}$$

This objective function is subjected to the following constraints:

(a) Zero resultants of total forces and moments as discussed in the section entitled "Equilibrium".

$$\mathbf{C_6\ x\ 3 \cdot F_3\ x\ 1 = A_6\ x\ 1} \tag{2.15}$$

(b) A force can be represented in by three force elements with respect to the X, Y, and Z axes. Thus, the sum of the squares of the X, Y, and Z force elements is equivalent to the square of the force magnitude. In order to ensure that there is no yielding due to localized stress, there should be a limitation on the maximum amount of force acting on a locator or a clamp. No yielding in turn would ensure the applicability of Coulomb's law of friction. If $F_{max.i}$ is the maximum force which is allowed then the constraint is:

$$F_{x.i}{}^2 + F_{y.i}{}^2 + F_{z.i}{}^2 < F_{max.i}{}^2 \tag{2.16}$$

(c) The force directions are constrained toward the workpiece according to the assumption defined in the section entitled "Force Direction and Limits."

$$F_{x.i}l_x + F_{y.i}m_y + F_{z.i}n_z < 0 \tag{2.17}$$

(d) The frictional force magnitude ($|F_{f.i}|$) is limited by the fractional normal force magnitude ($\mu|F_{n.i}|$). ($F_{f.i}$ and $F_{n.i}$ are functions of $F_{x.i}$, $F_{y.i}$, and $F_{z.i}$.)

$$\mu > \sqrt{\frac{|F_i|^2 - |F_i \cdot N_i|^2}{|F_{n.i}|^2}} \tag{2.18}$$

The matrices in constraint (a) (Equation 2.15) can be expressed as

$$\mathbf{C_{6\ x\ 3}} = \begin{bmatrix} 1 & 1 & 0 & 0 & 0 & 0 \\ 0 & 0 & 1 & 1 & 1 & 1 \\ 0 & 0 & 0 & 0 & 1 & 1 \\ 0 & 0 & -z_1 & -z_n & y_n & y_n \\ z_1 & z_n & 0 & 0 & -x_n & -x_n \\ -y_1 & -y_n & x_1 & x_n & 0 & 0 \end{bmatrix} \tag{2.19}$$

$$\mathbf{F_{3\ x\ 1}} = [F_{x.1}..F_{x.n}\ \ F_{y.1}..F_{y.n}\ \ F_{z.1}..Fz.n] \tag{2.20}$$

$$\mathbf{A_{6\ x\ 1}} = [-f_{cx} - f_{cy} - f_{cz} \quad (z_c f_{cy} - y_c f_{cz}) \quad (x_c f_c z - z_c f_{cx}) \quad (y_c f_{cx} - x_c f_{cy})]^T \tag{2.21}$$

Equation (2.15) represents three force equilibrium equations and three moment equilibrium equations. In the next section, a numerical example is discussed to demonstrate the use of this model for a fixture design verification purpose.

Numerical Example

The quadratic verification model described in the previous section is coded by using a nonlinear programming package GINO. A numerical example (shown in Figure 2.1) is given for a workpiece configured with three vertical supports, three horizontal locators, one vertical clamp, and one horizontal clamp for fixturing. The fixture configuration data are listed in Table 2.1. The friction coefficient for the contact of the workpiece and the fixture element is 1/3 (Higdon and Stiles, 1968). The maximum allowable locating force which a locator can take is conservatively set to be 500

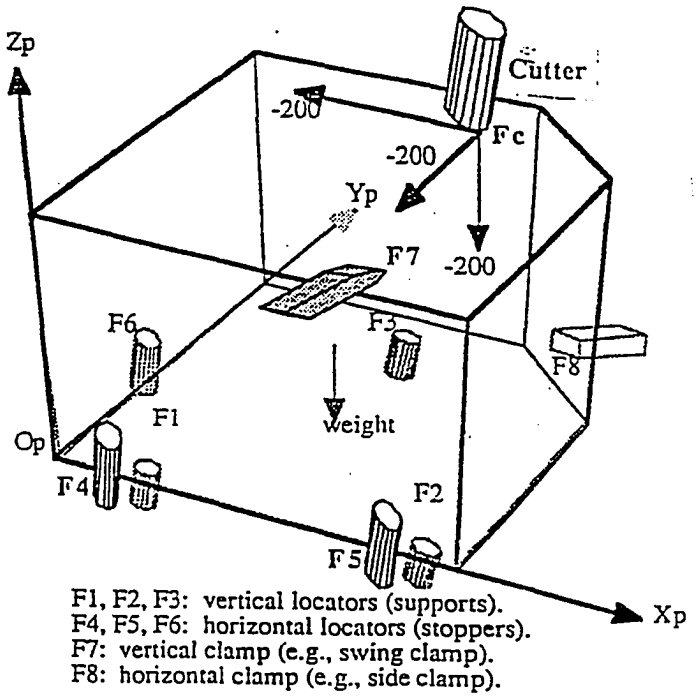

Figure 2.1: 3-D fixturing illustration

pounds (lbs.), and the maximum allowable clamping force which a clamp can take is set to be 350 lbs. (Colbert, 1985). The workpiece weighs 30 lbs. The center of weight of the workpiece is at the point (3.5, 3.5, 2.5). The maximum cutting force is at (4, 7, 5), and the maximum cutting force elements are (-200 lbs.. -200 lbs., -200 lbs.) with respect to the X, Y, and Z directions. The model is employed to check the feasibility of the fixture design. The complete results are shown in Table 2.2. These forces ensure the rigidity of the workpiece and in addition under the given constraints produce a minimum deformation (as defined by the objective function) of 22 micro-inches.

The complete resultant of the force system acting on the workpiece is zero. The

Table 2.1: Example of fixture configuration data.

Fixture	Type of Fixture Element	(x,y,z)
f1	vertical locator	(1,1,0)
f2	vertical locator	(6,1,0)
f3	vertical locator	(3,6,0)
f4	horizontal locator	(1,0,1)
f5	horizontal locator	(6,0,1)
f6	horizontal locator	(0,4,1)
f7	vertical clamp	(4,1,5)
f8	horizontal clamp	(6,6,1)

Table 2.2: Results of the example model.

Fixture	Computed Forces (Fx, Fy, Fz)
f1	(-1.94, 19.62, 75.88)
f2	(-2.99, -0.92, 9.39)
f3	(74.08, 23.66, 393.62)
f4	(-7.17, 167.44, -53.26)
f5	(-3.04, 174.91, -48.09)
f6	(213.3, 16.43, 69.05)
f7	(30.127, -6.84 , -242.31)
f8	(-102.35, -194.31, 25.71)

results demonstrate that the workpiece is completely restricted, the fixture elements are assigned to the right locations, and the allowable force magnitudes and directions are verified.

Conclusion

This research establishes a verification procedure that can be applied with the a computer-aided workholding interface to check the correctness of the workholding configuration in situations such as fixture design or robot hand grasping. Moreover, it can minimize deformation to meet the low tolerance band-width required for precision

parts. The model can be further embedded into the automatic fixture design system (Trappey and Liu, 1990) and used as an analytical tool to determine the proper fixture positions. The direction of future research is to develop a complete automatic workholding design system utilizing heuristic decision rules as well as the mechanical and geometrical knowledge developed in this paper.

References

Asada, H., and By, A.B., 1985, "Kinematics of work-part fixturing," IEEE Conf. on Robotics and Automation, pp. 337-345.

Chou, Y.C., Chandru, V., and Barash, M.M., 1987, "A mathematical approach to automatic design of fixtures: Analysis and synthesis," Proceedings, ASME Winter Annual Meeting, Boston, Mass., pp. 11-27.

Colbert, J.L., 1985, "Workholding technology in flexible manufacturing and the design of a modular fixturing system," M.S. Thesis, Rensselaer Polytechnic Institute, Troy, NY.

Higdon, A., and Stiles, W.B., 1968, Engineering Mechanics, 3rd Edition, Prentice Hall, Inc., Englewood Cliffs, New Jersey.

Hoffman, E.G., 1985, Jig and Fixture Design, Second Edition, Delmar Publishers Inc., Albany, NY.

Malvern, L.E., 1976, Engineering Mechanics, Volume I: Statics, Prentice-Hall, Inc., Englewood Cliffs, New Jersey.

Mani, M., and Wilson, W.R.D., 1988, "Automated design of workholding fixtures using kinematic constraint synthesis," Proceedings, 19th North American Mfg. Research Conference, SME, University of Illinois, Urbana, Illinois, pp. 437-444.

Ohwovoriol, M.S., and Roth, B., 1981, "An extension of screw theory." Journal of Mechanical Design, Vol. 103, pp. 725-735.

Shoham, Y., 1985, "Naive kinematics," Proceedings, International Joint Conference on Artificial Intelligence, pp. 436-442.

Trappey, J.C., and Liu, C.R., 1990, "Automatic generation of configuration for fixturing an arbitrary workpiece using projective spatial occupancy enumeration approach," Proceedings, Symposium on Advances in Integrated Product Design and Manufacturing, ASME Winter Annual Meeting, Dallas, TX, November 25-30, pp. 191-202.

Appendix

Example Model Formulated in GINO:

```
MODEL:
1) FX1 + FX2 + FX3 + FX4 + FX5 + FX6 + FX7 + FX8 - 200 = 0 ;
2) FY1 + FY2 + FY3 + FY4 + FY5 + FY6 + FY7 + FY8 - 200 = 0 ;
3) FZ1 + FZ2 + FZ3 + FZ4 + FZ5 + FZ6 + FZ7 + FZ8 - 200 - 30 = 0 ;
4) - FY4 - FY5 - FY6 - 5*FY7 - FY8 + FZ1+ FZ2 + 6*FZ3 + 4*FZ6 +
 FZ7 + 6*FZ8 - 5*200 - 7*200 - 3.5 *30 = 0;
5) FX4 + FX5 + FX6 + 5*FX7 + FX8 - FZ1 - 6*FZ2 - 3*FZ3 - FZ4 -
 6*FZ5 - 4*FZ7 - 6*FZ8 - 5*200  + 4*200  + 3.5*30 = 0 ;
6) - FX1 -FX2 - 6*FX3 -4*FX6 - FX7 -6*FX8 + FY1 + 6*FY2 + 3*FY3 +
 FY4 + 6*FY5 + 4*FY7 + 6*FY8 + 7*200 - 4*200 = 0 ;
7) - FZ1 < 0 ;
8)   - FZ2 < 0 ;
```

```
9)   - FZ3 < 0 ;
10)  - FY4 < 0 ;
11)  - FY5 < 0 ;
12)  - FX6 < 0 ;
13)   FZ7 < 0 ;
14)  0.707*FX8 + 0.707*FY8 < 0 ;
15)  ( FX1 ^ 2 + FY1 ^ 2 ) / ( FZ1 ^ 2 ) < 1/9 ;
16)  ( FX2 ^ 2 + FY2 ^ 2 ) / ( FZ2 ^ 2 ) < 1/9 ;
17)  ( FX3 ^ 2 + FY3 ^ 2 ) / ( FZ3 ^ 2 ) < 1/9 ;
18)  ( FX4 ^ 2 + FZ4 ^ 2 ) / ( FY4 ^ 2 ) < 1/9 ;
19)  ( FX5 ^ 2 + FZ5 ^ 2 ) / ( FY5 ^ 2 ) < 1/9 ;
20)  ( FY6 ^ 2 + FZ6 ^ 2 ) / ( FX6 ^ 2 ) < 1/9 ;
21)  ( FX7 ^ 2 + FY7 ^ 2 ) / ( FZ7 ^ 2 ) < 1/9 ;
22)  ( FX8 ^ 2 + FY8 ^ 2 + 2* (FZ8 ^ 2 ) - 2*FX8*FY8 ) / ( FX8 ^ 2 +
 FY8 ^ 2 + 2*FX8*FY8 ) < 1/9 ;
23)  FX1 ^ 2 + FY1 ^ 2 + FZ1 ^ 2 < 250000 ;
24)  FX2 ^ 2 + FY2 ^ 2 + FZ2 ^ 2 < 250000 ;
25)  FX3 ^ 2 + FY3 ^ 2 + FZ3 ^ 2 < 250000 ;
26)  FX4 ^ 2 + FY4 ^ 2 + FZ4 ^ 2 < 250000 ;
27)  FX5 ^ 2 + FY5 ^ 2 + FZ5 ^ 2 < 250000 ;
28)  FX6 ^ 2 + FY6 ^ 2 + FZ6 ^ 2 < 250000 ;
29)  FX7 ^ 2 + FY7 ^ 2 + FZ7 ^ 2 < 122500 ;
30)  FX8 ^ 2 + FY8 ^ 2 + FZ8 ^ 2 < 122500 ;
31)  XTERM = ABS( FX1 ) + ABS( FX2 ) + ABS( FX3 ) + ABS( FX4 )  +
```

```
 ABS( FX5 ) + ABS( FX6) + ABS( FX7 ) + ABS( FX8)  +  200 ;
32)  YTERM = ABS( FY1 ) + ABS( FY2 ) + ABS( FY3 ) + ABS( FY4 ) +
 ABS( FY5 ) + ABS( FY6) + ABS( FY7 ) + ABS( FY8)  + 200 ;
33)  ZTERM = ABS( FZ1 ) + ABS( FZ2 ) + ABS( FZ3 ) + ABS( FZ4 ) +
ABS( FZ5 ) + ABS( FZ6) + ABS( FZ7 ) + ABS( FZ8)  +  230 ;
34)  MIN = ABS( (1/( 10000000 ^ 2 ) )*(49*(-( XTERM / 33.57 ) +
0.05*( YTERM /  33.57 ) + 0.05*( ZTERM / 47 ) ) ^ 2 +
49*( 0.05 * ( XTERM /33.57 )  - ( YTERM / 33.57) +
0.05*( ZTERM / 47) ) ^ 2 + 25*( 0.05 * ( XTERM / 33.57 ) +
 0.05 * ( YTERM / 33.57) - ( ZTERM / 47) ) ^ 2 ) ) ^ 0.5 ;
END
```

Example Output from GINO:

```
SOLUTION STATUS:  OPTIMAL TO TOLERANCES.  DUAL CONDITIONS:
 SATISFIED.
OBJECTIVE FUNCTION VALUE
34) .000022
```

VARIABLE	VALUE	REDUCED COST
FX1	-001.940474	0.000000
FX2	-002.994801	0.000000
FX3	0074.080698	0.000000
FX4	-007.171431	0.000000
FX5	-003.048294	0.000000
FX6	0213.30296	0.000000
FX7	0030.127334	0.000000
FX8	-102.356001	0.000000
FY1	0019.623131	0.000000
FY2	-000.921439	0.000000
FY3	0023.664606	0.000000
FY4	0167.441511	0.000000
FY5	0174.916865	0.000000
FY6	0016.437538	0.000000
FY7	0006.847188	0.000000
FY8	-194.315026	0.000000
FZ1	0075.882110	0.000000
FZ2	0009.397702	0.000000
FZ3	0393.626052	0.000000
FZ4	-053.268695	0.000000
FZ5	-048.094998	0.000000
FZ6	0069.053000	0.000000
FZ7	-242.313570	0.000000
FZ8	0025.718399	0.000000
XTERM	0635.022002	0.000000
YTERM	0804.167304	0.000000
ZTERM	1147.354527	0.000000

ROW	SLACK OR SURPLUS	PRICE
1)	000000.000000	.000000
2)	000000.000000	.000000
3)	000000.000000	.000000
4)	000000.000000	.000000
5)	000000.000000	.000000
6)	000000.000000	.000000
7)	000075.882110	.000000
8)	000009.3977027	.000000
9)	000393.626052	.000000
10)	000167.441511	.000000
11)	000174.916865	.000000
12)	000213.302969	.000000
13)	000242.313570	.000000
14)	000209.746421	.000000
15)	000000.043583	.000000
16)	-00000.000056	.000000
17)	000000.072077	.000000
18)	000000.008068	.000000
19)	000000.035205	.000000
20)	000000.000370	.00000
21)	000000.094854	.000000
22)	000000.000000	.000007
23)	243853.072698	.000000
24)	249901.865310	.000000
25)	089010.567631	.000000
26)	219074.357061	.000000
27)	217081.669340	.000000
28)	199463.333984	.000000
29)	062829.593453	.000000
30)	073603.483869	.000000
31)	-00000.000000	.000000
32)	-00000.000000	.000000
33)	-00000.000000	.000000

CHAPTER 3. USING FINITE ELEMENT ANALYSIS TO CONTROL WORKPIECE RIGIDITY AND DEFORMATION IN WORK-HOLDING TO ACHIEVE PRECISION MACHINING

A paper submitted to International Journal of Machine Tool and Manufacture

Parag Gupta[1] and Jerry Lee Hall[1]

Abstract

The basic goal in precision machining is to machine a workpiece that satisfies dimensional accuracies, surface finish specification and low tolerance variations. To achieve the required accuracy and precision, the workpiece must be rigidly fixed during machining. Sufficient clamping forces must be applied to achieve workpiece rigidity and this often leads to deformation of the workpiece. Deformation also may be caused by cutting tool forces during the machining process. The deformation of the workpiece due to cutting and clamping forces hinders the final goal of the machinist, which is to machine within the specified dimensional and geometric tolerance bandwidths. An extensive literature review of previous research was performed. It was noted that previous models did not model flexible fixtures along with friction

[1]Department of Mechanical Engineering, Iowa State University, Ames, Iowa 50011

which makes them incapable of accurately determining the optimal clamping forces. In this paper a simple workpiece along with flexible fixtures having friction is modeled by using the finite element method. The model determines the optimal clamping forces to ensure workpiece rigidity as well as minimum deformation in the workpiece. It also determines the deformation at any point in the workpiece as well as the maximum deformation. It ensures that the workpiece and the fixtures do not yield under the forces which would violate the applicability of Coulomb's law of friction.

Introduction

Fixtures are employed in a gamut of manufacturing operations–machining, assembly, welding, inspection, and packaging. In the past decade researchers in manufacturing have realized the importance of fixtures or work-holding devices used for machining. Present day technology is capable of machining parts within low tolerance bandwidth by using rigid positional control strategies. However, to achieve such low tolerance requires that the workpiece be rigidly fixed during machining. "Rigidly fixed" is synonymous with high clamping forces achieving great frictional forces, which in turn may cause deformation of the workpiece. The deformation is also caused by cutting forces and clamping forces during machining; this hinders the final goal of the machinist–to machine within low tolerance bandwidth.

Review of Literature

The work-holding device serves three primary functions: location, clamping,and support. The workpiece has to be positioned correctly with respect to the machine tool and the cutting tool to maintain the specified tolerances (location). This position

of the workpiece must be maintained while it is being subjected to cutting forces (clamping). Finally, the deflection of the workpiece caused by the tool and the clamping forces must be minimized (support) (Cohen 1991). Weck and Bibring (1984) have defined "locating" as using faces of the component as reference planes. Location establishes a desired relationship between the fixture and the workpiece, which in turn establishes the relationship between the workpiece and the cutting tool. The common method for location is the 3-2-1 location. For example, if the machinist is to machine one face, control of dimension "a" is necessary and hence only one locating plane is necessary. Two locating planes are required for machining an open slot, as dimensions "a" and "b" need to be controlled. Full location (three planes) is necessary for milling a blind slot i.e. at least three dimensions need to be controlled by three datum planes as shown in Figure 3.1.

The clamping device is used to apply and maintain sufficient counteracting holding forces to cutting forces on a workpiece during machining. The workpiece can deflect within its elastic limit caused by clamping forces, cutting forces, or its own weight. A support is used to limit or stop deflection of the workpiece. Supports (or vertical locators) can be fixed, adjustable, or equalizing (Eary and Johnson 1962).

The clamping must maintain the workpiece contact with all locators despite cutting force variations, inertia forces, or dead weight as well as vibrations in the machine-tool-fixture-workpiece system. A recently developed method of clamping to avoid distortion in the workpiece is SAFE (self-adapting fixture element), which uses "flat contact areas" of hardened steel balls that are free to swivel within their sockets (Kuznetsov 1986). The ball automatically accommodates irregularities in the workpiece surface and provides contoured support without causing distortion. For

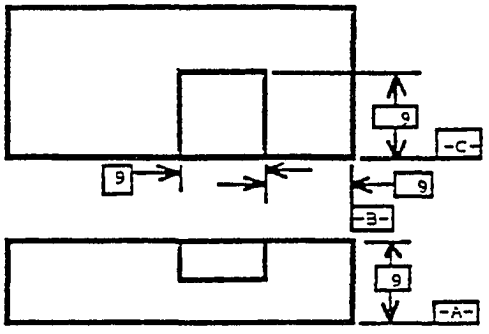

-A- Primary datum feature <-> primary datum plane
-B- Secondary datum feature <-> secondary datum plane
-C- Tertiary datum feature <-> tertiary datum plane

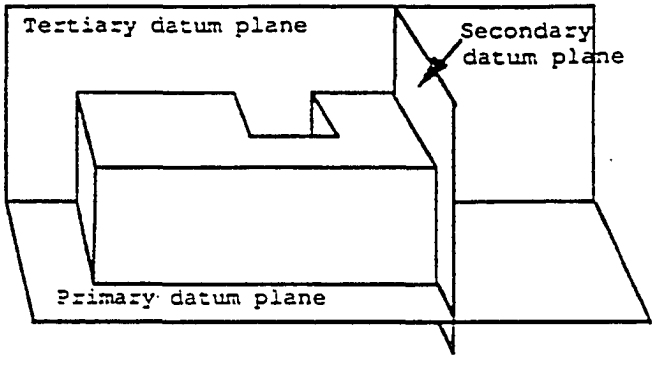

Figure 3.1: Primary, secondary, and tertiary datum planes are required to machine a blind slot.

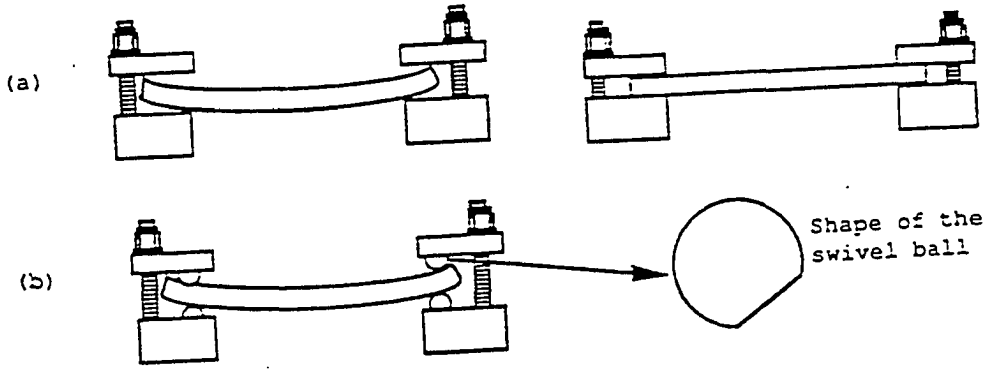

Figure 3.2: Blanks held by vertical locators and vertical clamps (a) with stiff and plane fixture components and (b) with adjustable ball-end fixture components

example, Figure 3.2(a) shows a traditional fixture with stiff locating elements and plane clamps. In this case a blank with an initial form error (curvilinear locating face) is deformed on clamping and, as a result, machining errors occur. However. when a blank is clamped in a fixture with ball supports, as shown in Figure 3.2(b). the blank is not deformed and no machining error is caused.

Shawki and Abdel-Aal (1965) developed formulas for various cases of dimensional inaccuracy in machined workpieces caused by various factors. The authors considered the effect of fixturing rigidity under clamping conditions. The inaccuracies caused by clamping could be due to (1) inaccuracies in the initial mislocation of the workpiece in the fixture components, (2) the inconsistency of the clamping force in fixturing where clamping devices are hand operated, and (3) non-homogeneity of the surface layers of the workpiece. The effect of fixture rigidity under machining conditions was also considered. The authors also took into account the inaccuracies caused by machining and workpiece withdrawal, which include the effects caused by variations in the magnitude of the cutting force or in the deformation of locating elements as a result of tool movement. Also considered was the workpiece withdrawal from the fixture, which causes the elastic deformation to be restored. In addition, the effects of fixture wear and other locating conditions were accounted for by considering inaccuracies caused by mechanical wear in the fixture, non- coinciding disposition of datum surfaces, or inherent errors in the fixture. For each of the above mentioned inaccuracies, the authors developed an analytical formula and used the "Combined Limit Theorem" to calculate the effect of these inaccuracies.

Further experiments of Shawki and Abdel-Aal (1966a) have determined the performance characteristics under various dimensional conditions for both screwed and

hinged clamping elements in a miniature press especially developed for the purpose. Their investigations established that the force versus deflection characteristics for the clamping elements tested were linear in nature and that clamp rigidity considerably increased with screw or pivot size, as with the height of the nut in a screwed clamp. Comparison between the stiffness of screwed and hinged clamps revealed the superiority of the former. The rigidity of relatively large-size screw clamps was found to be comparable with that of flat locators with excellent surface finish. The authors claimed that the behavior of the fixture and workpiece system can be represented by linear characteristics for the clamping elements together with nonlinear characteristics for the locating elements. They also showed that rigidity is impaired with an increase in the number of contacts in the fixture and workpiece system, which implies the need for maintaining a minimum number of contacts in the system. Contact deformation at static surfaces may be reduced by applying high initial-tightening loads to the assembled fixture components. Therefore, according to these workers, stresses induced in the fixture elements, under the influence of clamping and working loads, did not normally exceed the limit of elasticity.

In another research project, Shawki and Abdel-Aal (1966b) investigated the contact rigidity of fixtures for three types of locating elements (spherical, flat, and V-shaped), where the force deflection characteristic was obtained in a miniature hydraulic press for a wide range of operating conditions. The experimental results showed that the performance characteristics were nonlinear in nature. Deformation at contact surfaces between workpiece and locator was found to be affected by workpiece material, hardness, and surface finish, as well as by the size and form of the locating elements. They found that higher contact rigidity in a fixture may be es-

tablished with greater workpiece hardness, better surface quality, and larger contact area. Larger values of the workpiece diameter (for V-shaped and radius-of-curvature for spherical locators) led to increased contact rigidity. Test results for all three types of locators were compared with the theory of contact between elastic bodies and showed that the experimental values greatly exceed theoretical predictions. The discrepancy between experiment and theory may be attributed to the fact that the influence of hardness and of the actual area of contact (as affected by surface finish) were not included in the theory.

In a later study, Shawki and Abdel-Aal (1967) analytically investigated the fixture workpiece system under eccentric clamping conditions for both spherical and flat locators. The analysis was based on linearized deflection but nonlinear reaction distributions at the contact surface. Under the same operating conditions, the flat locator was found to display a higher rigidity than did spherical locators of the same metallic area.

The kinematic model was developed by Asada and By (1985). In this model, the characteristics of the work- holding (such as the deterministic position, accessibility, detach-ability, and complete restriction) were formulated as geometric constraints. The constraints were structured in terms of the boundary Jacobian matrix and the fixture displacement vector. Asada and By considered only the relationship between the workpiece boundary and the fixture elements. The possible force impact of the machining process was not included in the work-holding analysis.

Screw theory (Ohwovoriol and Roth 1981) was applied by Chou et al. (1989) to model the fixturing equilibrium problem for a prismatic workpiece. A linear programming formulation was used to solve the unknown, optimal clamping force magnitudes

given fixturing and cutting torques. Some issues were not addressed by Chou et al. First, it was presumed that all of the unit clamping and locating torques were under a friction-free condition. In contrast, in this work the locating wrenches only occurred dynamically to counterbalance the clamping torques with respect to the clamping force magnitudes and directions as well as the friction coefficient. However. most previous researchers did not consider the frictional effect. Because of the simplified direction definition for the fixturing force (perpendicular to the planar boundary surface), only prismatic workpiece fixturing could be verified.

Later, Chou (1990) extended his work to consider the cutting force effects of several machining operations such as drilling, boring, and milling. An algebraic representation for cutting forces and their effects on fixtures was introduced. This representation allowed the effect of all cutting forces to be considered as constituting a "force field," which was a function of both time and space. The "envelope" of the force field was then computed. The envelope was an upper bound estimate for the effects of cutting forces, which were taken as the goal to be counteracted by a proper layout of fixture components.

The kinematic (Shoham 1985) approach was applied by Mani and Wilson (1988) to construct the constraints and to ensure the validity of the fixture configuration. The counter-clockwise (CCW) and the clockwise (CW) rotational triangles were used to model and prevent the rotational movement. Although this approach was rather easy to implement in a knowledge-based expert system, the application domain was limited to a 2 1/2 dimensional prismatic workpiece. The friction factor between the workpiece and the fixture was not considered (i.e., a friction free surface was assumed). Further, the counteracting concept was not modeled in the analysis so the

system was possibly too restrictive in some situations (see Figure 3.3). Because the force magnitude was not defined for each force, the allowable fixturing force limits were not considered.

Lee and Haynes (1987) proposed a finite element formulation for a fixturing system for prismatic parts. The deformation of the workpiece, the clamping forces of the fixture elements, and the resulting stress distribution were computed with their model. The workpiece was modeled as a linear isotropic solid and Coulomb's law of friction was used to calculate the frictional forces acting at the nodal points at which the machining took place. All the fixturing elements were assumed to be rigid and in contact with nodal points on the workpiece surface. The nodal point force or the nodal point displacement were specified for every degree of freedom. The boundary conditions were the primary factors influencing the behavior of the workpiece under the clamping and cutting forces. Since the boundary conditions were not known in advance, analyzing a fixturing system involved the validation of boundary conditions based on the nature of the solution obtained or discrepancies in the solution, if any. This was accomplished iteratively. At the end of iterations, the nodal point forces, displacements, deformation of the workpiece, and the stress values at every nodal point were obtained. Lee and Haynes concluded that after initial tightening of the clamping elements, the work caused by the friction force dominated, which gave rise to frictional forces opposite in direction to the tangential displacement. As the tightness increased, the work done by the fixturing elements increased monotonically with tightness and sticking conditions were assumed to apply. However, the analysis assumed that the frictional force obeyed Coulomb's law of friction, which is not true when local yielding occurs.

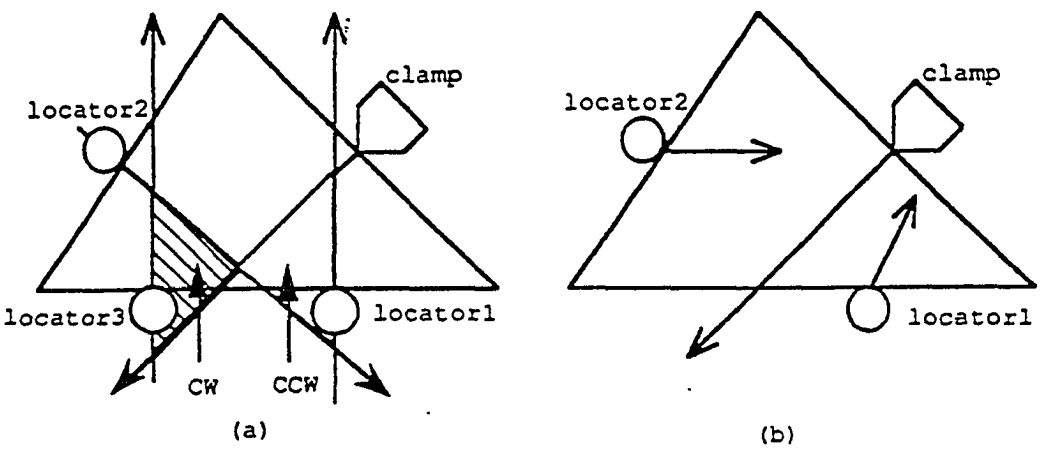

Figure 3.3: Without considering friction, fixture configuration shown in (a) is valid with the pair of clockwise and counterclockwise triangles; however, the configuration in (b) cannot be verified.

Trappey and Liu (1989) extended the work of Chou et al.(1989) by incorporating friction. The reactive force equilibrium approach was developed to verify the fixture configuration. To ensure complete absence of motion of a workpiece during machining, assembling, transporting, the resultant force and moment needed to be zero. The research included consideration of the following situations, (1) time-varying acting and reacting force equilibrium, (2) limits of force magnitudes to prevent excessive deflection, (3) constraints of force directions based upon the part geometry, and (4) frictional effects. Force elements included the horizontal and vertical locating forces, the horizontal and vertical clamping forces, and the machining forces, which were all acting and reacting with each other. Finally, a quadratic programming model was used to implement the general verification system.

Trappey, Gupta and Liu (1992) extended the work by using an analytical nonlinear optimization model to minimize the deformation in a workpiece. This model is suitable for simple workpieces but is not be suitable for complex shapes.

In another study, Cabadaj (1990) developed a force model of the fixture to evaluate the influences of cutting and clamping forces on the workpiece and fixture system. The model was based on the equilibrium of all forces and moments in x, y, and z directions. However, the model avoided practical complexities such as the effects of coefficient of friction or fluctuation of cutting forces.

Lee and Cutkosky (1991) found that the clamping forces depended on various factors such as the workpiece material (e.g., aluminum versus plastic), geometry (whether the part has thin walls or other easily deformed sections). Also if the clamping forces were high, the resultant deformation could affect accuracy. On the other hand, if the clamping forces were smaller, the workpiece could slip. The machinist

estimates clamping forces by the resistance developed in the vise. However, errors could occur because of unexpected variations in cutting forces or the coefficient of friction.

In the same study, Lee and Cutkosky (1991) divided the general fixture planning analysis into four sections, namely geometric, kinematic, force, and deformation analysis. The geometric analysis was performed to ensure that the fixtures did not restrict access to features being machined. After geometric constraints were satisfied, heuristic objective functions were applied to reduce the number of candidate clamping arrangements. The kinematic analysis of fixturing was used to determine whether it would constrain the part with respect to cutting forces. Force analysis tested whether the forces applied by the fixtures were sufficient to maintain static equilibrium in the presence of cutting forces. Lee and Cutkosky (1991) emphasized only the kinematic and force analysis. They developed a novel technique to determine whether a part under given frictional constraint would slip or not when additional cutting forces or moments were introduced. To determine this, the authors determined the limit surface in a space defined by x and y components of frictional force and maximum moment. However, to determine the limit surface for a simple case, such as a block held in vise, five minutes of 68020-based workstation time was required.

According to Table 3.1, some researchers have restricted their analyses to a limited number of factors that affect rigidity and deformation of a workpiece. For example, none considered that Coulomb's law of friction may not be valid when yielding occurs. Some models took friction into account. However, they assumed rigid fixtures. Some researchers developed analytical models which are limited only to simple workpiece shapes which is far from reality.

Table 3.1: Summary of the relevant works

REFERENCE	MODEL DESCRIPTION	ADVANTAGES	DISADVANTAGES
Shawki and Abdel-Aal (1965, 1966a, 1966b, 1967)	Analytical formula for dimensional inaccuracy	Gives an idea of maximum possible error	Discrepancy between theory and experiment because hardness and actual area of contact ignored
Asada and By (1985)	Kinematic model applying Jacobian matrix to ensure geometric constraints	Total constraint of a 3-D workpiece	No machining force effect is considered
Lee and Haynes (1987)	Fixture analysis by finite element method	Deformation of workpiece is obtained	Assumes rigid fixturing elements
Mani and Wilson (1988)	Using naive kinematic reasoning to ensure complete workpiece restraint	Simple implementation	Only apply up to 2-1/2 D workpiece
Chou et al (1989), Chou (1990)	Stability of a workpiece under cutting forces using screw theory	Considered empirical formulas to estimate cutting forces for few processes to make the system pragmatic	Ignored friction
Trappey and Liu (1989), Trappey, Gupta and Liu (1992)	Reactive equilibrium approach to verify the work-holding rigidity	Considers friction, can solve cases that are not solved by naive kinematic approach	Assumes Coulomb's law of friction and rigid clamping elements
Cabadaj (1990)	Force model evaluates influence of cutting & clamping forces	Can find whether the workpiece is in equilibrium if the forces are provided	Did not consider friction and fluctuation of cutting force
Cutkosky and Lee (1989), Lee and Cutkosky (1991)	Effect of friction in fixture design	Determined maximum forces and moments within which no slippage occurs	High computation time, assumed coulomb's law of friction (not true for yielding)

A new finite element model has been developed herein which (1) computes the deformation at any place on the workpiece or fixturing element, (2) computes the optimal clamping forces under which there is no slippage (3) ensures that workpiece and fixtures do not yield thus allowing applicability of Coulomb's law of friction (4) can be used for workpiece and fixturing elements of any complex shape and (5) does not assume rigid fixtures.

Finite Element Model

A workpiece (7"x 7"x 5") with a cut at one corner as shown in Figure 3.4. is configured with three vertical supports (F1, F2 and F3), three horizontal locators (F4, F5 and F6), one vertical clamp (F7) and one horizontal clamp (F8) for fixturing. The maximum cutting force is (-100lb, -100lb, -100lb) at (3,4,5,5). Forces are applied by a vertical clamp and a horizontal clamp at (4,1,5) and (6,6,1) respectively. Table 3.2 provides the configuration of the fixtures.

A solid model of the workpiece having three vertical supports and three horizontal locators as shown in Figure 3.5 was developed in the solid modeling module

Table 3.2: Fixture configuration data

Fixture	fixture element	Nodal coordinates of fixture contact
F1	vertical locator	(.5..5.0), (1..5.0), (1,1.0), (.5,1.0)
F2	vertical locator	(6..5.0), (6.5..5.0), (6.5,1.0), (6,1.0)
F3	vertical locator	(2.5,6.0), (3,6.0), (3,6.5.0), (2.5,6.5.0)
F4	horizontal locator	(0.5.0.0), (1.0.0), (.5.0..5), (1.0..5), (.5.0.1), (1.0,1)
F5	horizontal locator	(6.0.0), (6.5.0.0), (6,0..5), (6.5.0..5), (6.0.1), (6.5.0.1)
F6	horizontal locator	(0.3.5.0), (0.4.0), (0.3.5..5), (0.4..5), (0.3.5.1), (0.4.1)
F7	vertical clamp	(4,1,5)
F8	horizontal clamp	(6,6,1)

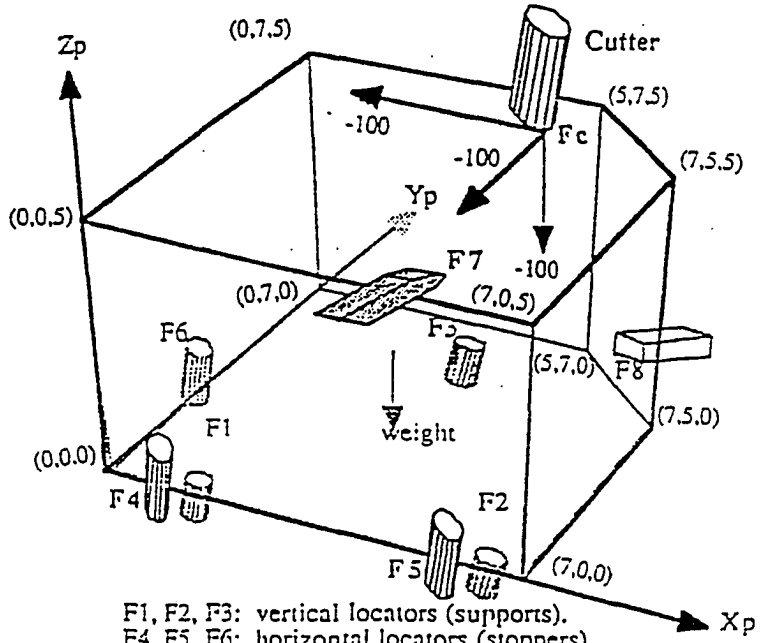

F1, F2, F3: vertical locators (supports).
F4, F5, F6: horizontal locators (stoppers).
F7: vertical clamp (e.g., swing clamp).
F8: horizontal clamp (e.g., side clamp).

Figure 3.4: 3-D fixturing illustration

of I-DEAS software. The clamps were not modeled because the nodes at the location of the clamps are restrained in an appropriate direction to determine required frictional force. The workpiece is located by three fixtures (F1, F2 and F3) in the bottom XY plane, two fixtures (F4 and F5) in the front XZ plane and one fixture (F6) in the YZ plane. The solid model was then transferred to the Finite Element Analysis module of I-DEAS software. The horizontal locators, vertical supports and workpiece surface were then meshed by quadrilateral thin shell elements as shown in Figure 3.6. However, the workpiece has no cavity so the volume enclosed by the quadrilateral thin shell elements required meshing. Moreover, it was realized that solid linear brick elements would provide a better solution than thin shell elements when a workpiece does not have a cavity. Therefore, the thin shell elements were extruded in appropriate directions to develop solid linear brick elements having dimensions of 1/2"x1/2"x1/2") as shown in Figure 3.7. All horizontal locators were modeled by a single linear brick elements whereas the vertical locators were modeled by two linear brick elements. The configurations of the fixtures are provided in Table 3.2. After the brick elements were generated the thin shell elements were deleted. The method of extruding a thin shell element to mesh the volume with linear brick elements is a better method than directly meshing the whole volume by a linear brick element. The former process allows the thin shell meshing to be changed before extruding. Extrusion generates higher regularity in elements than free meshing does. The material property table of the linear brick element was developed assuming all the fixtures and the workpiece to be made of steel with a coefficient of friction between the workpiece and fixture element of 1/3. The material property table of the solid linear brick element is provided in Appendix 1. The physical property table

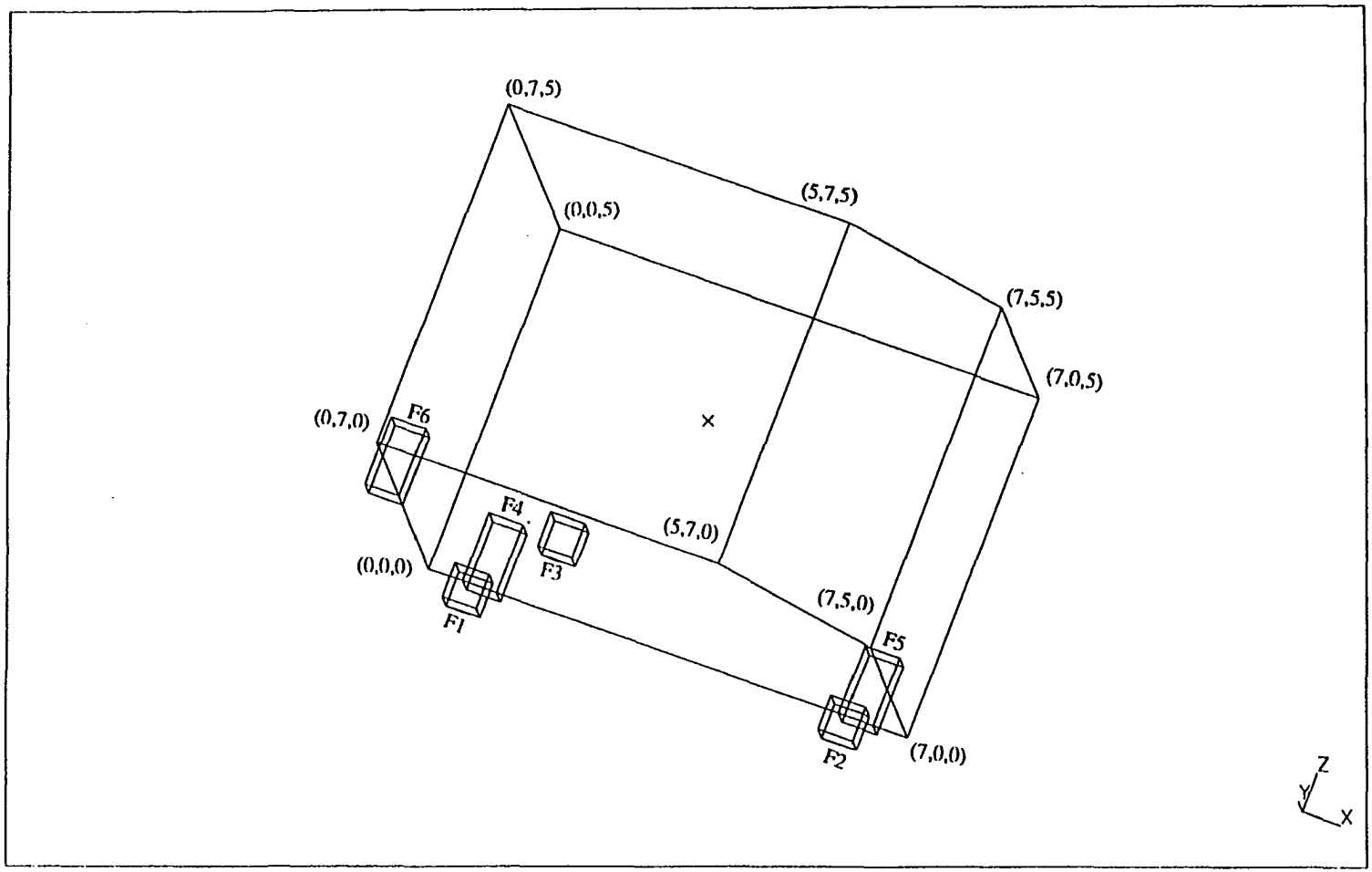

Figure 3.5: Solid model of the workpiece and fixtures

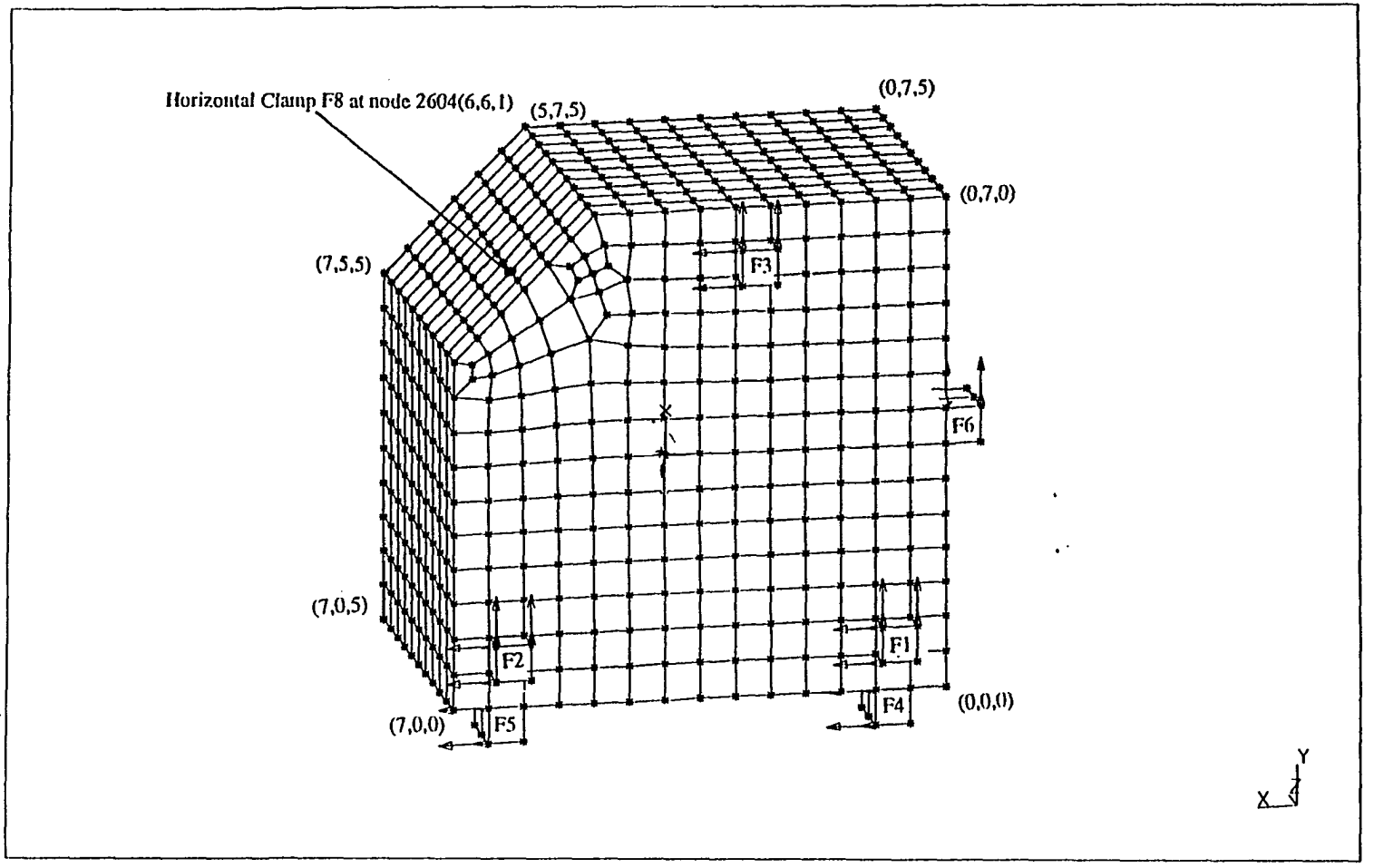

Figure 3.6: Workpiece and fixtures meshed with thin shell quadrilateral elements.

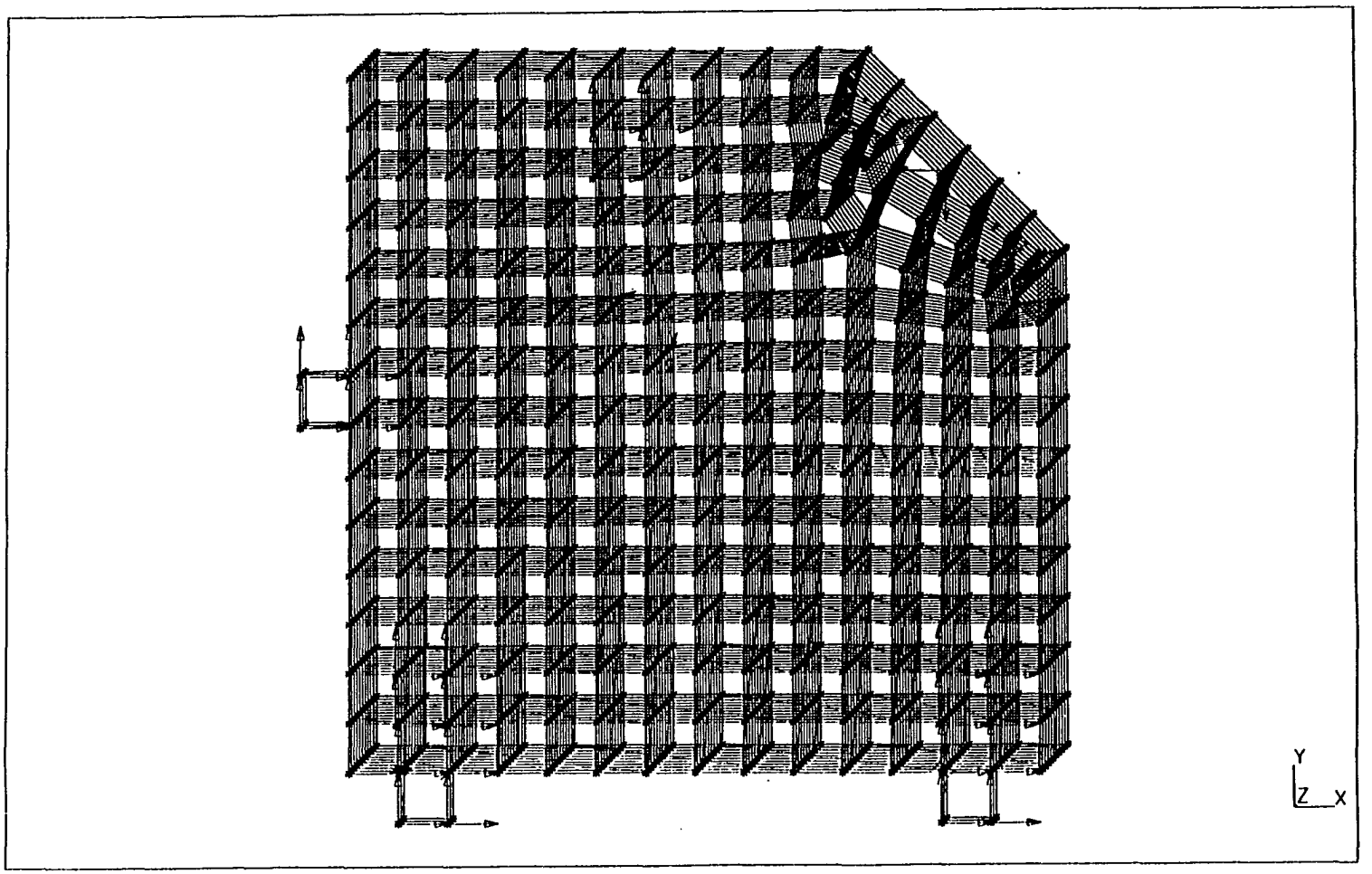

Figure 3.7: Workpiece and fixtures meshed with solid linear brick elements

was developed by using the default values of an isotropic material. The six fixtures used in locating and supporting the workpiece were assumed to be rigidly fixed to the base plate. The linear brick element has three translational degrees of freedom and no rotational degree of freedom. Therefore the bottom four nodes of each fixture for all six fixtures were restrained in the X, Y and Z directions as shown in Figure 3.6.

To model friction between the fixture and the workpiece , node-to-node gap elements were generated between those nodes of fixtures and the workpiece which were coincident. There were four such nodes for each horizontal locator and six such nodes for each vertical locator the coordinates of which are provided in Table 3.2. Therefore a total of 4x3 + 6x3 = 30 node-to-node gap elements were created. The initial gap between the pin surface and the block surface was assumed to be 0.00001 inches. If a gap of zero inches were provided then the software assumes it to be a press fit problem. The maximum value of cutting force (-100lbs, -100lbs, -100lbs) is applied as a nodal force at (3,4.5,5) as shown in Figure 3.8. It is assumed that the friction caused by the vertical clamp restrains the workpiece in the X and Y directions whereas the friction caused by the horizontal clamp restrains it in the Z direction. Therefore the node 220 at (4,1,5) at the location of the vertical clamp is restrained in the X and Y directions as shown in Figure 3.8, and node 2604 at (6,6,1) at the location of the horizontal clamp is restrained in the Z direction. Initially no forces are applied at these nodes. The model is then solved only with the cutting force applied. The model then provides the reaction forces in the X and Y directions as being equal to 164.2 lbs and 266.1 lbs respectively at the location of the vertical clamp (node 220). The reaction force in the Z direction at the location of the horizontal

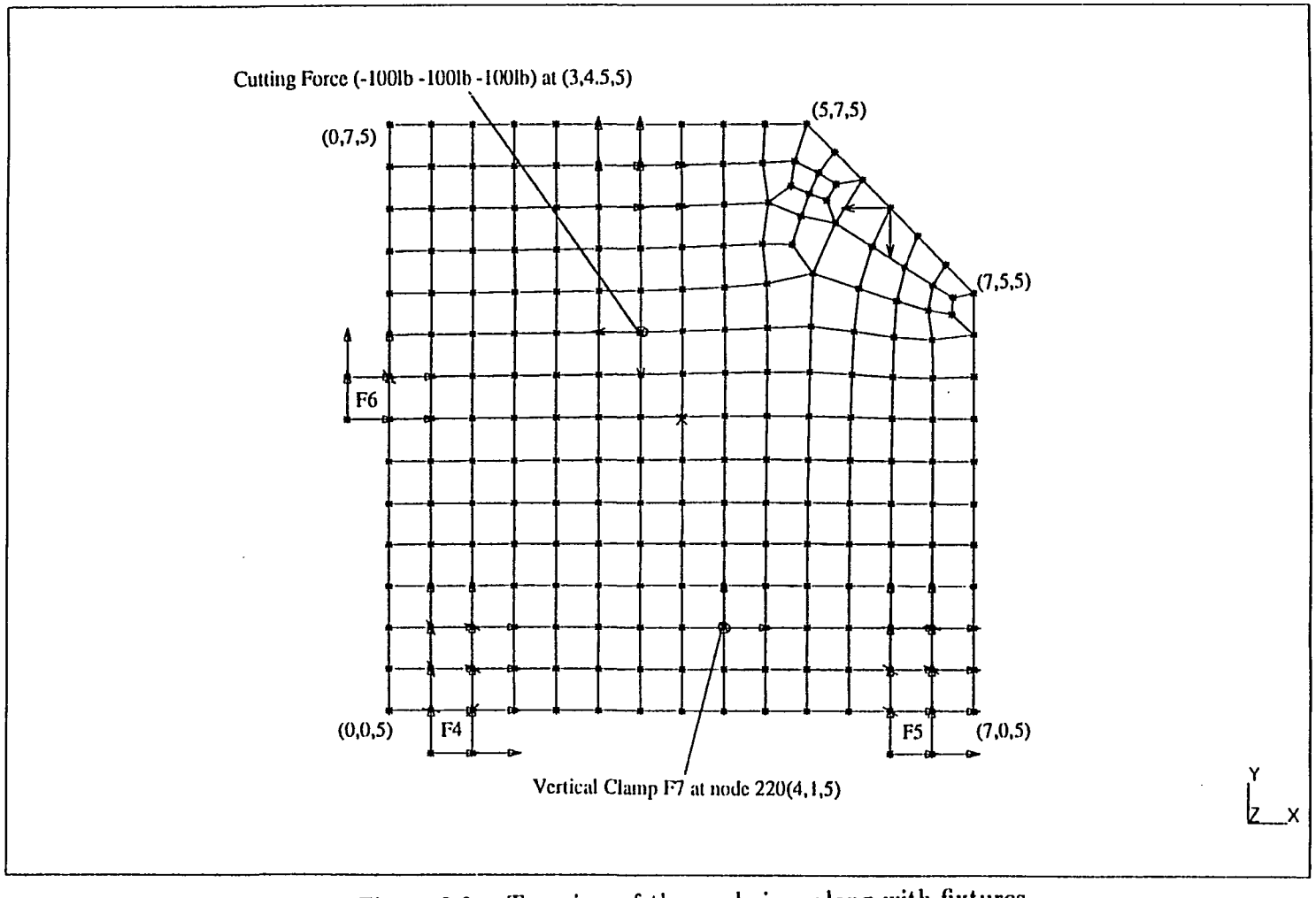

Figure 3.8: Top view of the workpiece along with fixtures

clamp (node 2604) was found to be 226.8 lbs. The reaction forces for load-set-1 are provided in Appendix 1. The reaction forces are merely the required friction forces required to avoid slippage of the workpiece caused by the cutting force. The normal forces required to generate the equivalent friction forces are computed by assuming the coefficient of friction to be 1/3 between the clamp surface and the workpiece surface. The normal force at node 220 is $(Fx^2 + Fy^2)^{1/2}$/(coefficient of friction) = 938.0499lbs, where Fx and Fy are the reaction forces at node 220 for load-set-1. The direction cosines of the unit normal force vector are (0, 0, -1) so the force applied is (938.0449x0 lbs, 938.0449x0 lbs, 938.0449x-1 lbs) = (0 lbs, 0 lbs, -938.0449 lbs). The normal force at the horizontal clamp (node 2604) is Fz/(coefficient of friction) = 226.8 x 3 = 680.4 lbs. The unit normal force vector has direction cosines (-0.7071, -0.7071, 0). Therefore the normal force acting at node 2604 is (680.4x-0.7071lbs , 680.4x- 0.7071lbs ,680.4x0lbs) or (-481.115lbs, -481.115lbs, 0lbs). The model is once again solved with these normal forces and the cutting force. The reaction forces obtained by the model for load-set-2 are provided in Appendix-1. The reaction forces in the X and Y directions for node 220 (vertical clamp F7) were found to be 630.1 lbs and 1301 lbs respectively. The reaction force in the Z direction at node 2604 (Horizontal clamp F8) was found to be 1148 lbs. The resultant reaction forces for load-set-2 are greater than the product of the normal force and the coefficient of friction which implies the workpiece would slip. Therefore it is necessary to change the clamping forces in order to obtain the initial reaction forces. However the normal component of clamping forces should remain the same to provide the required friction. So additional X and Y component forces must be applied at node 220 (vertical clamp). The X component = Reaction force in X direction for load set 2 - Reaction force in X

direction for load set 1 =465.9 lbs . Similarly the Y component = 1034.9 lbs at node 220 (vertical clamp) and Z component = 921.2 lbs at node 2604 (horizontal clamp) is determined. Therefore the horizontal and vertical clamping forces are modified to (465.19 lbs, 1034.9 lbs, -938.0449 lbs) and (-481.115 lbs,-481.115 lbs, 921.2 lbs) respectively. Once again the model is solved for load-set-3 which consists of the above mentioned modified clamping force and cutting force. This time the reaction forces obtained at the horizontal and vertical clamp are the same as those obtained in load set-1 as can be seen in Appendix-1. This implies that clamping forces are just optimal to restrain the movement of the workpiece due to the cutting and clamping forces. In other words these clamping forces would ensure rigidity and minimum inaccuracy due to deformation. The maximum deformation obtained by cutting and optimal clamping forces was found to be $1.644X10^{-3}$ inches as shown in Figure 3.9. The deformation would be much higher if the part had a cavity or if it were made of plastic or aluminum. The stresses caused by the vertical clamp and cutting force can be seen in Figure 3.10. From the reaction force data provided for load set-3 in Appendix 2, it was noticed that the horizontal locator F5 and the vertical locator F2 supported most of the clamping and cutting load which is evident from the stresses shown in Figure 3.11. Figure 3.11 also shows the stress caused by the horizontal clamp. The reaction forces at the restrained nodes of the fixtures are also provided for all load sets in Appendix1.

Conclusions

The model uses a unique but simple algorithm as shown above in determining the optimal clamping forces which unlike other methods does not require trial and

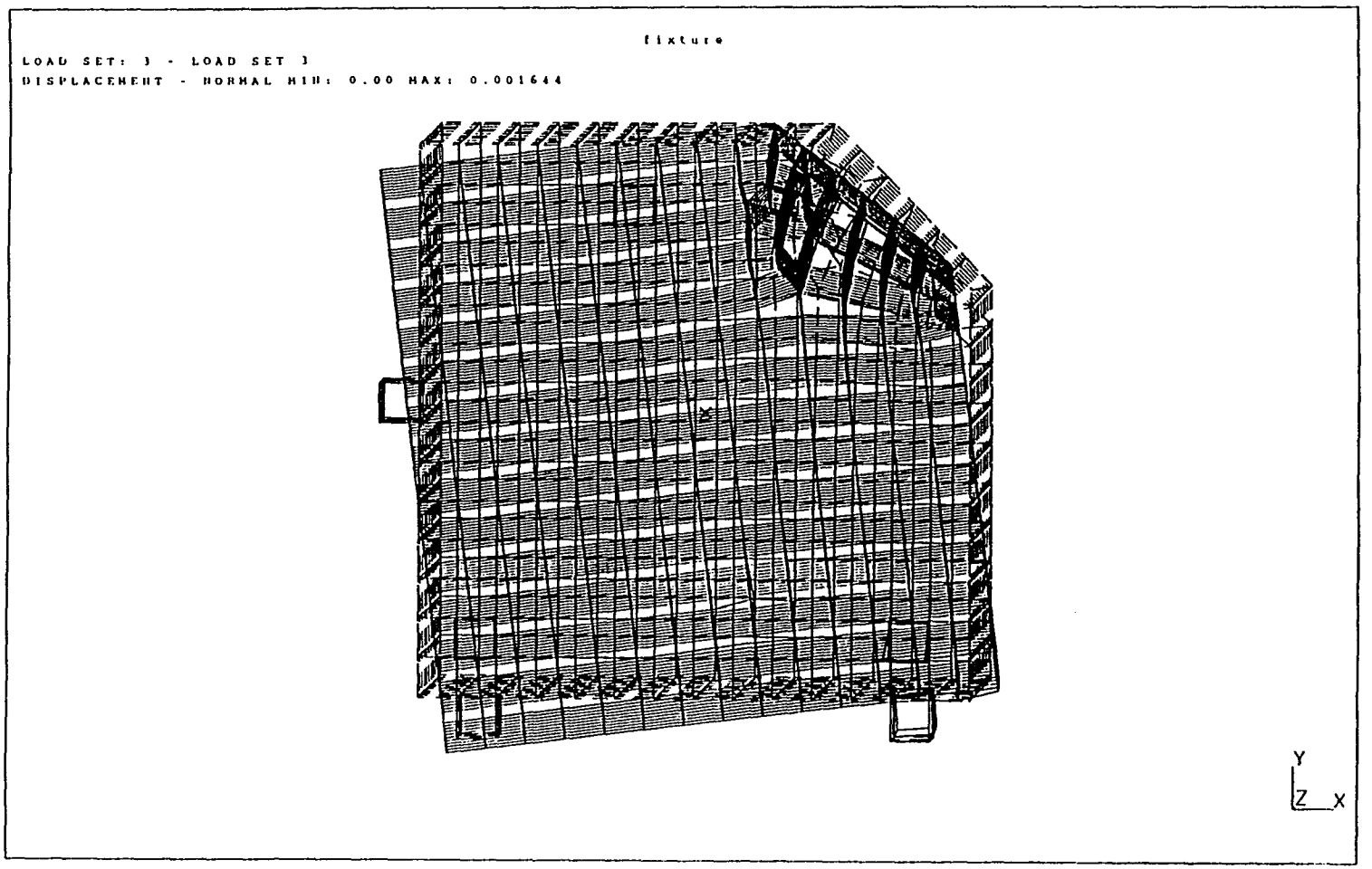

Figure 3.9: Deformation of the workpiece and fixtures

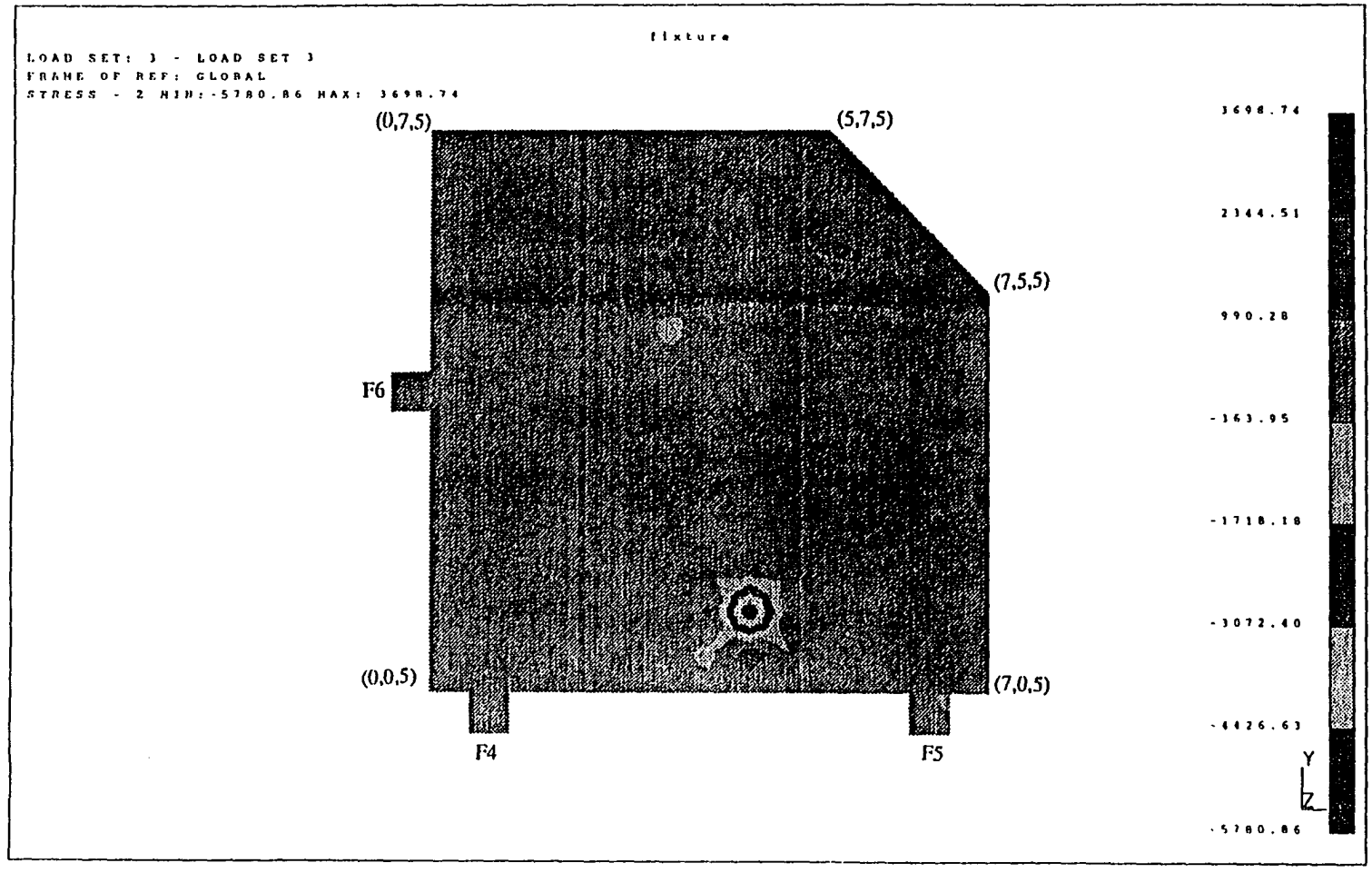

Figure 3.10: Stresses developed in the top surface of the workpiece

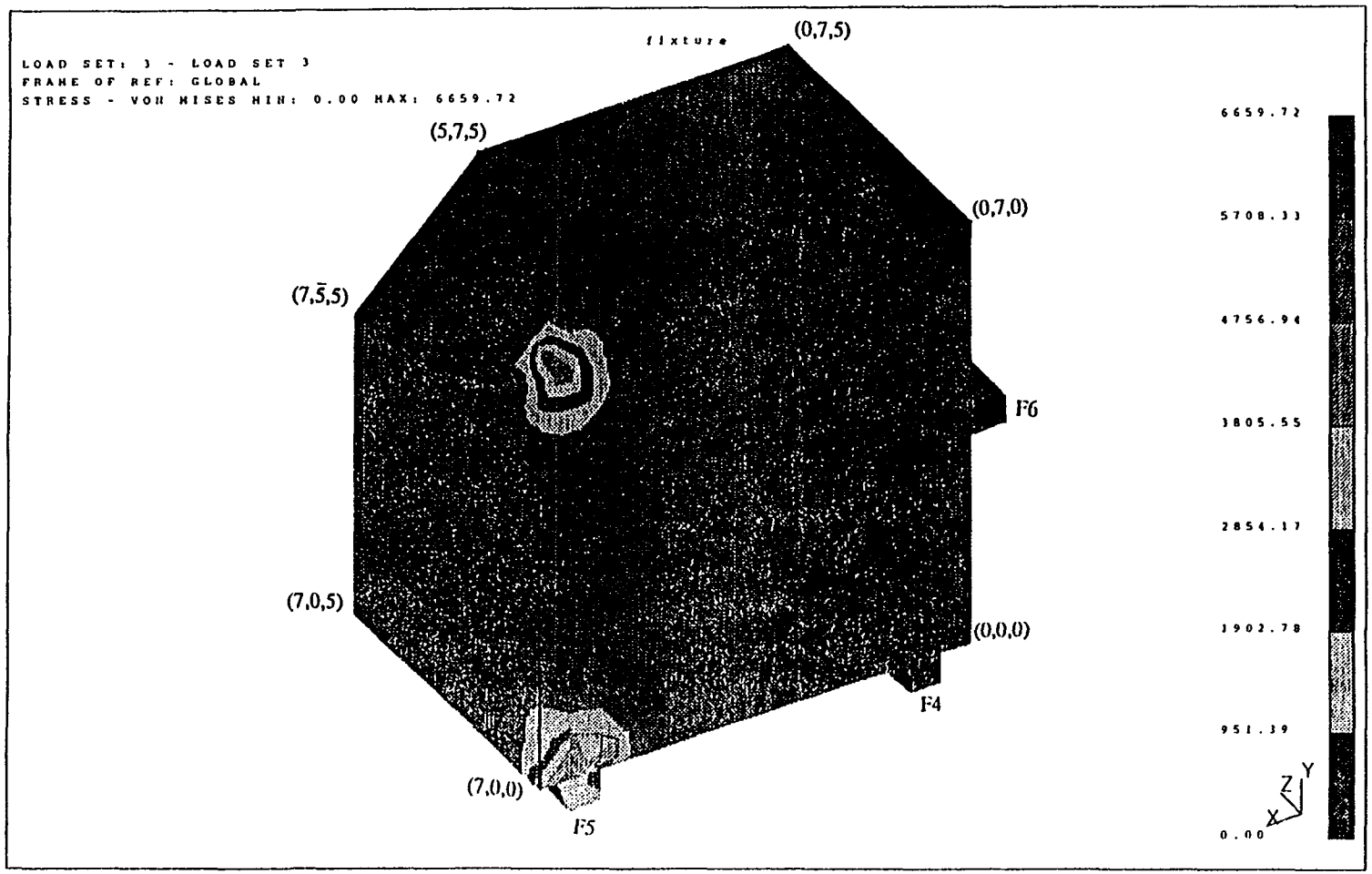

Figure 3.11: Stresses developed in fixtures as well as bottom and side surfaces of the workpiece

error or several iterations to reach an optimal solution. Unlike other models, the deformation at any place on the workpiece or fixture can be determined and it ensures the validity of Coulomb's law of friction under optimal clamping forces. It can be used for workpiece and fixturing elements having any possible complex shapes. In this model flexible fixtures have been modeled for the first time and this has also eliminated the disadvantages which were encountered by the previous models except that it requires a relatively large amount of computational time. Approximately 2.5 hours were required for each load set on a DEC 5000 60MHz machine which implies that a total of 7.5 hours were required to solve the problem. This technique would be especially useful for aircraft industries in determining the optimal clamping forces for clamping composite, plastic or aluminum parts which have low stiffness because of their material property. The shape of the part is also a major factor. For example an aluminum part having a cavity may have large deflections if clamping forces are high which would imply higher inaccuracy and higher rejection rates.

References

Asada, H., and By, A. B., 1985, "Kinematics of work part fixturing," IEEE Conf. on Robotics and Automation, pp. 337-345.

Cabadaj, J., 1990, "Theory of computer aided fixture design," Third International Seminar on Intelligent Manufacturing Systems- IMS '89, Computers in Industry, Vol. 15, 1-2 Oct. 1990, pp. 142-147.

Chou, Y. C., Chandru, V., and Barash, H. H., 1989, "A mathematical approach to automatic configuration of machining fixtures: Analysis and synthesis," Transactions of the ASME, Journal of Engineering for Industry, Vol. Ill, Nov., pp. 299-306.

Chou, Y. C., 1990, "A methodology for automatic layout of fixture elements based on machining forces considerations," Advances in Integrated Design and Manufacturing, PED-Vol.47, ASME, New York, pp. 181-190.

Cohen, P. H., 1991, "Automated fixture design," Proceedings of the 1991 NSF Design and Manufacturing Systems Conference, Jan. 9-Il, pp. 405-414. published by Society of Manufacturing Engineers, One SHE drive, P. O. Box 930, Dearborn, Michigan. 48121, USA.

Eary, D. F., and Johnson, G. E., 1962, Process Engineering for Manufacturing, Prentice-Hall, Inc., Englewood Cliffs, N.J.

I-DEAS Mechanical CAE/CAD/CAM software, Structural Dynamics Research Corporation, 2000 Eastman Dr., Milford, OH 45150

Kuznetsov, Y. I., 1986, "A range of resettable fixtures," Soviet Engineering Research, Vol.6, No. 10, Oct., pp. 74-75.

Lee, J. D., and Haynes.L. S., 1987, "Finite element analysis of flexible fixturing system." Transactions of the ASME, Journal of Engineering for Industry, Vol. 109, No. 2, Hay, pp. 134-139.

Lee, S. H., and Cutkosky, H. R., 1991, "Fixture planning with friction." Transactions of the ASME, Journal of Engineering for Industry, Vol. 113, Aug., pp. 320-327.

Mani, M., and Wilson, W. R. D., 1988, "Automated design of workholding fixtures using kinematic constraint synthesis." Proceedings, 16th North American Manufacturing Research Conference, SME, University of Illinois, Urbana, pp. 437-444.

Ohwovoriol, M. S., and Roth, B., 1981, "An extension of screw theory," Journal of Mechanical Design, Vol. 103, pp. 725-735.

Shawki, G. S. A., and Abdel-Aal, M. M., 1965, "Effect of fixture rigidity and wear on dimensional accuracy," International Journal of Machine Tool Design and Research, Vol 5, pp. 183-202.

Shawki, G. S. A., and Abdel-Aal, M. M., 1966a, "Rigidity considerations in fixture design-contact rigidity at locating elements," International Journal of Machine Tool Design and Research, Vol. 6, pp. 31-43.

Shawki, G. S. A., and Abdel-Aal, M. M., 1966b, "Rigidity considerations in fixture design-contact rigidity at clamping elements," International Journal of Machine Tool Design and Research, Vol.6, pp. 207-220.

Shawki, G. S. A., and Abdel-Aal, M. M., 1967, "Rigidity considerations in fixture design-contact rigidity for eccentric clamping," International Journal of Machine Tool Design and Research, Vol.7, pp. 195-209.

Shoham, Y., 1985, "Naive kinematics," Proceedings, International Joint Conference on Artificial Intelligence, pp. 436-442.

Trappey, J. C and Liu, C. R., 1989, "An automatic workholding verification system" Proceedings of International Conference on Manufacturing Science and Technology of the Future (MSTF), Stockholm, Sweden, June 6-9.

Trappey, A. J . C. , Gupta Parag and Liu C.R. 1993 "Using Optimization Model to Control Workpiece Rigidity and Deformation in Workholding to Achieve Precision Machining" Published in "Operations Research in Production Planning and Control" A Springer Verlag publication edited by Fandel, Gulledge, and Jones, pp. 138-150.

Weck, M. and Bibring, H., 1984, Handbook of Machine Tools, Vol.1, John Wiley and Sons, Chichester West Sussex, New York 1984.

Appendix

Table 3.3: Load Set 1

Node	Force-X (lb)	Force-Y (lb)	Force-Z (lb)	Fixture
220	164.2	0	0	F7
2604	0	0	226.8	F8
3374	012.45	002.148	-36.25	F2
3376	000.8232	-01.621	-12.25	F2
3378	004.486	020.96	-47.27	F2
3380	-03.535	010.17	-24.38	F2
3382	0	0	0	F1
3384	0	0	0	F1
3386	0	0	0	F1
3388	0	0	0	F1
3390	0	0	0	F3
3392	0	0	0	F3
3394	0	0	0	F3
3396	0	0	0	F3
3399	0	0	0	F4
3402	0	0	0	F4
3405	0	0	0	F4
3408	0	0	0	F4
3411	-12.98	-16.26	-35.32	F5
3414	-04.502	-18.76	-19.05	F5
3417	001.961	-07.972	017.23	F5
3420	-02.638	-11.48	037.14	F5
3423	0	0	0	F6
3426	0	0	0	F6
3429	0	0	0	F6
3432	0	0	0	F6

Table 3.4: Load Set 2

Node	Force-X (lb)	Force-Y (lb)	Force-Z (lb)	Fixture
220	630.1	1301	0	F7
2604	0	0	1148	F8
3374	112.6	024.94	-129.1	F2
3376	020.13	-23.43	0059.86	F2
3378	056.41	063.51	-110.8	F2
3380	016.84	-17.16	0050.81	F2
3382	0	0	0	F1
3384	0	0	0	F1
3386	0	0	0	F1
3388	0	0	0	F1
3390	0	0	0	F3
3392	0	0	0	F3
3394	0	0	0	F3
3396	0	0	0	F3
3399	0	0	0	F4
3402	0	0	0	F4
3405	0	0	0	F4
3408	0	0	0	F4
3411	-46.46	-60.81	-122.7	F5
3414	-13.88	-80.62	-093.4	F5
3417	005.251	-33.58	0080.16	F5
3420	-12.39	-42.12	0124.9	F5
3423	0	0	0	F6
3426	0	0	0	F6
3429	0	0	0	F6
3432	0	0	0	F6

Table 3.5: Load Set 3

Node	Force-X (lb)	Force-Y (lb)	Force-Z (lb)	Fixture
220	164.2	0	0	F7
2604	0	0	226.8	F8
3374	012.45	002.148	-36.25	F2
3376	000.8232	-01.621	-12.25	F2
3378	004.486	020.96	-47.27	F2
3380	-03.535	010.17	-24.38	F2
3382	0	0	0	F1
3384	0	0	0	F1
3386	0	0	0	F1
3388	0	0	0	F1
3390	0	0	0	F3
3392	0	0	0	F3
3394	0	0	0	F3
3396	0	0	0	F3
3399	0	0	0	F4
3402	0	0	0	F4
3405	0	0	0	F4
3408	0	0	0	F4
3411	-12.98	-16.26	-35.32	F5
3414	-04.502	-18.76	-19.05	F5
3417	001.961	-07.972	017.23	F5
3420	-02.638	-11.48	037.14	F5
3423	0	0	0	F6
3426	0	0	0	F6
3429	0	0	0	F6
3432	0	0	0	F6

CHAPTER 4. ANALYTICAL AND FINITE ELEMENT MODELING OF AN END MILL

A paper submitted to International Journal of Machine Tool and Manufacture

Parag Gupta[1] and Jerry Lee Hall[1]

Abstract

In this paper, an analytical equation has been developed to determine the deflection of an end mill under a cutting force. The equation is also verified by modeling the complete geometry of a four flute end mill cutter on a computer and analyzing by using the finite element analysis module of I-DEAS software. The deflection obtained from the finite element model were exactly the same as those predicted by the analytical equation.

Introduction

The dimensional accuracy of machined parts has improved with the implementation of positional feedback control systems in machining. One of the most common

[1]Department of Mechanical Engineering, Iowa State University, Ames, Iowa 50011, USA

machining processes in industry is the end milling process. However, it has become increasingly difficult to obtain a high degree of accuracy in end milling due to the low stiffness of the tool. The demand for accuracy improvement and machining cost reduction in machining center operations has increased considerably in recent years. Due to the complexity of end mill geometry, the analysis of end mill deflection has presented a seemingly insoluble problem.

Previous researchers [1-4] have obtained approximate results by assuming the cutter to be a cylinder. Matsurba et al[5,6] went a step further and assumed the helical part of the end mill to consist of a number of equivalent straight members. However, such approximations and assumptions introduce unknown errors in estimating the stiffness of the cutter.

Analytical Model

An analytical derivation of the deflection of an end mill due to a single concentrated force P is performed here. The end mill is similar to a cantilever beam with varying cross-section. The tool has a shank length L_s, flute length L_f, total length L and diameter d. The tool shank cross-section has a moment of inertia I_1 whereas I_2 is the moment of inertia of the flute section as can be seen in the Figure 4.1(a).

The y-z coordinate system shown is introduced where the z axis coincides with the original unbent position of the end mill. The deflected profile of the beam can be seen in Figure 4.1(b). The reaction force exerted by the spindle and is equivalent to a vertical force P and a moment PL. Initially considering the tool shank only, the moment M at a distance z_1 from the tool end gripped in the spindle is given by

$$M = -PL + Pz_1 \tag{4.1}$$

The differential equation of the bent beam is

$$EI_1 \frac{d^2y_1}{dz_1^2} = M \tag{4.2}$$

From equations 1 and 2 we have

$$EI_1 \frac{d^2y_1}{dz_1^2} = -PL + Pz_1 \tag{4.3}$$

The equation is readily integrated once to yield

$$EI_1 \frac{dy_1}{dz_1} = -PLz_1 + \frac{Pz_1^2}{2} + C_1 \tag{4.4}$$

which represents the equation of the slope, where C_1 denotes a constant of integration. This constant may be evaluated by use of the condition that the slope dy/dz of the end mill at the spindle is zero because it is rigidly clamped there. Thus $(dy/dz)_{z_1=0}$ = 0. If the condition $z_1 = 0$ is substituted we obtain $0 = 0 + 0 + C_1$ or $C_1 = 0$. Next integration of equation 4.4 yields

$$EI_1 y_1 = \frac{-PLz_1^2}{2} + \frac{Pz_1^3}{6} + C_2 \tag{4.5}$$

where C_2 is a second constant of integration. Again, the condition at the spindle will determine this constant. There, at z = 0, the deflection y_1 is zero because the tool is rigidly clamped to the spindle which is assumed to be rigid. Substituting $(y_1)_{z_1=0}$ = 0 in equation 4.5 , we find $0 = 0 + 0 + C_2$ or $C_2 = 0$. An equation similar to equation 4.3 can be written for the flute length of the tool which is

$$EI_2 \frac{d^2y_2}{dz_2^2} = -PL_f + Pz_2 \tag{4.6}$$

Integrating it once, we have

$$EI_2\frac{dy_2}{dz_2} = -PL_f z_2 + \frac{P{z_2}^2}{2} + C_3 \tag{4.7}$$

It is reasonable to assume

$$(\frac{dy_2}{dz_2})_{z_2=0} = (\frac{dy_1}{dz_1})_{z_1=L_s} \tag{4.8}$$

because the deflection profile of the end mill will be a smooth curve. From equations 4.4, 4.7 and 4.8 we have

$$EI_2(\frac{-PLL_s}{EI_1} + \frac{P{L_s}^2}{2EI_1}) = -PL_f z_2 + \frac{P{z_2}^2}{2} + C3 \tag{4.9}$$

Substituting $z_2 = 0$ we get

$$C_3 = \frac{-PI_2L_s}{I_1}(L - Ls/2) \tag{4.10}$$

Now substituting the value of C_3 in equation 4.7 and integrating it once we get

$$EI_2y_2 = \frac{-Pl_f{z_2}^2}{2} + \frac{P{z_2}^3}{6} - \frac{PI_2L_sz_2}{I_1}(L - Ls/2) + C_4 \tag{4.11}$$

At $z_2 = 0$, $y_2 = y_1$. Substituting $z_2 = 0$ and $y_2 = y_1$ in the above equation we get $C_4 = EI_2y_1$. Substituting the value of C_4 along with value of y_1 at $X_1 = L_s$ from equation 4.5 in equation 4.11 we have

$$EI_2y_2 = -\frac{P{L_f}^3}{2EI_2} + \frac{P{L_f}^3}{6EI_2} - \frac{PL_sL_f}{EI_1}(L - L_s/2) - \frac{PL{L_s}^2}{2EI_1} + \frac{P{L_s}^3}{6EI_1} \tag{4.12}$$

After simplification the equation becomes

$$y_2 = -\frac{P}{3E}(\frac{{L_f}^3}{I_2} + \frac{{L_s}^3}{I_1} + \frac{3L_sL_fL}{I_1}) \tag{4.13}$$

In the above equation L = L_s + L_f and if $I_1 = I_2 =$ I then the equation converges to the well known deflection equation of a cantilever beam [8] which is

$$y = -\frac{PL^3}{3EI} \tag{4.14}$$

In equation 4.13, $I_1 = \pi d^4/64$ where 'd' is the diameter of the end mill. I_2 is the moment of inertia of the helical section. The moment of inertia of the helical section depends on the shape of the cross-section of the helical section. The shapes of cross-sections of two flute, three flute and four flute half inch diameter end mill are shown in Figure 4.2, 4.3 and 4.4[9]. The moments of inertia for these cross-sections were found to be 1.5125e-03 $inch^4$, 1.539e-03 $inch^4$ and 1.760e-03 $inch^4$ using IDEAS[10] software. It is not necessary that the moment of inertia of the cross-section of a four flute end mill be greater than that of a two flute or three flute cutter because the shape of the cross-section is the determining factor. For example, a cross-section of another four flute half inch end mill is shown in Figure 4.5 and it has a moment of inertia of 1.330e-03 $inch^4$ which is less than moment of inertia of the other three. This latter is the cross-section of the end mill for which a finite element model was developed. The force P applied on the cutter will has an x component P_x, a y component P_y and a z component P_z. The deformation caused by the x and y component can be computed by substituting the resultant of P_x and P_y in equation in equation 4.13 instead of P. So equation 4.13 can be rewritten as

$$y_2 = -\frac{\sqrt{P_x{}^2 + P_y{}^2}}{3E}\left(\frac{L_f{}^3}{I_2} + \frac{L_s{}^3}{I_1} + \frac{3L_sL_fL}{I_1}\right) \tag{4.15}$$

The deformation z caused by the P_z component can be computed by using the equation below

$$z = \frac{P_zL_s}{A_sE} + \frac{P_zL_f}{A_fE} \tag{4.16}$$

where A_s is the cross-sectional area of the tool shank and A_f is the cross-sectional area of the flute section of the tool, ($I_1 = \pi d^4/64$). The total deformation D=$(y_2{}^2 + z^2)^{1/2}$, which can be rewritten as

$$D = \sqrt{(\frac{\sqrt{P_x{}^2 + P_y{}^2}}{3E}(\frac{L_f{}^3}{I_2} + \frac{64L_s{}^3}{\pi d^4} + \frac{192L_sL_fL}{\pi d^4}))^2 + (\frac{4P_zL_s}{\pi d^2E} + \frac{P_zL_f}{A_fE})^2} \qquad (4.17)$$

Computer Model of an End Mill

A cross-section of a helical portion of a half inch diameter four-flute end mill was obtained from the end mill catalog[7]. After suitable magnification this was drawn in the construction geometry module in I-DEAS as shown in Figure 4.5. The cross-section was reproduced 20 times at equal intervals along the 1.25 inch axial portion of the cutter. However, each cross-section was rotated by a predetermined angle before being reproduced to incorporate the helical nature of the flutes. A skin was developed over these cross sections for surface modeling of the helical section of the tool. The 2 inch cylindrical section of the tool shank was also created and joined to the helical section. The surface model is shown in Figure 4.6. Finally the surface model was converted into a solid model. The shaded image of the solid model of the tool is shown in Figure.4.7. Once the solid model was made, an automatic mesh generation was performed in the Finite Element Analysis module of I-DEAS software. 4200 parabolic tetrahedron elements were used for meshing the solid model. Figures 4.8 and 4.9 show the surface elements of the model. The distortion in the elements was removed by using the 'tetra fixes' command. The nodes on the top of the cylindrical section of the tool in a plane parallel to XY were restrained in the X,Y and Z directions. A nodal force was applied to the tip of the flute. The model was

solved for four different loads, namely (-25lb, -25lb,-25lb), (-50,-50lb,-50lb), (-75lb, -75lb, -75lb) and (-100lb, -100lb, -100lb). The maximum displacement in each case was determined. The milling cutter can be seen in the deformed condition under a (-100lb, -100lb, -100lb) load in Figure 4.10. The dashed line indicates the deformed condition. Figure 4.11 shows the Von mises stress distribution in the end mill under the load.

The displacement was also computed for the same loads applied on one end of a cylinder having a length of 3.25 inch and a 0.5 inch diameter. The other end of the cylinder was restrained. Figure 4.12 shows the geometry of the cylinder. Figure 4.9 shows the cylinder meshed with solid parabolic tetrahedron elements with restraints and also under load. Figure 4.14 shows the deformed cylinder under a (-100lb, -100lb, -100lb) load. Displacements were also computed for a cylindrical component as shown in Figure 4.15. In this component the thicker portion was 2 inch in length and 0.5 inch in diameter. The thinner portion was 1.25inch in length and 0.32inch in diameter which happens to be the diameter of the core of the helical section of the milling cutter. Figure 4.16 shows the meshing of the cylinder component with the solid parabolic tetrahedron elements along with the restraints and the load. Figure 4.17 shows the deformation of the shaft under a (-100lb, -100lb, -100lb) load. The deformations of the cylinder and the cylindrical component were computed in order to estimate the error committed by previous researchers in approximating an end mill by a cylinder or a cylindrical component. The maximum displacement of each model was plotted against the resultant force. Figure 4.18 shows the linear relationship between the deflection and the resultant force. The deflections obtained under various loads are given in Table 4.1.

Table 4.1: Deflection under Cutting Force

Force applied in lb (x lb, y lb, z lb)	**Cylindrical Component(inch)**	**Milling Cutter(inch)**	**Cylinder (inch)**
(-25, -25, -25)	05.551e-03	04.724e-03	04.251e-03
(-50, -50, -50)	11.102e-03	09.488e-03	08.503e-03
(-75, -75, -75)	16.653e-03	14.213e-03	12.755e-03
(-100, -100, -100)	22.244e-03	18.976e-03	16.969e-03

For verification of the analytical equation developed in the previous section the area of the cross-section (A_f) of the flute section profile shown in Figure 4.5 was computed by IDEAS and found to be 0.1242 $inch^2$. This along with other parameters L=3.25, L_s=2, L_f=1.25, d=.5, P_x=-25, P_y=-25, P_z=-25, I_2=1.330e-03 were substituted in equation 4.17 and a deformation D value of 4.724e-03 inch was obtained which is the same as above in the table 4.1. Similarly the equation was also tested for other three set of forces which were(-50,-50,-50), (-75,-75,-75) and (-100,-100,-100) and the deformation values of 9.488e-03inch, 14.213e-03 inch and 18.976e-03 inch were obtained respectively. These values are exactly the same as that obtained by the finite element model.

Conclusions

The deflection of all three computer models varied linearly with applied load. As expected the deflection of the cutter was found to be intermediate in value between the cylinder and cylindrical component. Seven hours were required on a DEC 5000/240MHz computer to solve the finite element model to calculate the deformation of the end mill under a force. However, in the future I-DEAS software or any other software could be used to calculate the moment of inertia and area of the cross-

section of the flute portion of the cutter. This along with other tool parameters could be used in the tool deflection equation to calculate the exact tool deflection without even developing a finite element model. This would save computational time without any loss of accuracy.

References

1) Bablin, T.S., Lee, J.M., Sutherland, J.W., and Kapoor, S.G.."A model for end milled surface topography",Proceedings of 13^{th} North American Manufacturing Research Conference, 1985, pp. 362-368.

2) Devor, R.E., Sutherland, J.W. and Kline, W.A.,"Control of surface error in milling",Proceedings of 11^{th} North American Manufacturing Research Conference. Wisconsin, 1983, pp.356-362.

3) Devor, R.E, Kline, W.A., and Zdeblick, W.J.,"A mechanistic model for the force system in end milling with application to machining airframe structures", Proceedings of 8^{th} North American Manufacturing Research Conference, 1980, pp. 297-303.

4) Sutherland, J.W., and Devor, R.E.,"An improved method for cutting force and surface error prediction in flexible end milling systems", Journal of Engineering for Industry, November 1986, Vol. 108, pp. 269-279.

5) Matsubara, T., Yamamoto, H., and Mizumoto, H.,"Study on accuracy in end mill operations (1^{st} Report)-stiffness of end mill and machining accuracy in side cutting"Bull. Japan Soc. of Prec. Engg., Vol. 21, No. 2, June 1987, pp.95-100.

6) Matsubara, T, Tanaka, H., and Mizumoto, H.,"Study on accuracy in end mill operations (2^{nd} report)-machining accuracy in side cutting tests" Int. J. Japan Soc.

Prec. Engg., Vol.25, No.4 (Dec 1991), pp.291-296.

7) Nachi catalog no.T1004"End mills and milling cutters"

8) S.Timoshenko,"Strength of Materials - Part I- elementary theory and problems"Third edition, Robert E. Krieger Publishing Company, Malabar, Florida.

9) Mohawk cutting tools- A Thesaurus, Form no. THE-7(2/78), Montpelier, Ohio.

10) I-DEAS mechanical CAE/CAD/CAM software, Structural Dynamics Research Corporation, 2000 Eastman Dr., Milford, OH 45150

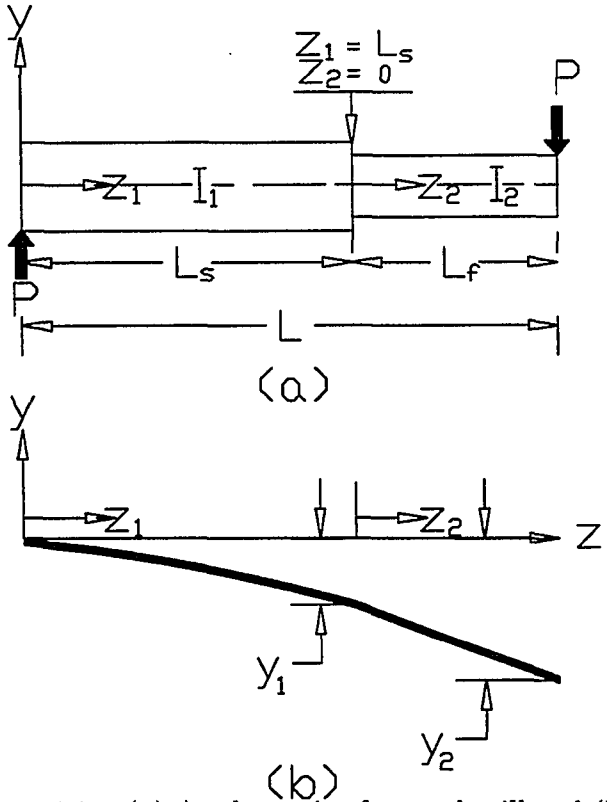

Figure 4.1: (a) A schematic of an end mill and (b) it's deflection profile

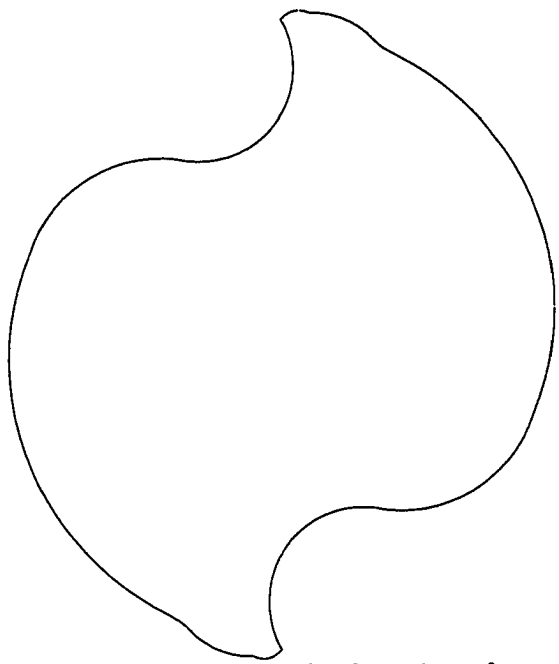

Figure 4.2: Cross-section of the helical section of a two flute end mill

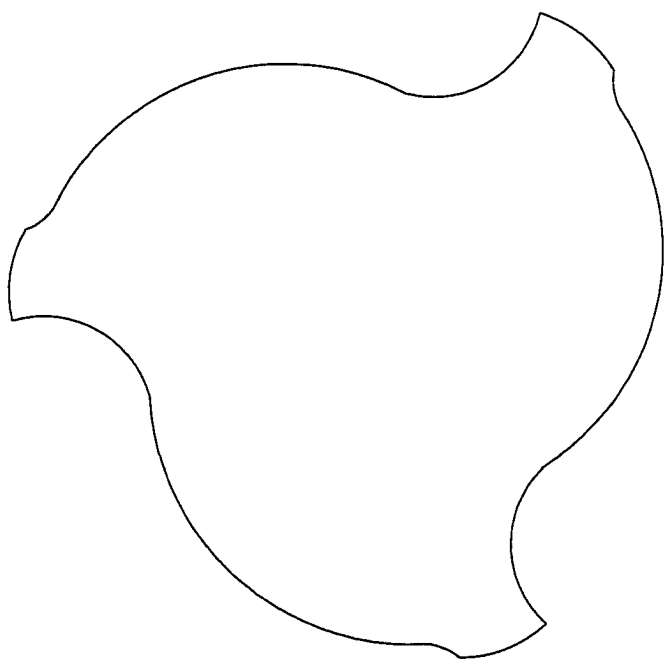

Figure 4.3: Cross-section of the helical section of a three flute end mill

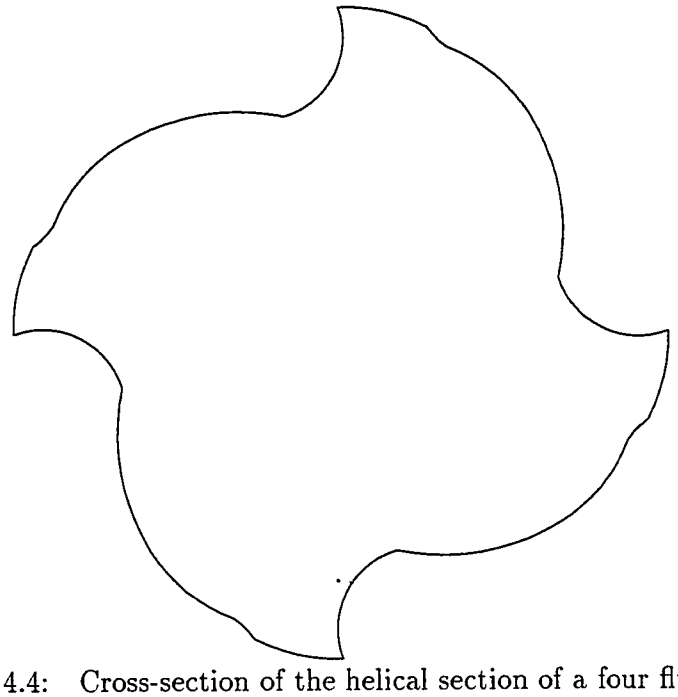

Figure 4.4: Cross-section of the helical section of a four flute end mill

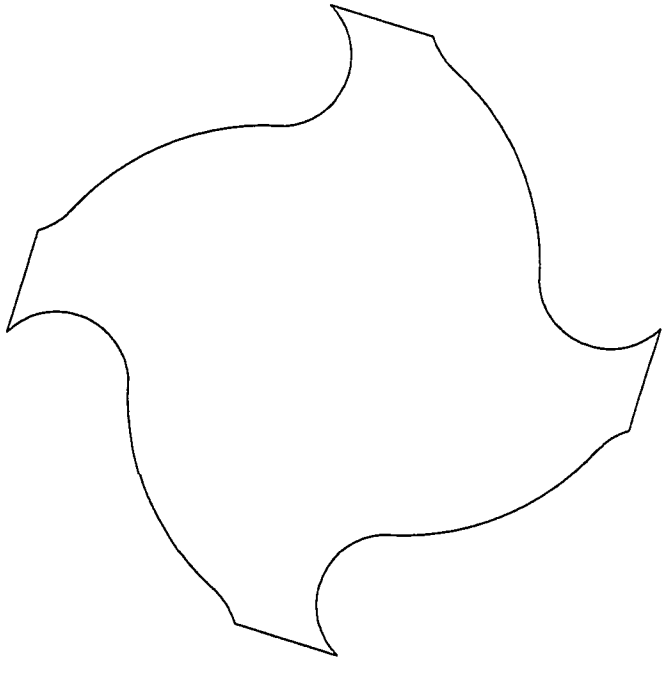

Figure 4.5: Cross-section of another four flute end mill

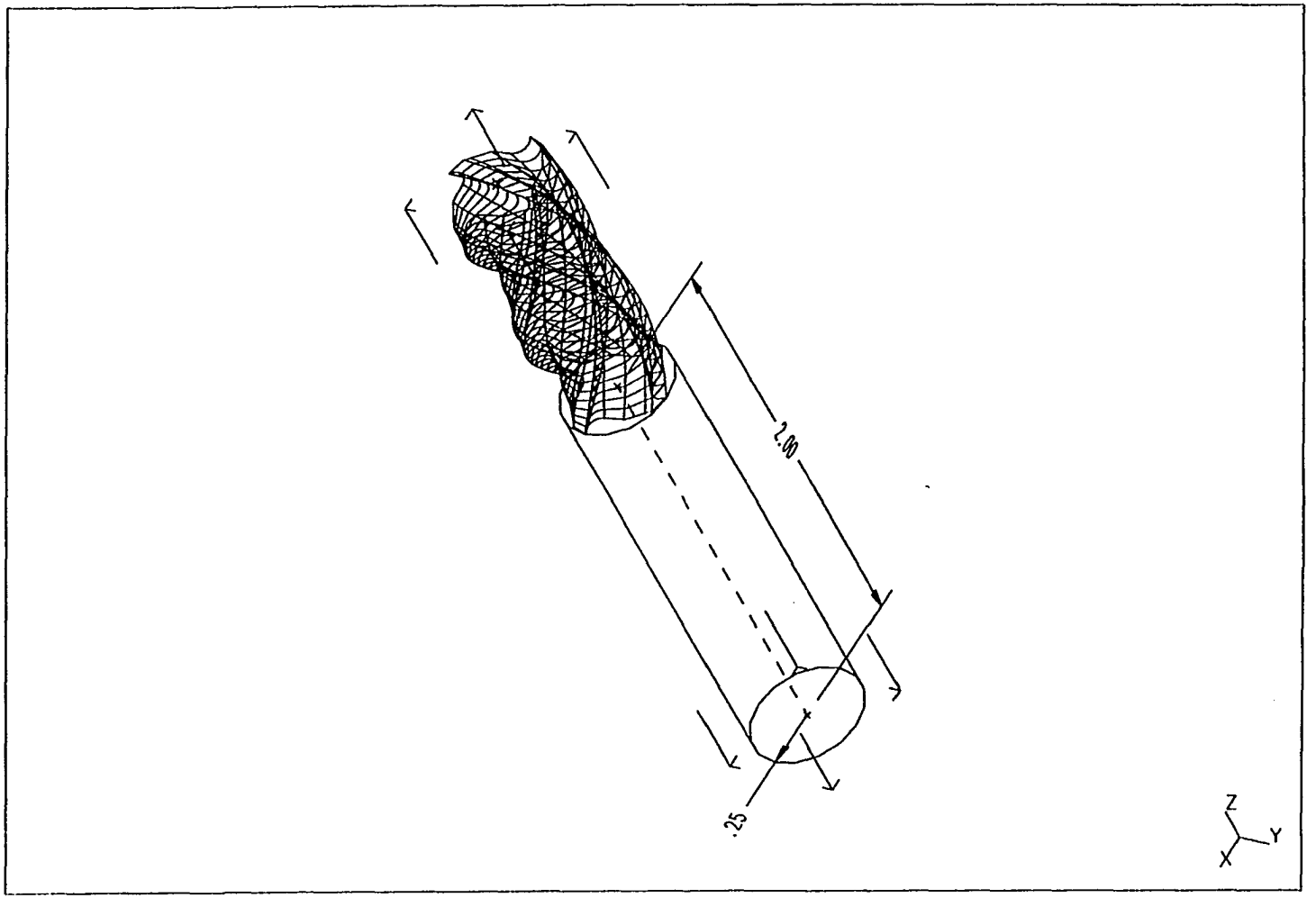

Figure 4.6: Surface model of the end mill cutter

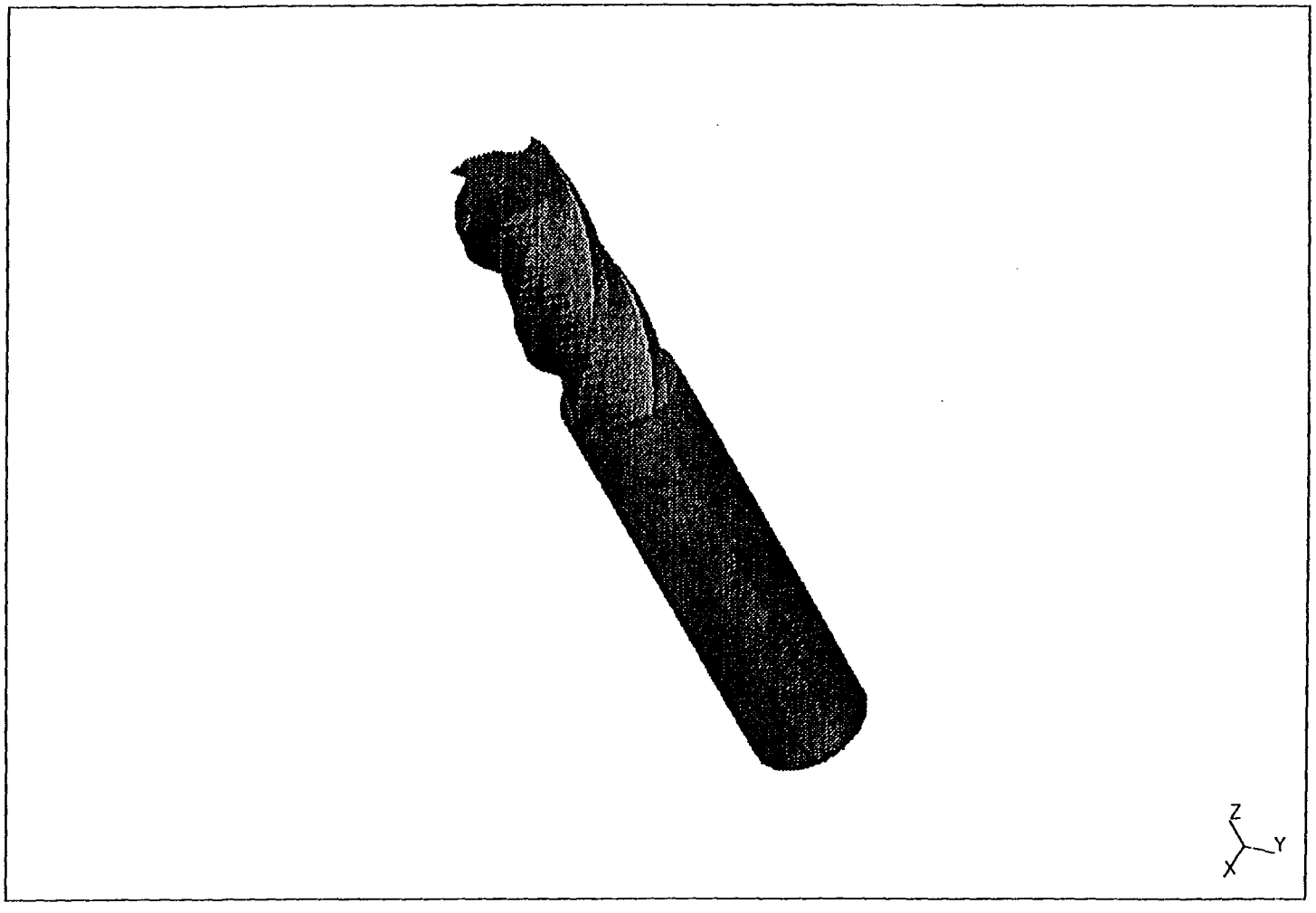

Figure 4.7: Shaded solid model of the end mill cutter

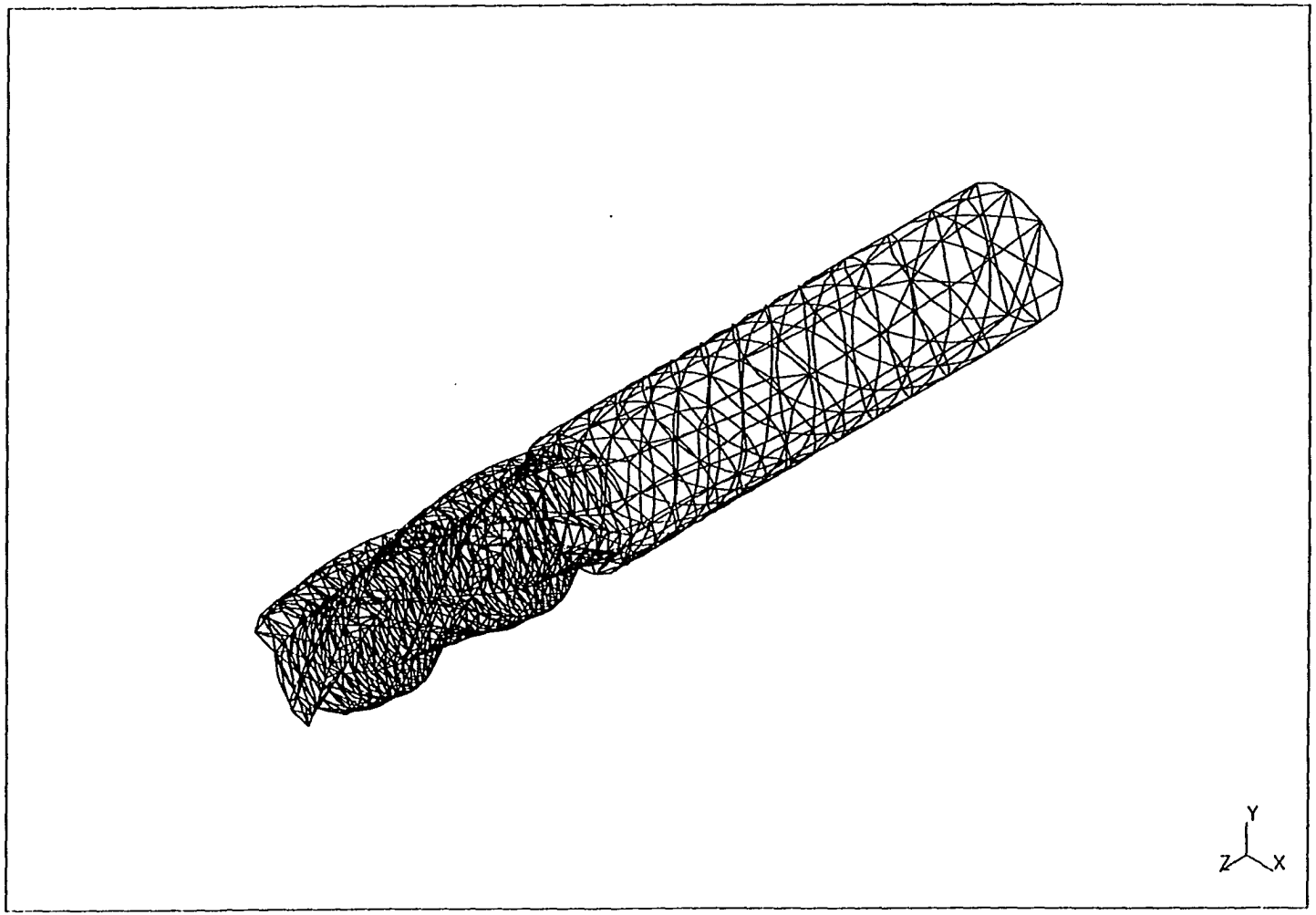

Figure 4.8: Surface elements of the meshed model of the end mill

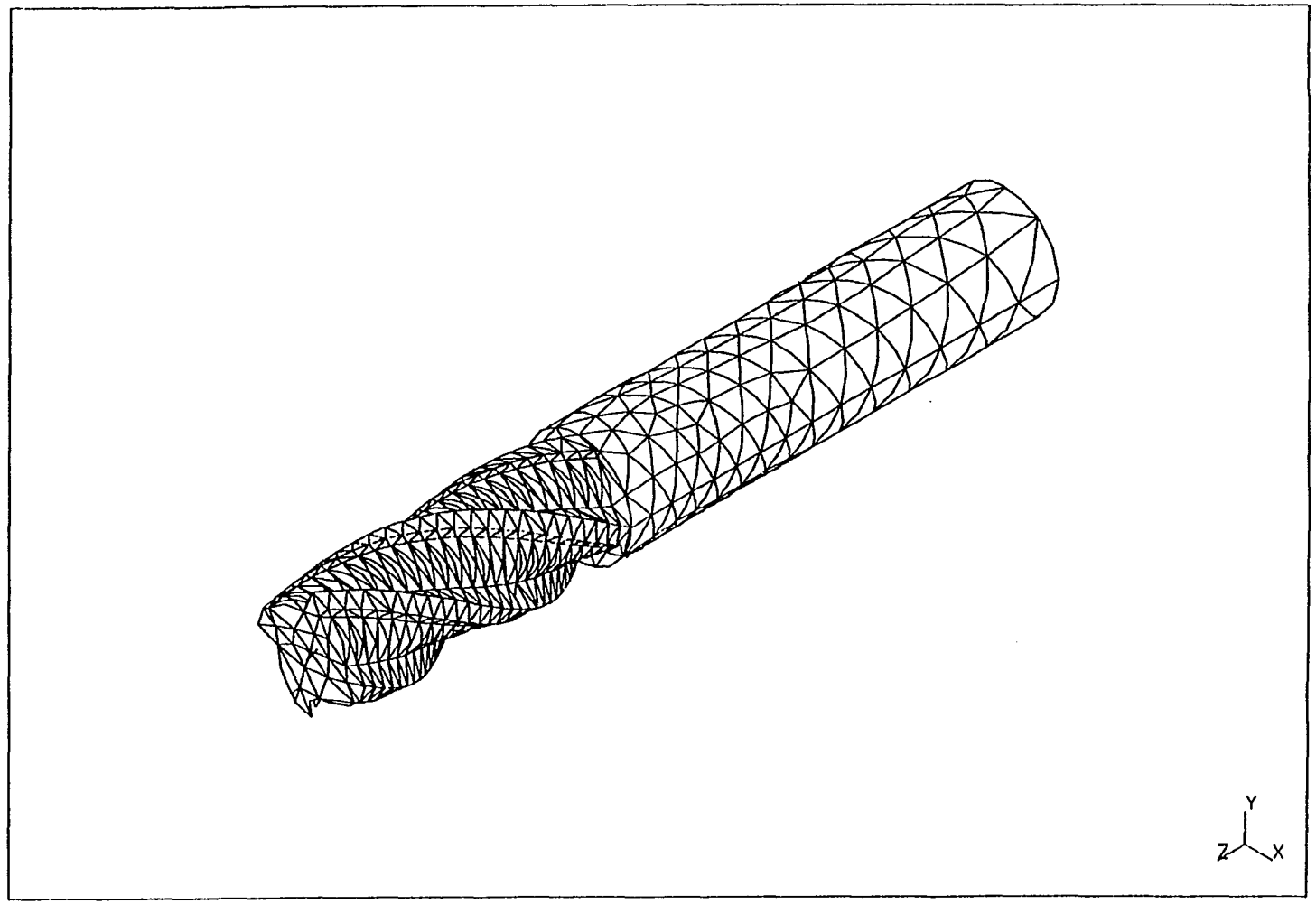

Figure 4.9: Surface elements with hidden lines of the end mill

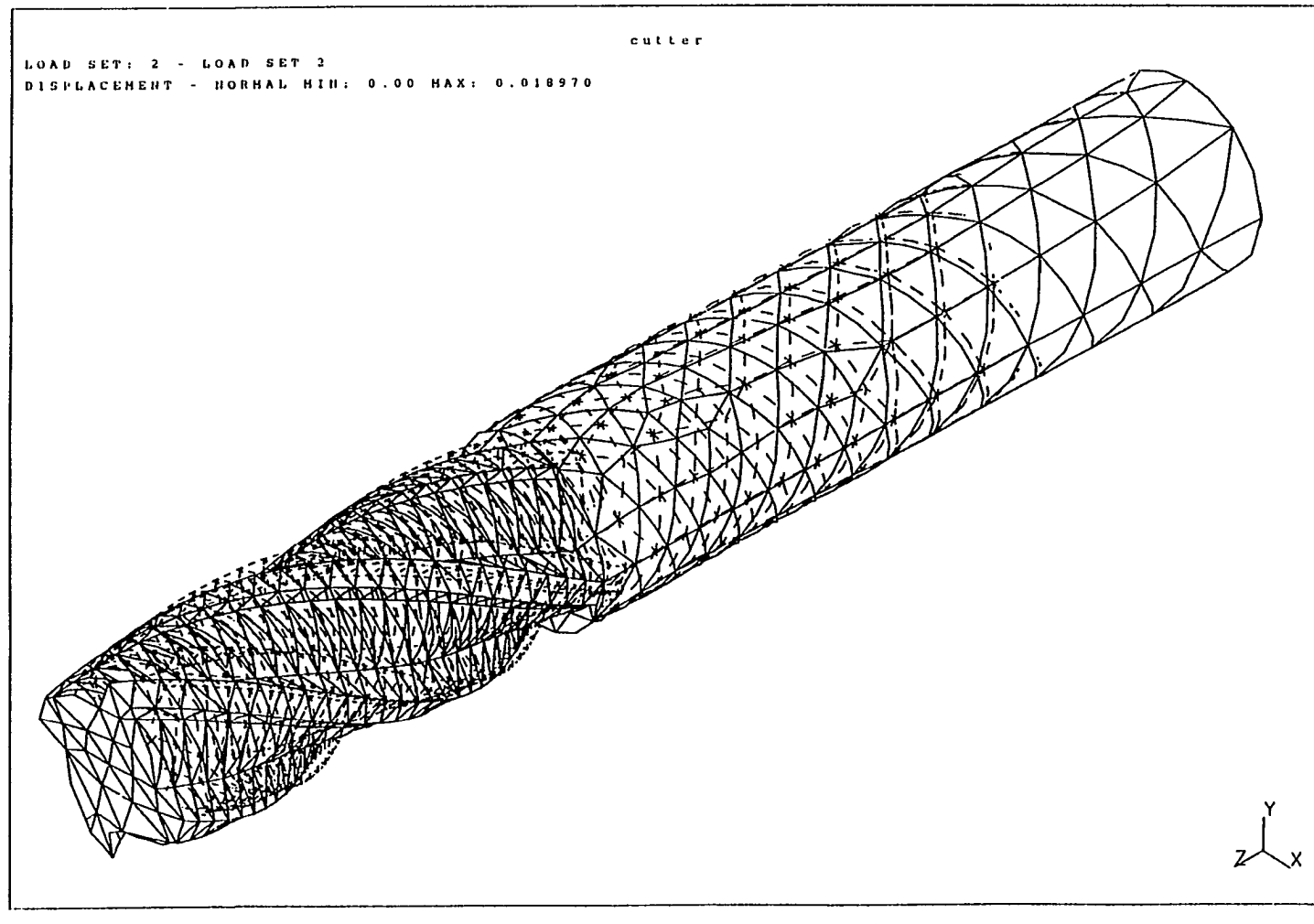

Figure 4.10: Deformed End mill

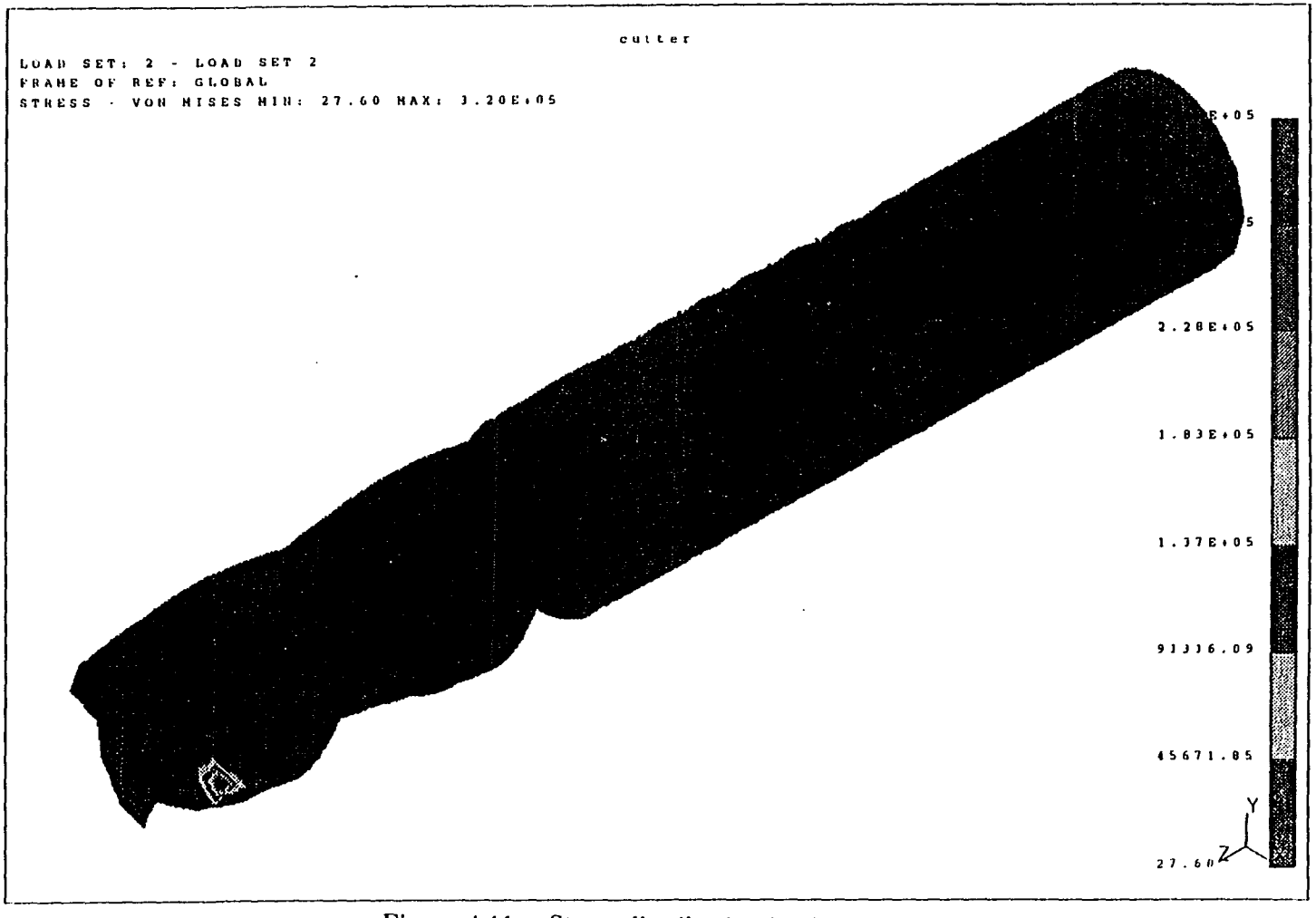

Figure 4.11: Stress distribution in the end mill

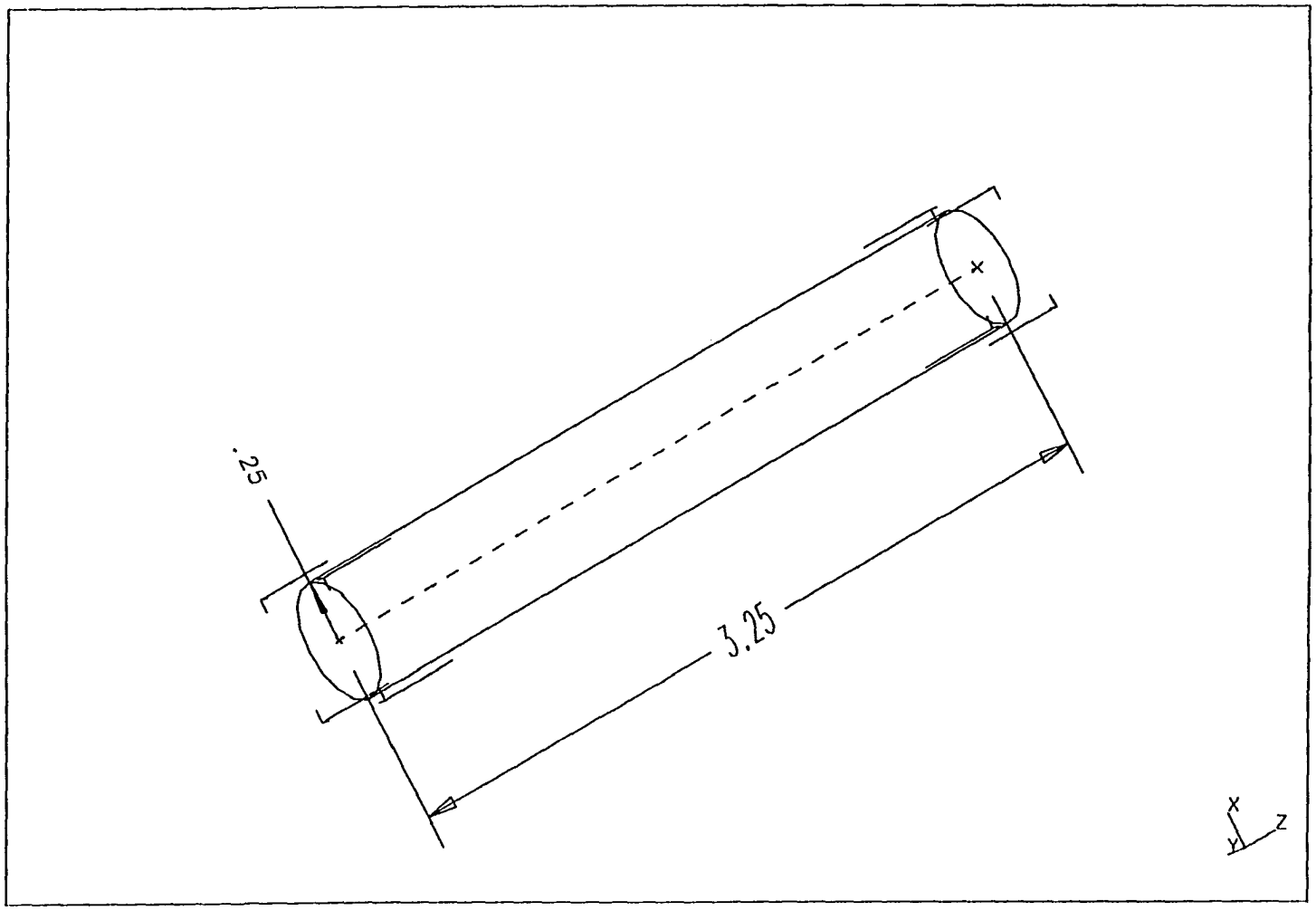

Figure 4.12: Geometry of the cylinder

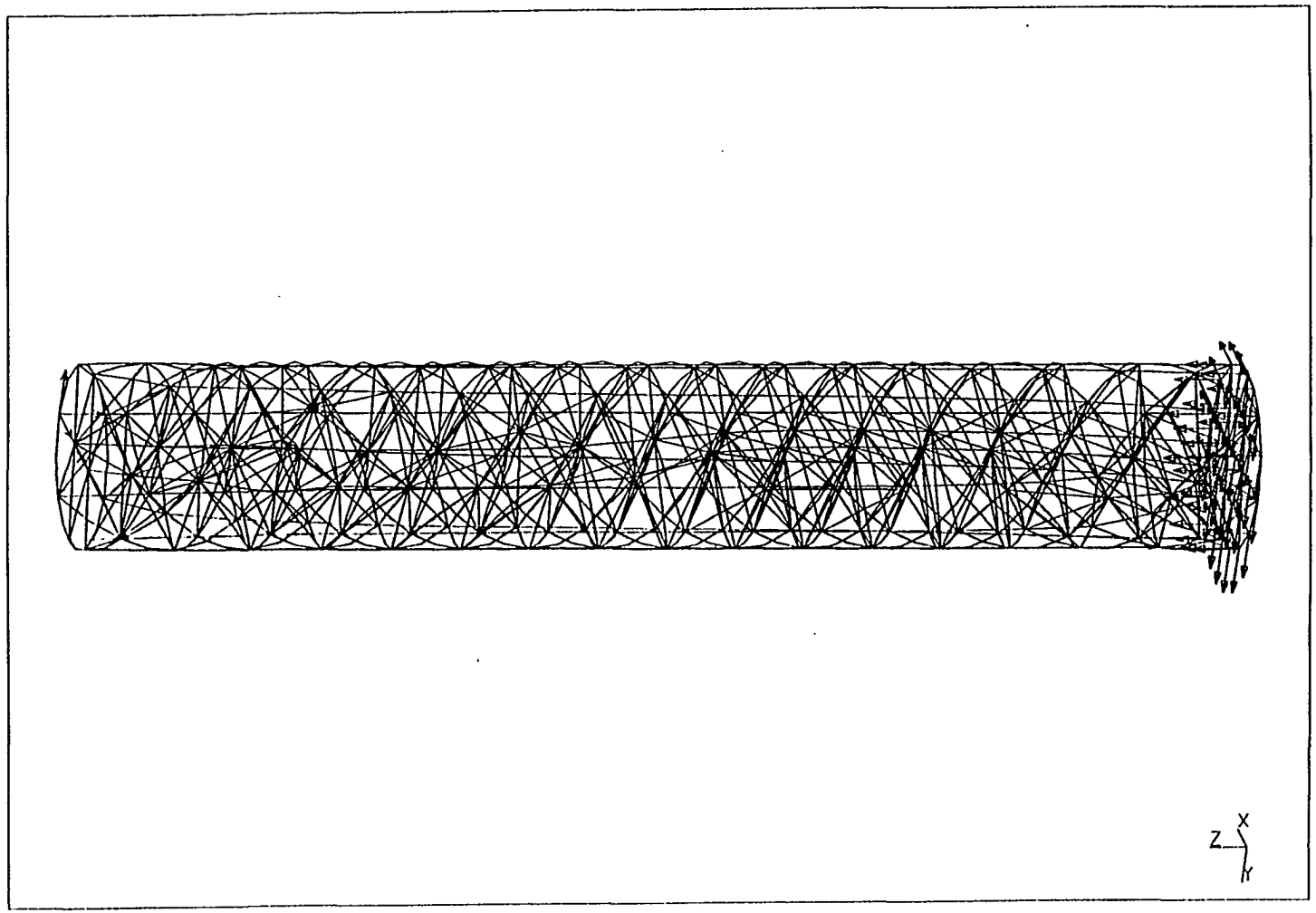

Figure 4.13: Meshed cylinder showing restraints and loads

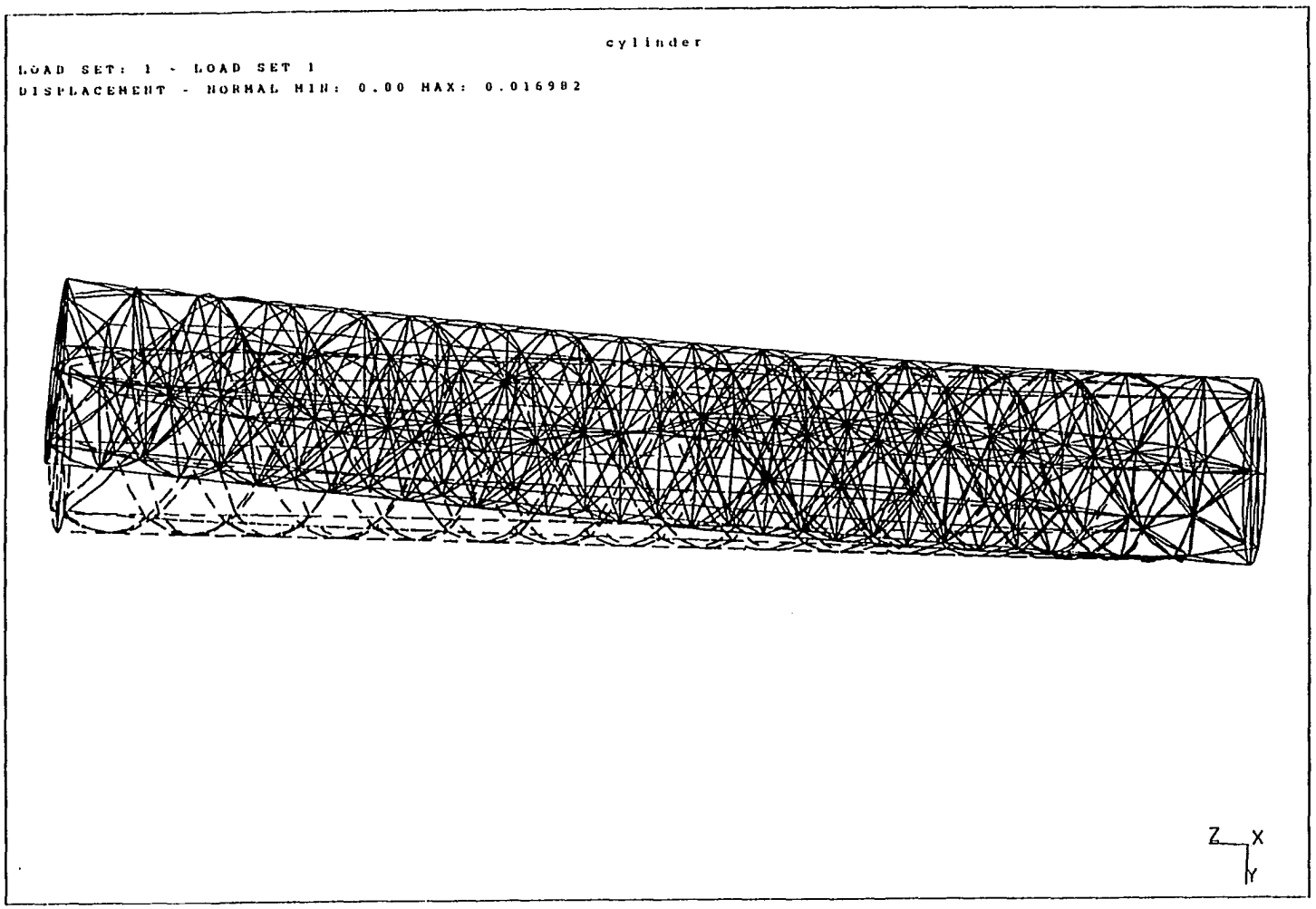

Figure 4.14: Deformed cylinder

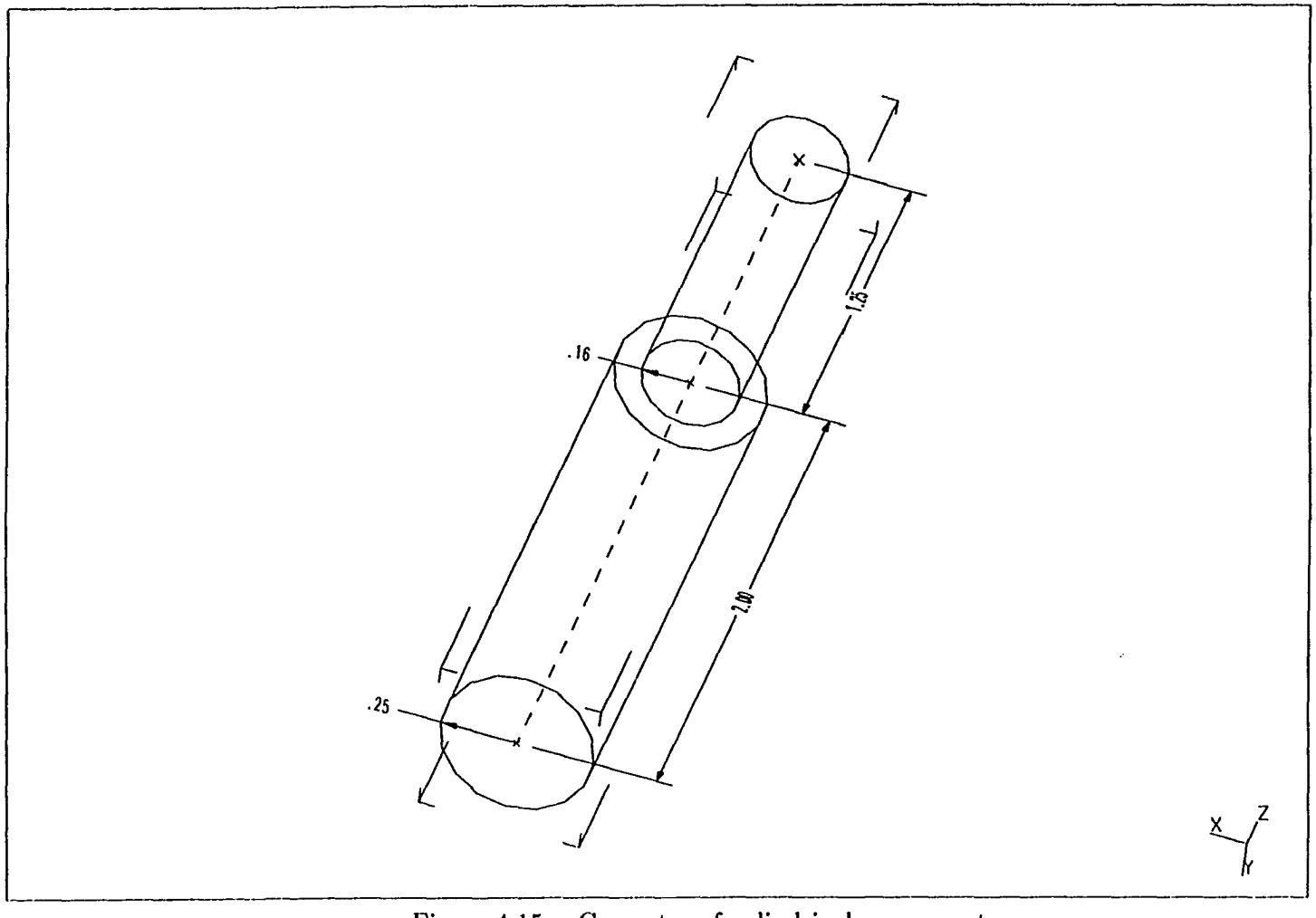

Figure 4.15: Geometry of cylindrical component

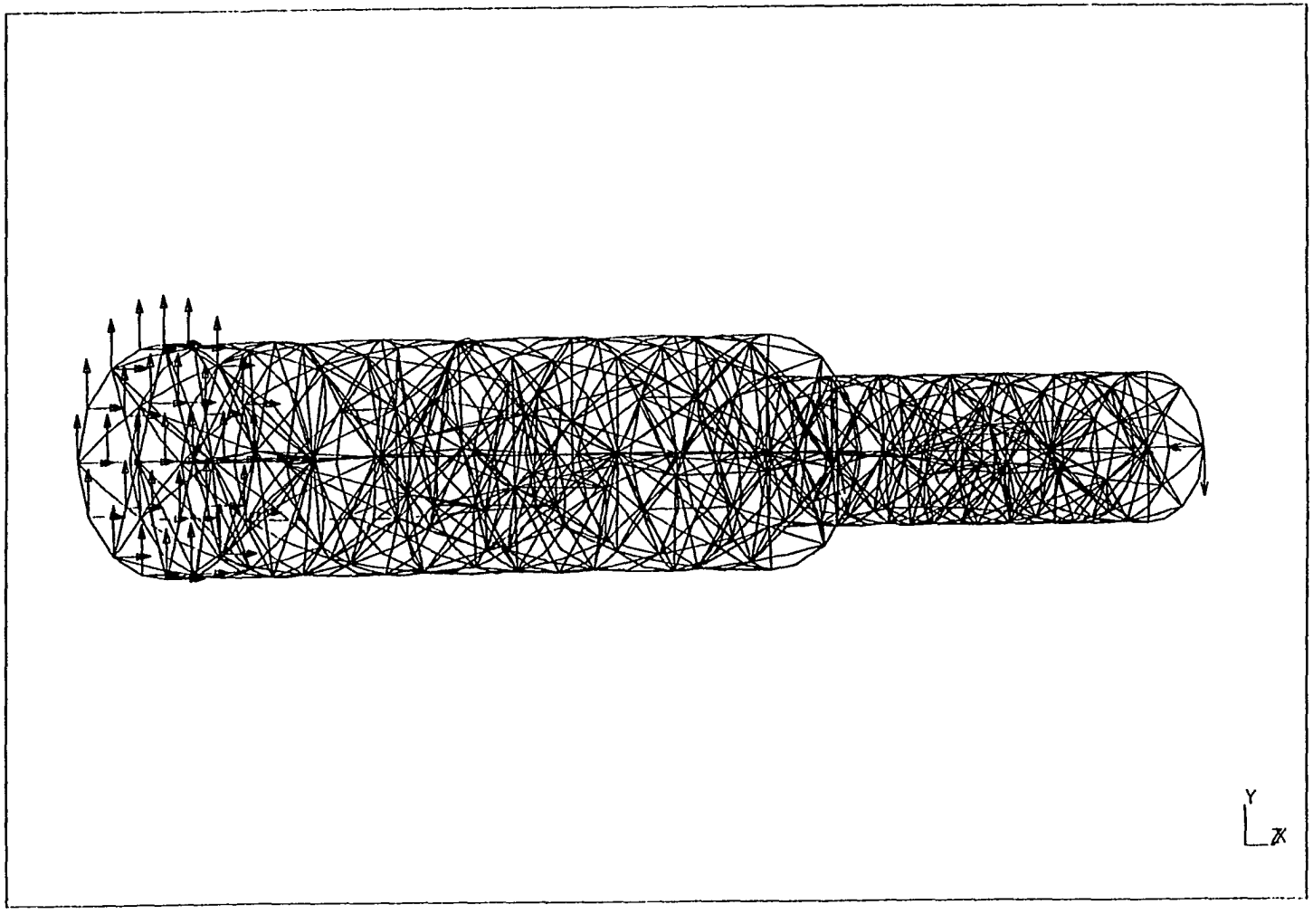

Figure 4.16: Meshed cylindrical component showing restraints and loads

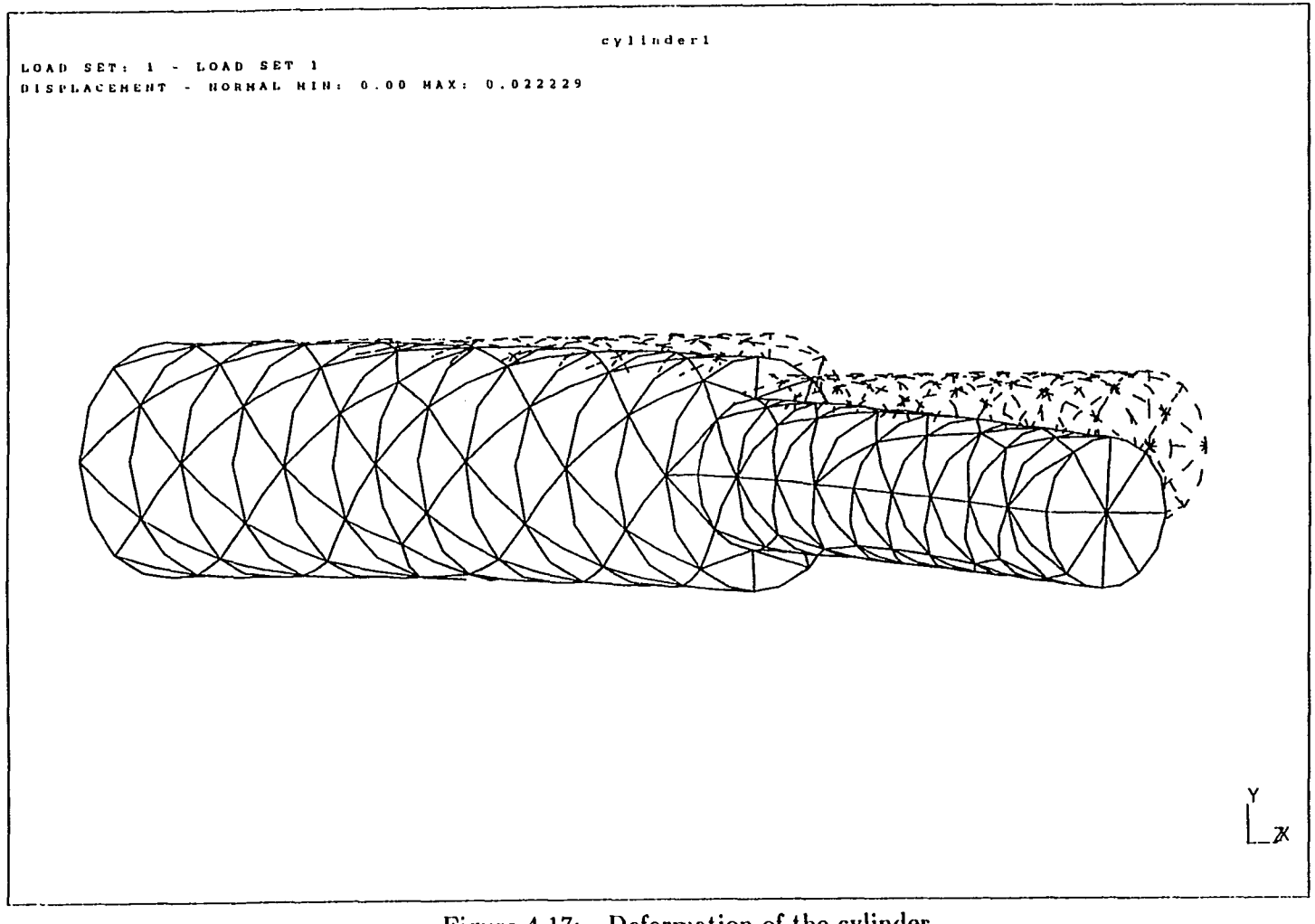

Figure 4.17: Deformation of the cylinder

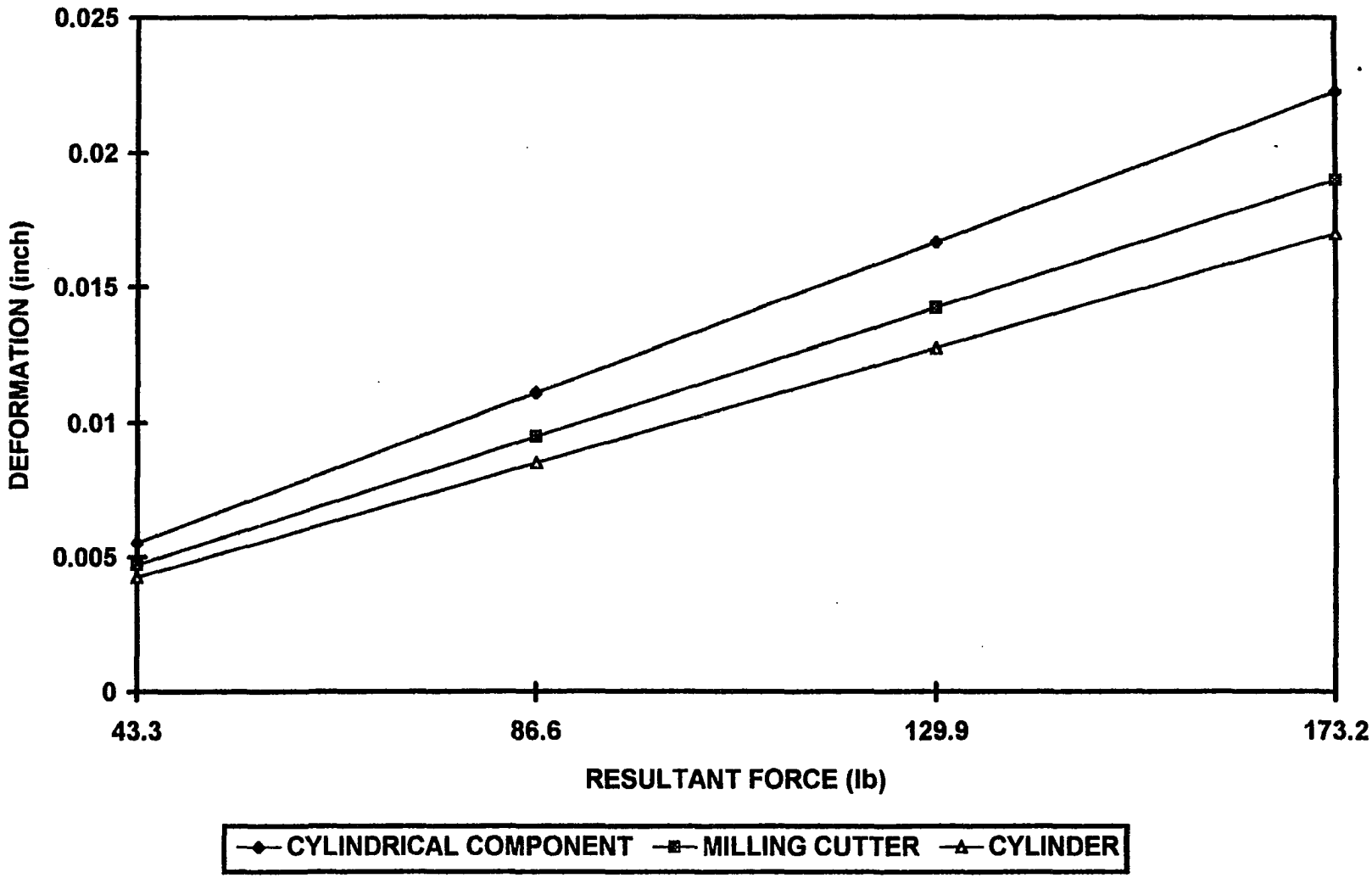

Figure 4.18: Maximum deformation under different loads

CHAPTER 5. RAPID PROTOTYPING IN DIE MANUFACTURING

A paper published in the book"Rapid Prototyping Systems-fast track to product realization", Society of Manufacturing Engineers, pp.3-17, 1994 and Proceedings of Rapid Prototyping Conference held in Dearborn, Michigan, section 16, May, 1993.

Parag Gupta[1] and Jerry Lee Hall[1]

Abstract

There are two conventional methods for manufacturing a die. Both methods require NC programming which requires a large amount of time and skilled people. Even though most parts today are designed by using CAD (Computer Aided Design), it takes a lot of time to generate an NC(Numerical Control) program from the CAD file because one has to specify the tool, the direction of tool path (chaining process), cutting parameters and the area to be machined for each and every surface separately. This becomes a tedious process for a complex die where there are a large number of different surfaces. However, by using rapid prototyping one can easily generate the negative or positive of the part.

Some researchers have considered copper electro-plating or copper spray painting

[1]Department of Mechanical Engineering, Iowa State University, Ames, IA 50011, U.S.A

the positive to develop an electrode for EDM (Electro discharge Machining). Compressing graphite powder in a negative and then curing to develop an electrode has also been suggested by previous researchers. The EDM process finally produces the die. However, these processes for making electrodes are time consuming and a copper spray painted electrodes produce poor surface finish.

This paper proposes three processes to produce dies for parts with too many surfaces in less time and at lower cost than conventional processes . Three processes are proposed rather than a single process because any one of the three can turn out to be more economical than the remaining two, depending on part size, complexity, and objectives of (a) minimizing total time or (b) minimizing manual labor.

Two of the three processes use EDM. A unique method is proposed to produce a copper prototype (copper electrode) that would take a few hours instead of the days required for previous processes and be the least expensive compared to previous methods. An example of production of an under-bracket (part of a Honda motorcycle) by the conventional method is also provided to examine problems faced in the industry in die manufacturing.

The capability to manufacture a wide variety of quality products in a timely and cost-effective fashion in response to market requirements is a key to global competitiveness. Although a large number of products are designed each day, they take a considerable amount of time to enter the market. This is because most parts that go into a product–or the product itself–require injection molding, forging, punching, or other processes requiring dies. The conventional method of making dies with NC programming is time consuming, especially when the design has a large number of complex surfaces. Presently, designers use more and more complex surfaces to im-

prove the aesthetic appearance and achieve compactness of the product. There are three proposed processes that can be used to manufacture dies for less cost and time. All three use the rapid prototyping process and do not require conventional time consuming NC programming, thus eliminating costs for skilled labor involved in NC programming. One process suitable for small dies also eliminates a labor-intensive copy milling process needed in conventional die manufacturing.

Introduction to Conventional Methods

Choosing one of two conventional methods for making a die depends on the complexity and size of the part as well as time availability. Following are explanations of the two methods.

Method 1 Computer aided manufacturing (CAM) software is used to write programs to generate sculptured surfaces. If the part is small and complex, it is difficult to write programs to make a negative (master die) of the part directly. In such a case programs are written to generate a positive, that is the part itself. NC data produced by these programs are then fed into the machining center, which machines a block of wood or wax. These materials are soft compared to metals and, with a high feed rate, can be machined faster. Moreover, any error made in machining can be rectified in wood or wax by using resin or molten wax respectively as a filler and again machining the surface. One can machine a block of copper directly but an error can not be rectified.

Once this wooden or wax part is created, a copy milling machine is used to make a copper prototype. This copper part is then used as a cathode in EDM to make a negative or master die of the given part. The wooden part generated in the beginning

should be slightly smaller than the part because the EDM process generates a cavity which is slightly bigger than the copper part. The degree of tolerance that should be given to make a wooden part of a slightly smaller size depends on the machine used for EDM because tolerance varies from machine to machine but it varies between 1 to 2%. Tables of tolerances are generally provided in operation manuals given along with EDM machines. Figure 5.1 shows a block diagram of the process.

Method 2 If the part is large, part programs to generate the surface of the negative or the master die can be written directly by using any CAM software. The NC data produced by the software is fed into a machining center, which is used to make the master die by machining a piece of wood or wax. Once the master die is made, a copy milling machine is used to prepare a final die. Figure 5.2 shows a schematic of the process.

If the part is small and complex, in the conventional process, most of the time and skilled labor (cost) is required to write or generate the Numerical Control (NC) program. To generate the NC Program from CAD file requires a chaining process or defining the Basic and Driving Curve, specifying tool diameter and cutting parameters for each and every surface. Moreover, the conventional technique (Method 1) apart from the tedious NC program generation also demands a labor intensive copy milling process. All this time and labor can be saved if a process could be developed to produce a copper prototype of the part which can be used as an EDM Electrode. This is also applicable to large parts, however, EDM is a slower process and will take more time as compared to conventional technique (Method 2). Although the EDM process may take more time but unlike copy milling it doesn't require human interaction. The author proposes three processes namely Casting Prototype, Copy

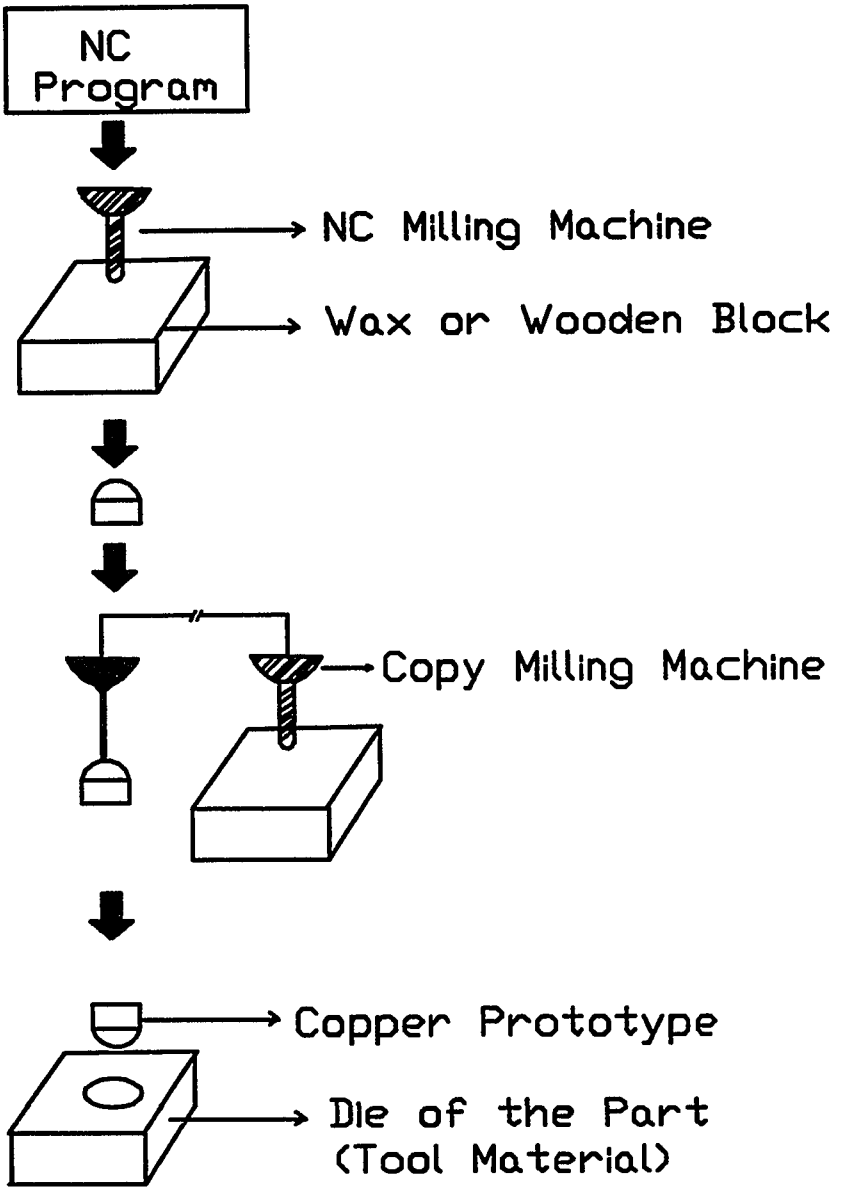

Figure 5.1: Conventional die manufacturing (Method 1)

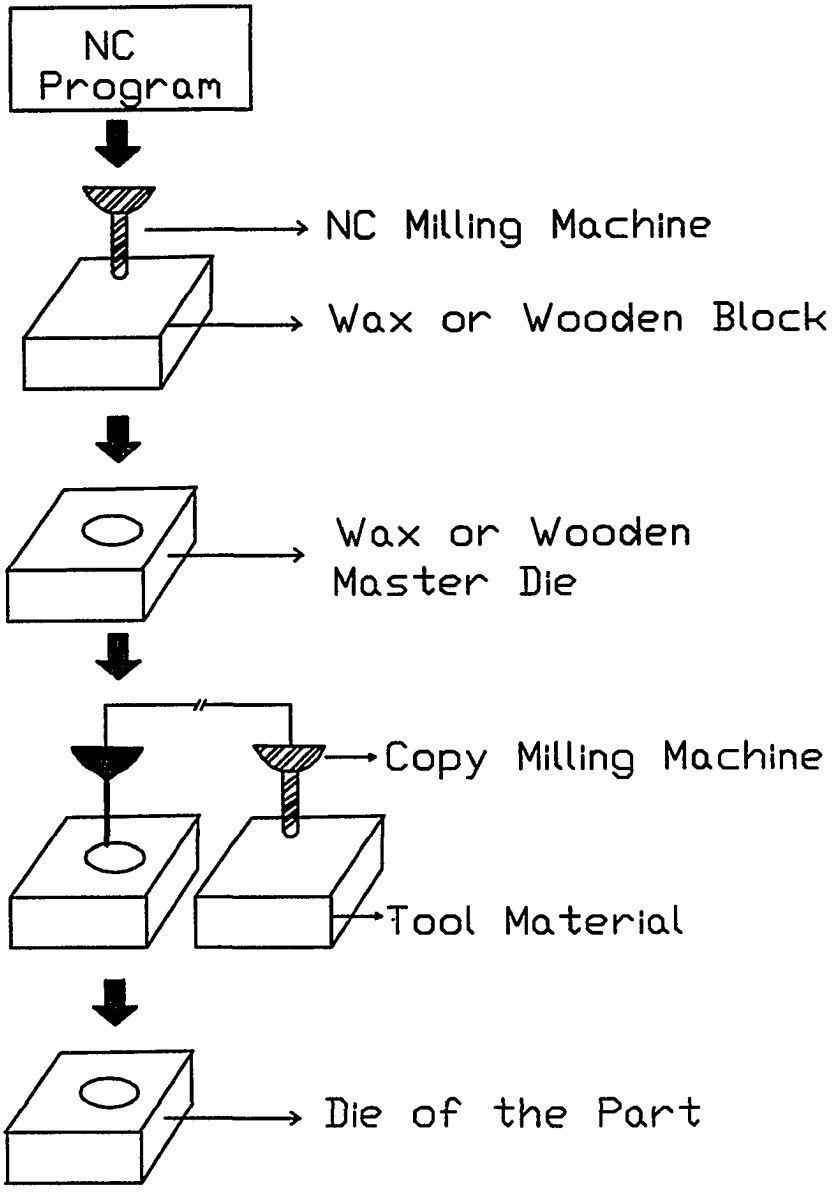

Figure 5.2: Conventional die manufacturing (Method 2)

Prototype and EDM Milling. The Casting Prototype is a process very suitable for small complex parts, however, it can also be used for large parts if the objective is to minimize manual labor. Casting Prototype will be a too time consuming of a process for large parts because the material removal rate of EDM is very low as comared to conventional milling. The other two processes are suitable for large parts. The EDM Milling process would produce a better surface finish than the Copy Prototype process because of the EDM process involved. In EDM process low current and high spark frequency will produce an excellent surface finish. However, the EDM Milling process will take more time. Therefore the process should be chosen dependent on surface finish requirement. All the three processes avoid NC programming and Copper Casting has an additional advantage of avoiding copy milling which requires human interaction.

Preparation before Machining

Before starting, the order of machining different surfaces should be considered to prevent tool breakage and avoid getting a master die of a totally different shape. The tool diameter should also be considered to avoid problems. For example, if a pocket has to be made and the ball end mill chosen is greater than the size of the pocket, then a pocket of a similar profile but greater size would be created. Such mistakes can not be completely avoided, but a machinable resin can be used to solve such problems. The holes or cavities that are made by such mistakes are filled by the resin, which transforms into a hard machinable substance in just three minutes. The short time resin takes to solidify saves production time, and it's excellent machinability results in a high grade surface finish. Air is generally used as a coolant for machining wood

because heat generated is not high and, if liquid coolant is used. the wood particles will not only create problems in the coolant pump but the wood itself would warp.

Practical Application

An engineering drawing of Underbracket KW7A, a part of the Honda 1990 NOVA-S motorcycle was given by Honda company to Thai Engineering Products Co. Ltd., Bangkok, Thailand, to get a master forging die for the part. An engineering drawing with 1.5% positive tolerance was made at Thai Engineering Products Co.Ltd. (Figure 5.3) because the master forging die should be bigger than the part.

The part programs for contoured surfaces were written by using FAPT DIE-II and part programs for remaining surfaces (which were flat) were written by using FAPT MILL software running on FANUC SYSTEM-P MODEL-G. These programs helped produce NC data that plotted all the contoured, as well as the flat surfaces of the upper and lower master forging die (Figures 5.4, 5.5, 5.6, and 5.7). Many errors appeared when all the surfaces were plotted on a single page with the same origin and scale. In particular, any intersection of surfaces at the wrong place clearly indicated that the reference coordinates of the surface were incorrect.

Plotting all the surfaces together gives an idea whether or not the surfaces generated by the part programs are aligned with the other surfaces in the right fashion. Though it is a time consuming process, it is advisable not to skip this step. The NC data generated by FANUC FAPT DIE-II is suitable for Fanuc machines only. Since Okuma MC 4VA was used for machining, the data were edited by FAPT TRACER software running on Fanuc System-P Model-G to make it suitable for the Okuma machine. The NC data was then transferred to Data Store FR-15 of Mori Seiki with

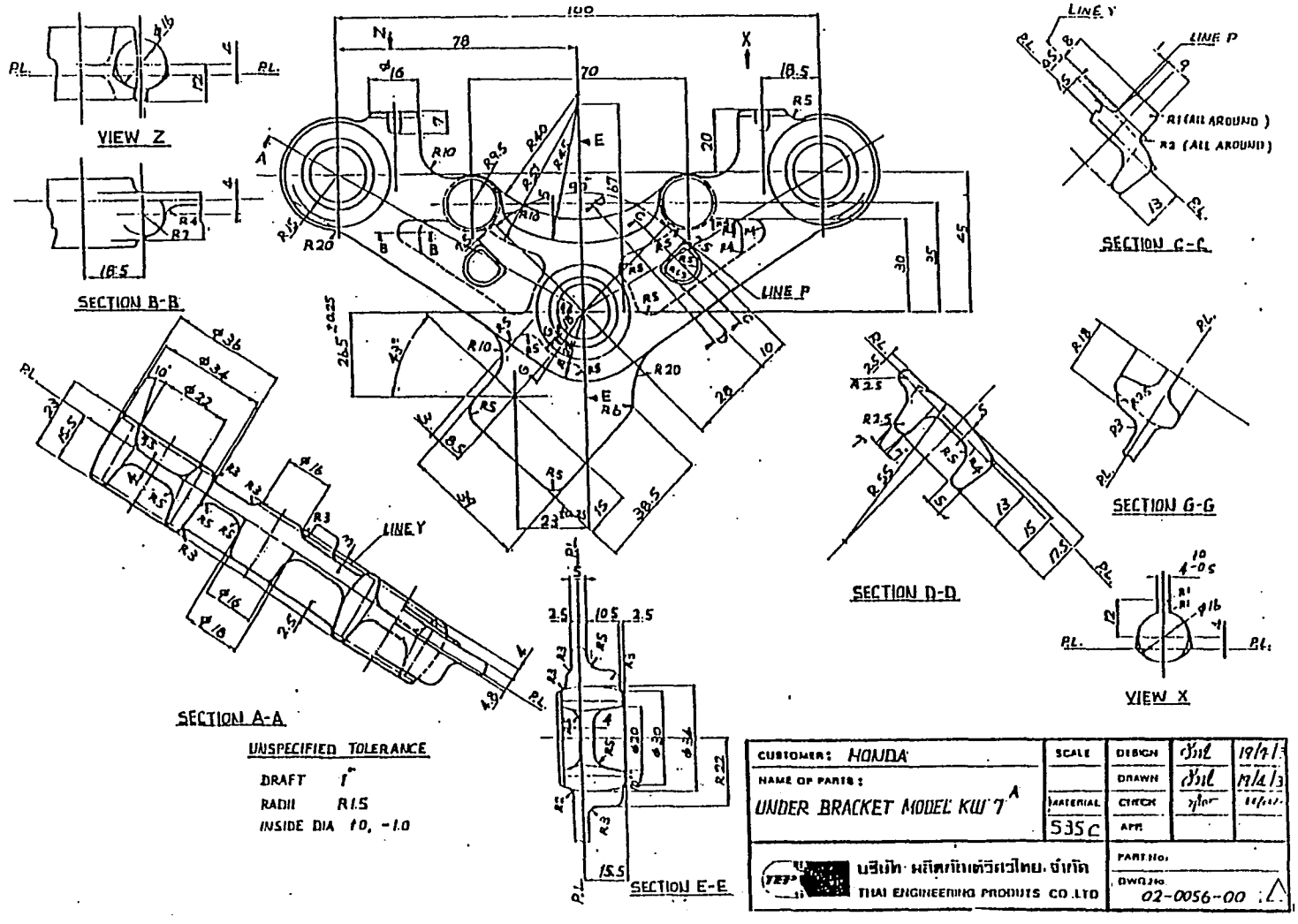

Figure 5.3: Engineering drawing of the underbracket

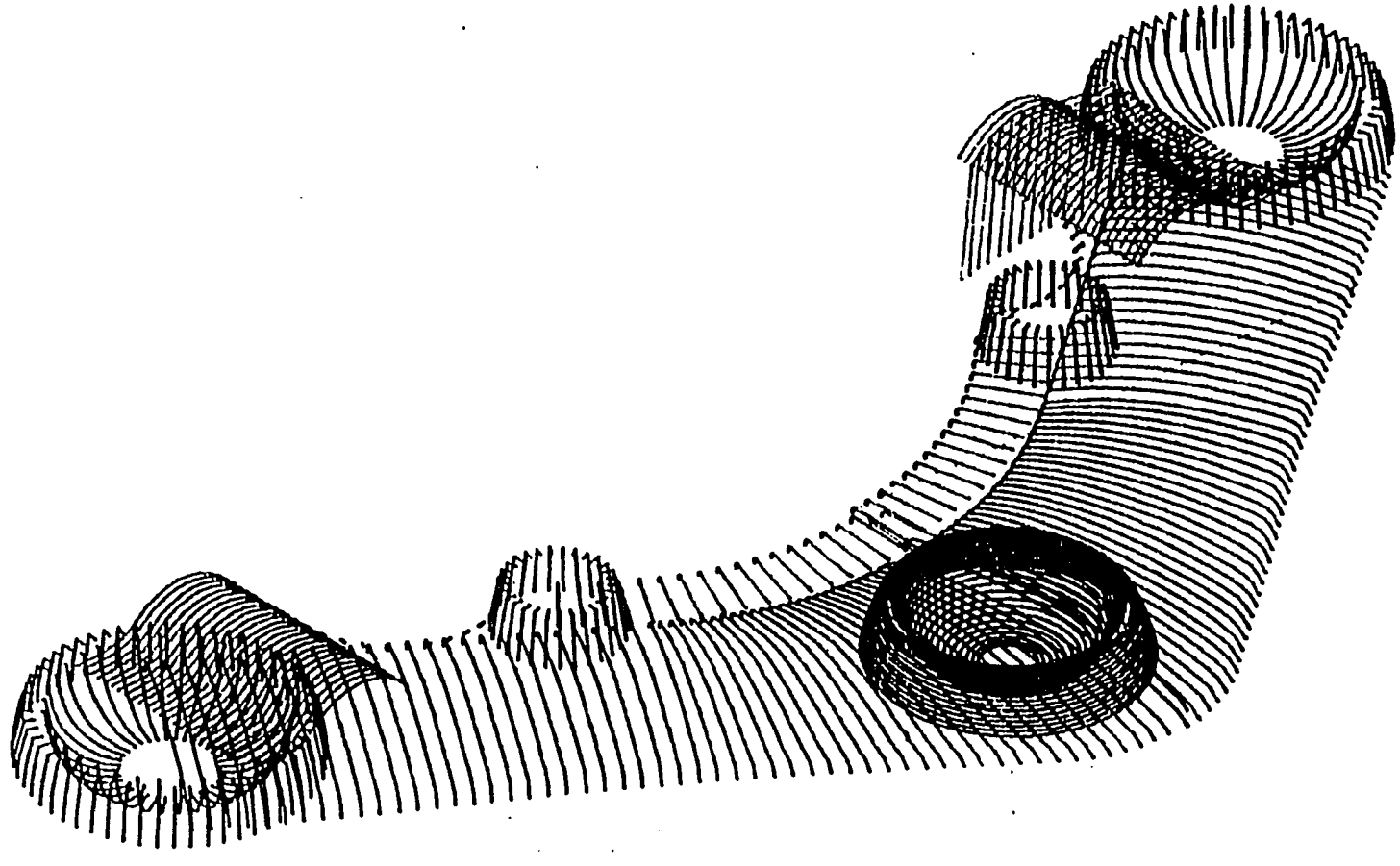

Figure 5.4: Tool path of sculptured surface of upper die

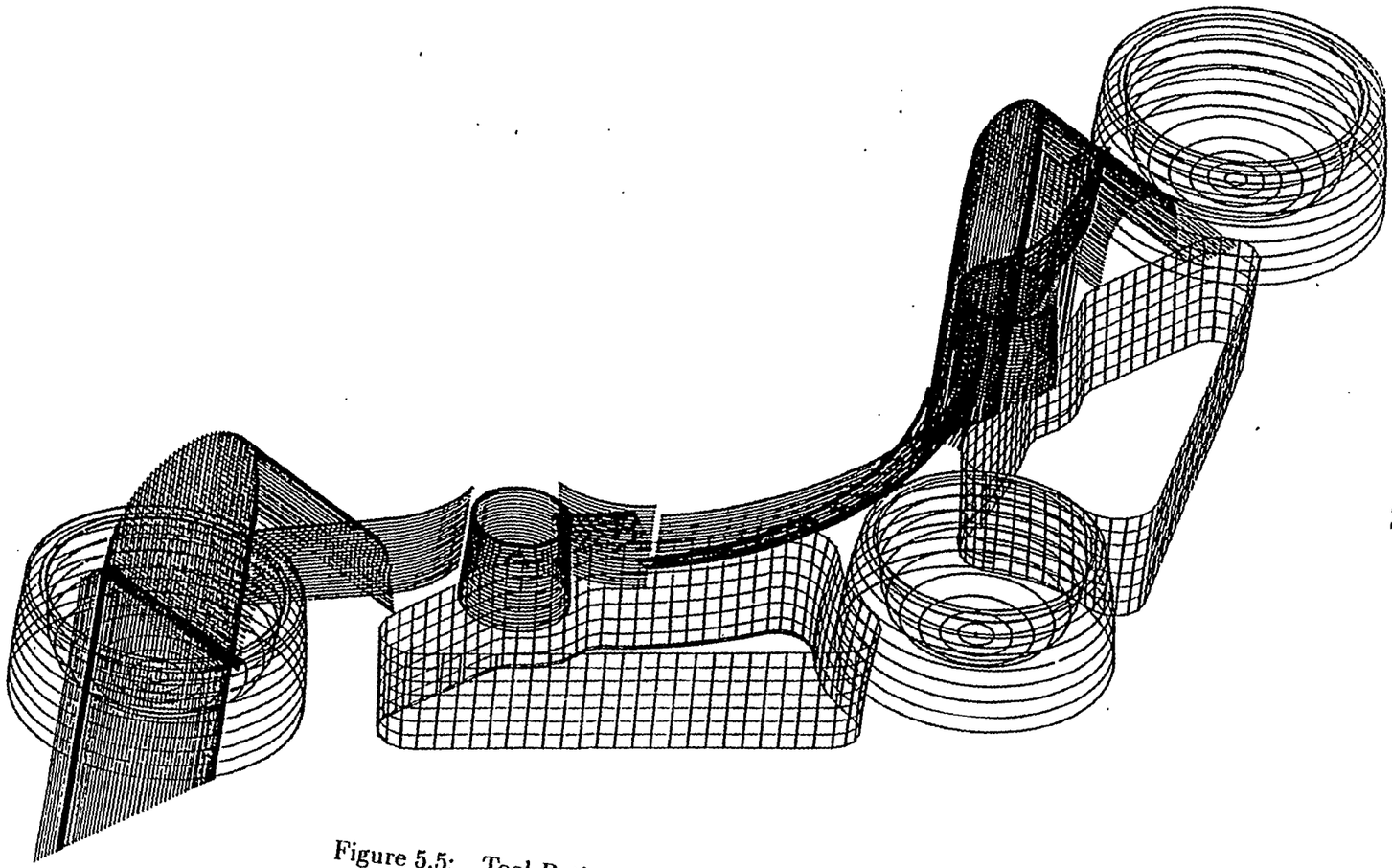

Figure 5.5: Tool Path of Sculptured surface of lower die

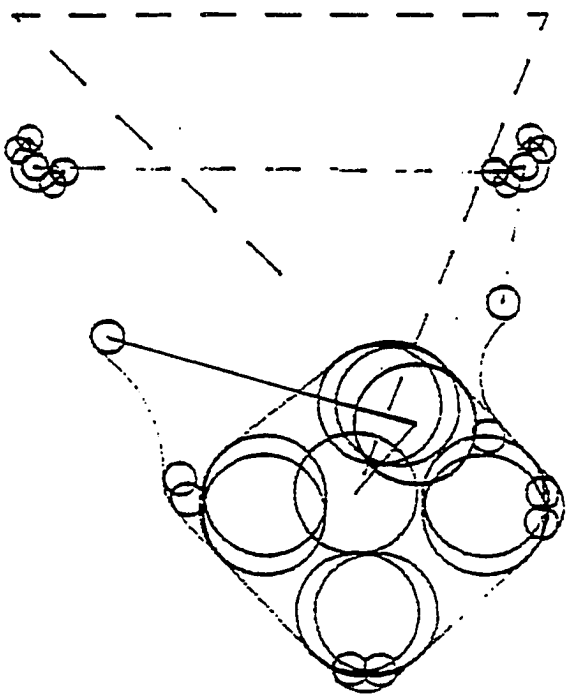

Figure 5.6: Tool path of flat milled surface of upper die

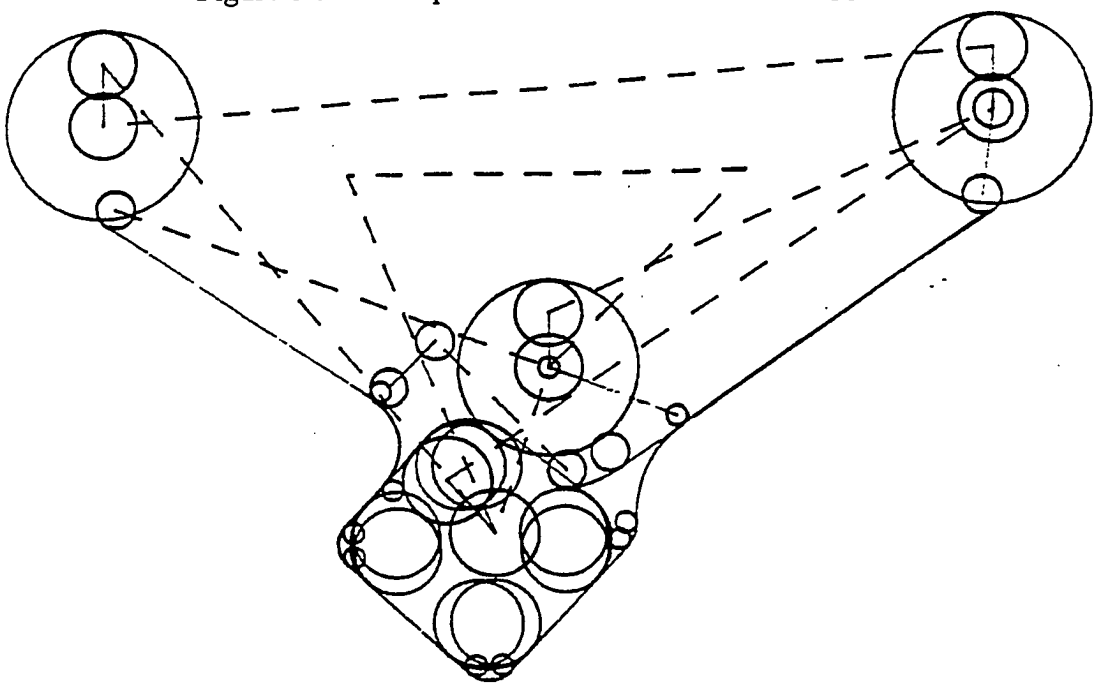

Figure 5.7: Tool Path of flat milled surface of lower die

the help of RS 232 interface. The Data Store FR-15 was used to transfer the data to the Okuma MC-4VA machining center on the shop floor. However a direct RS 232 interfacing between the computer and the machining center is also possible.

The workpiece was mounted on the table and workpiece offset was done by manual Pulse generator. The machining center was used to machine the surfaces in the required order one at a time to produce upper and lower master forging dies of the underbracket KW7A on wooden blocks. A copy milling machine was used to copy the sculptured surface of upper and lower master forging die onto two blocks of high speed steel. These two blocks of high speed steel with sculptured surfaces are nothing but forging dies, which could be used for mass production of the part. The first part produced with the help of forging die is shown in Figure 5.8.

In conventional processes, if the part is small and complex, most of the time and skilled labor (cost) is required to write or generate an NC program. To generate an NC program from a CAD file requires a chaining process or defining basic and driving curve to specify tool diameter and cutting parameters for each and every surface. Moreover, the conventional technique (Method 1) in addition to the tedious NC program generation also demands the labor-intensive copy milling process.

After producing large number of parts, dies wear out and need re-machining. Conventionally, a computer numerical control (CNC) machine is used for removing a thin layer of approximately one tenth of an inch. Although the volume of material removed is much less, the machining time required to re-machine the die is quite high because the whole NC program has to be executed again. However, an EDM electrode would drastically reduce re-machining time because the EDM process, unlike the conventional CNC milling process, machines all the surfaces simultaneously and

requires minimal labor.

All this time and labor could be saved if a process were developed to produce a copper prototype of the part that could be used as an EDM electrode. Although this approach is also applicable to large parts, EDM is a slower process and might take more time than a conventional technique (Method 2). Still, unlike copy milling, it doesn't require human interaction.

Previous Research and Proposed Methods

Generating an NC program for a part by using its CAD file is very time consuming because one has to specify the tool and cutting parameters, as well as do chaining operation (specifying the surface and the tool direction) for each and every surface separately. This becomes a tedious process for a complex die with hundreds of different surfaces. However, by using rapid prototyping, one can easily generate negative or positive of the part. Jensen [1] has suggested various methods to use the positive to develop an electrode for the EDM. One suggestion was metal spraying the positive with copper but in that method, the wear of the electrode during EDM process is unacceptably high because of porosity of sprayed copper. Jensen [1] also suggested electro-plating the positive but that method has a long processing time and the difficulty of deposition in holes and sharp corners may make inside details become problematic. In addition more deposition of copper on the edges occurs due to high current density or briefly nonuniform deposition of copper. Holes with depth greater than half the width can not be reproduced by electro-plating which limits the complexity of the die that can be produced by the process.

A compressing powder technique was also suggested by Jensen [1]. In this pro-

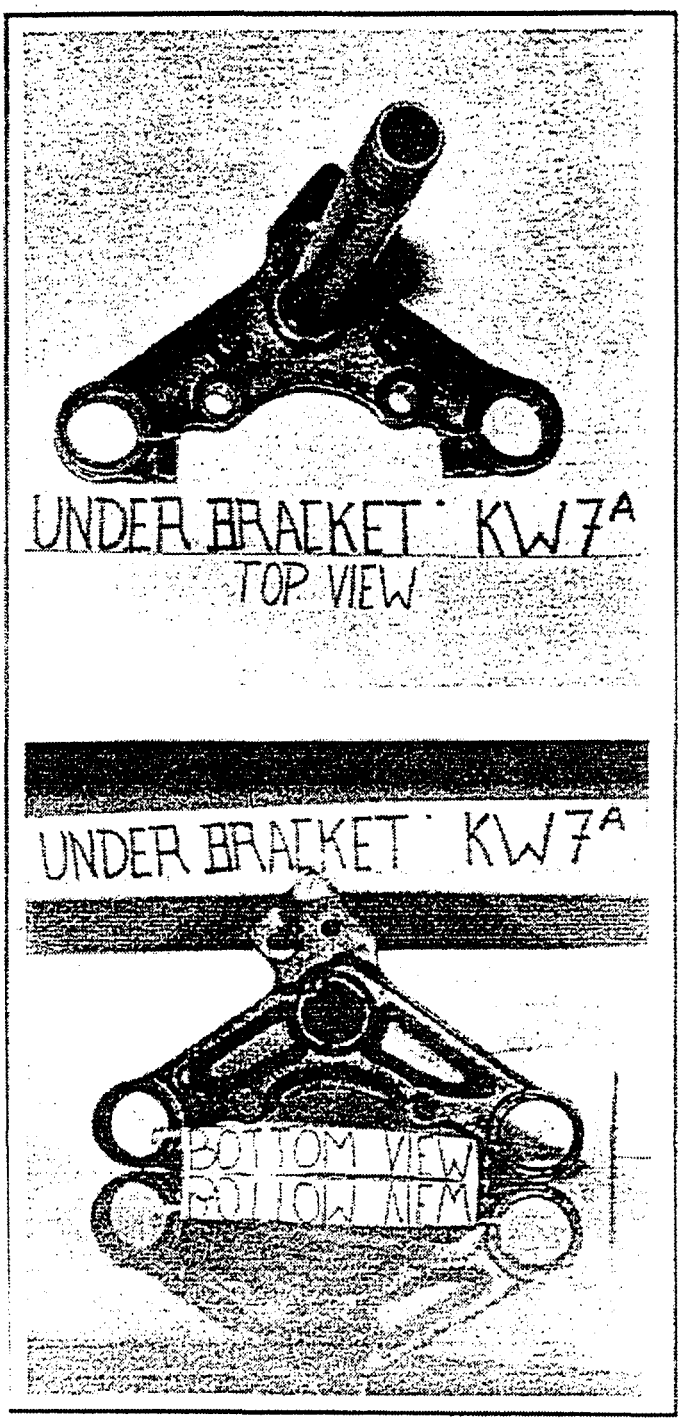

Figure 5.8: (Above) Top view of Underbracket produced with the help of forging die. (Below) Bottom view of the underbracket.

cess, a half filled cylinder of graphite powder is put in the negative and filled to the top with powder. A piston is used to compress the powder and the negative is exposed to hydrostatic pressure. The compressed block then requires twelve process steps and curing before it can be used as a graphite electrode making the process expensive. The processing time is about four days. Jensen [1] has reported that these methods are only suitable for die dimensions up to four inches. Furthermore, it has been reported that although electrodes can be made directly by adding copper or graphite powder to resin for rapid prototyping[1,2], the electrical conductivity of copper is lost so it is not practical to use it for EDM[1].

Three Better Processes

The authors propose three unique techniques: casting prototype, copy prototype, and EDM milling. The Casting prototype is a process very suitable for small complex parts, as well as large parts, if the objective is to minimize manual labor. The Casting prototype will be too time consuming for large parts because the material removal rate of EDM is much less than milling. The other two processes are suitable for large parts. The EDM milling process will produce a better surface finish than the copy prototype process because of the EDM process involved. In the EDM process, low current and high spark frequency will produce an excellent surface finish. However, the EDM milling process will take more time. Therefore the process should be chosen on the basis of surface finish requirement. All three processes avoid NC programming, and copper casting has an additional advantage of avoiding copy milling, which requires human interaction.

(a) Casting Prototype Method: Some negatives produced by rapid prototyping have low strength [2] and thus can not be used as a pattern to produce a sand mould without supports [3]. However, the strength of the negative can be increased by filling it with wax. A small amount of molten wax is poured into a negative, which is hydro-statically supported in cold water to allow faster heat dissipation and equal pressure distribution.

Once the layer solidifies, small amounts of molten wax should be added repetitively, providing sufficient time for each layer to solidify, until the negative is completely filled. This layering process is better than directly pouring in all the wax because it allows the solidified wax rather than the negative, to support the weight of the layers of molten material. This wax-filled negative with its higher strength acts as a pattern to make a sand mould.

A negative with sufficient strength can be directly used as a pattern. That helps produce a copper prototype by the conventional casting process. This copper prototype can be used as an electrode in EDM to produce the die. Indeed, one can produce many electrodes by the same negative. This is beneficial because a worn EDM electrode can be easily replaced. A schematic of the process is shown in Figure 5.9.

An experiment was performed to test the process. A copper casting of a simple donut shaped profile was made. This copper casting was then used as an EDM electrode to machine a die on a block of steel. The EDM machine used had a low current density because of which it took 2.5 hours to machine a half centimeter deep die. A photograph of the EDM electrode and the machined die can be seen in Figure 5.10.

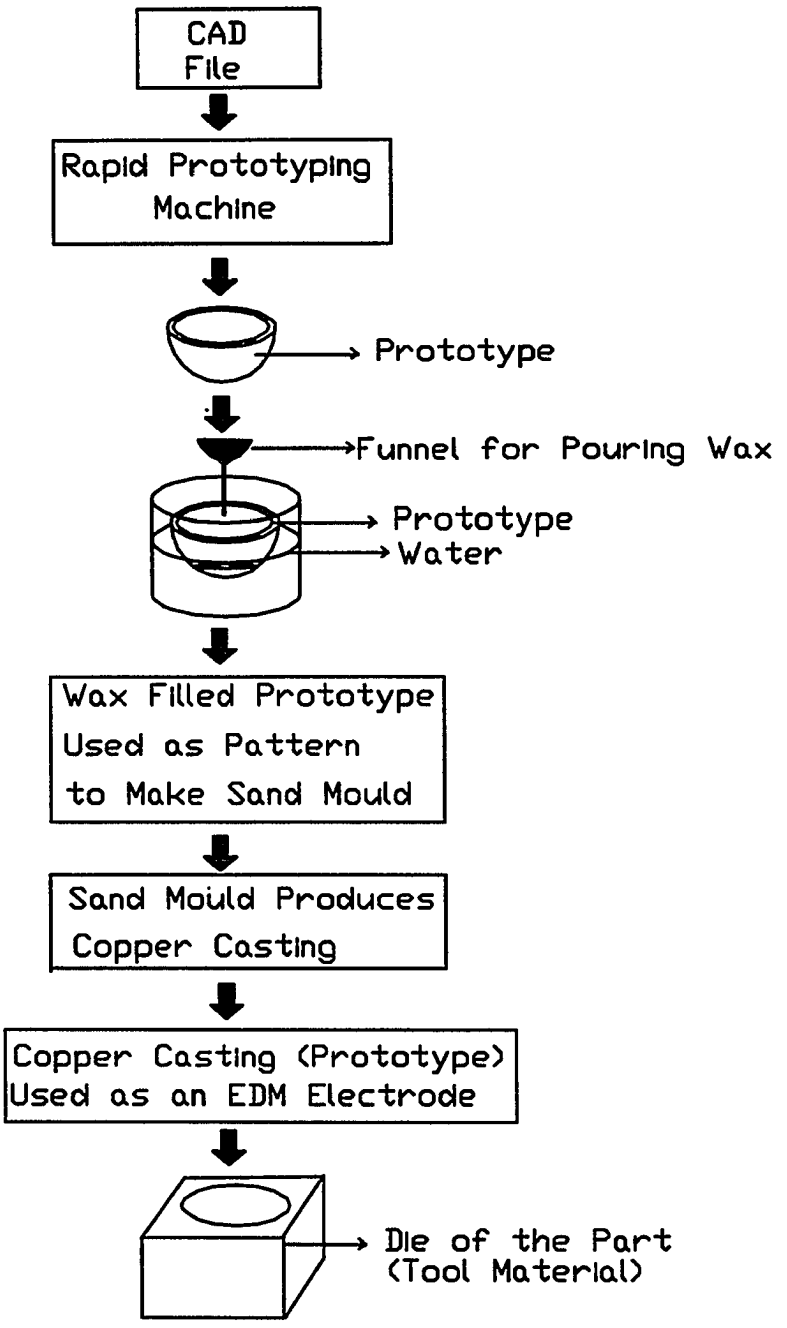

Figure 5.9: Casting Prototype Process

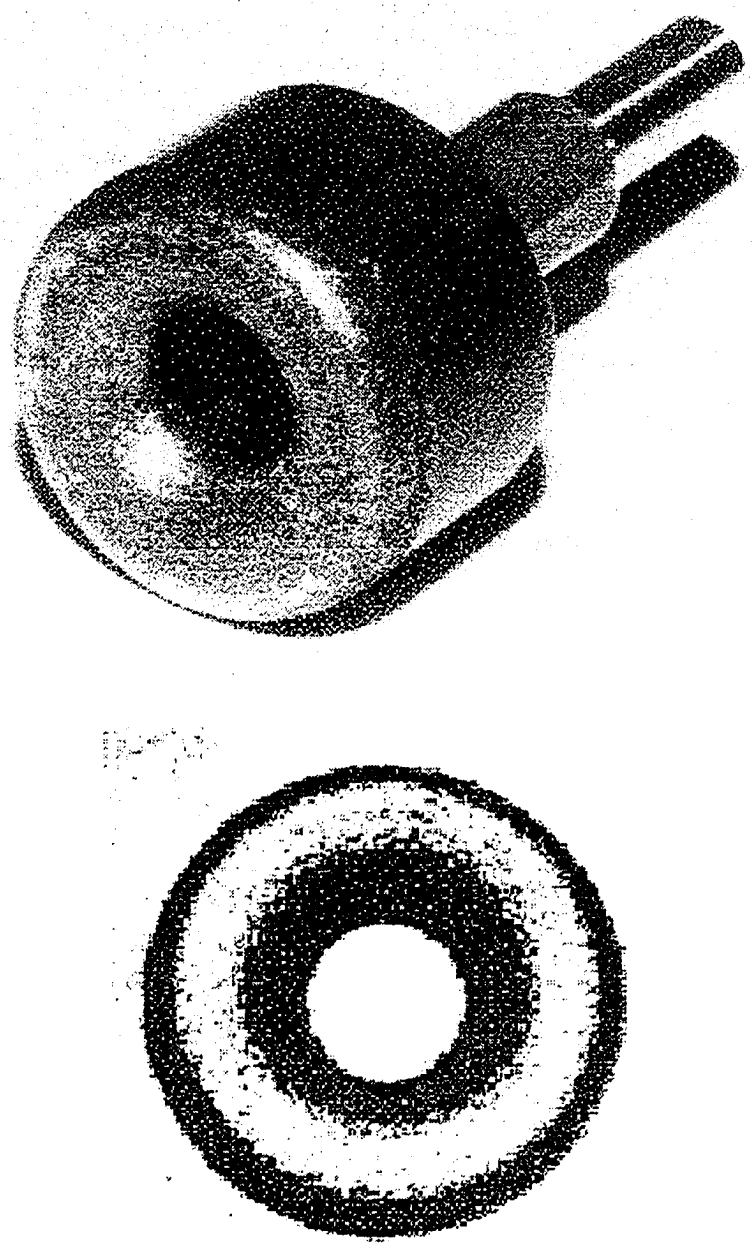

Figure 5.10: (Above) EDM electrode. (Below) machined die

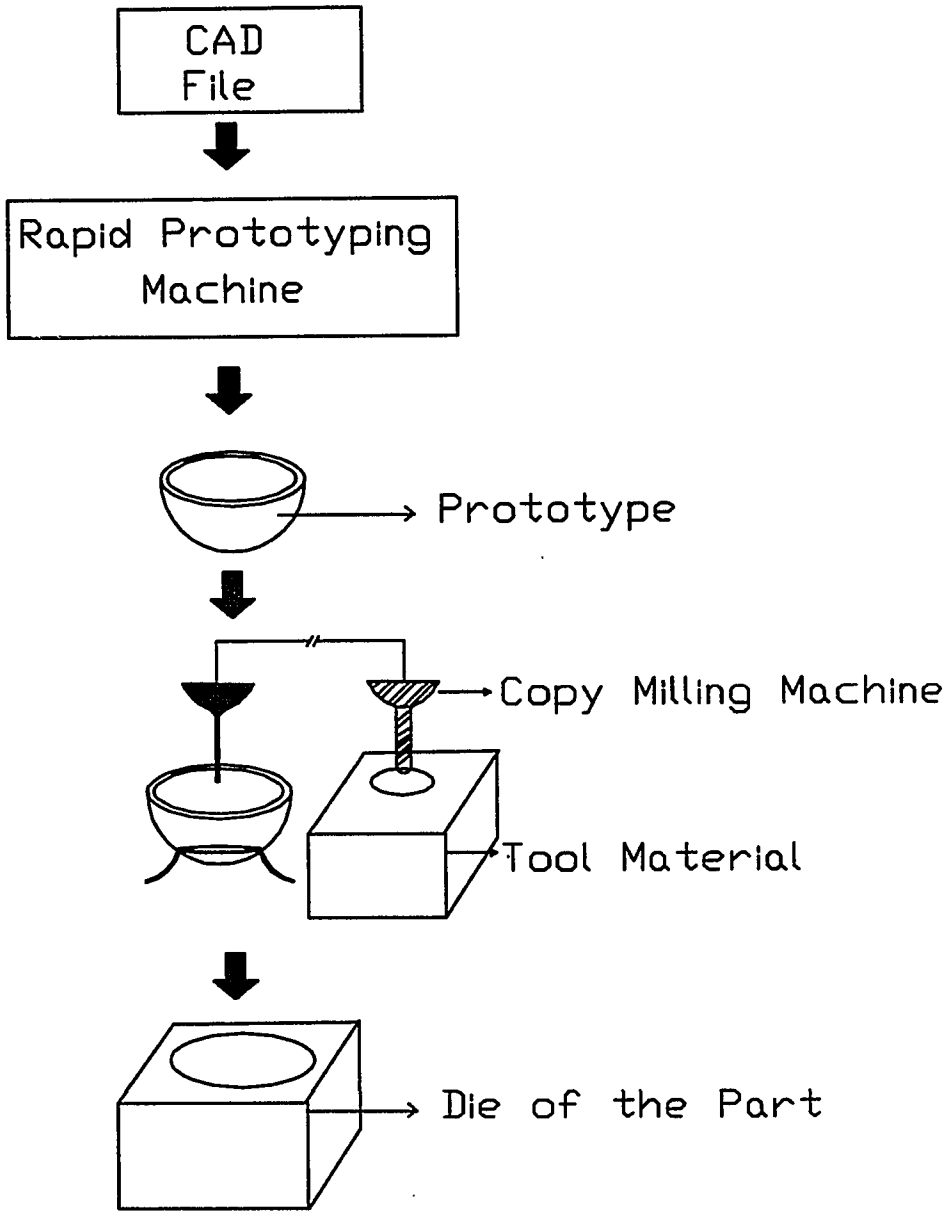

Figure 5.11: Copy Prototype Process

The EDM process is capable of producing a better surface finish than a conventional machining process, thus producing a better die surface. A die with a better surface finish will produce parts having better surface finish, with high aesthetic value and fewer micro-cracks. This process, unlike processes suggested by previous researchers, is expected to take a few hours instead of days and is quite economical.

(b) Copy Prototype Process: The CAD file is used by a rapid prototyping machine to produce a negative that can be copied onto the die material with a copy milling process. A schematic of the process is shown in Figure 5.11. The die will be produced in less time because no NC programming was involved and no NC data was generated. The method is fast because the milling process which has a high material removal rate. However, the method requires manual work because of the copy milling operation. This process would be more suitable for large and complex parts.

This process depends on accuracy of the milling procedure. To achieve the required accuracy and precision in a die, the workpiece must be rigidly fixed during copy milling.

The high clamping forces applied to achieve workpiece rigidity often lead to deformation of the workpiece, which is also caused by cutting and clamping forces during machining. Deformation of the workpiece due to cutting and clamping forces hinders the machinist's final goal, which is to machine the die within low dimensional and geometric tolerance bandwidth. A previously developed analytical model by Trappey, Gupta and Liu [4] can be used to determine optimal clamping forces to minimize the deformation in the workpiece and ensure no slippage as well as applicability of Coulomb's Law of Friction.

(c) Milling EDM Process: Most of the time required for copy milling is needed to remove the material close to the surfaces of the die. This is because low feed should be used near the surface to ensure less error due to tool deflection. Using the milling process to remove the bulk of the material and the EDM process for finishing work produces the die faster with better surface finish. This combination of processes can be achieved by making the tracer in the copy milling machine spherical. The sphere's radius would determine the thickness of material that has to be removed by the EDM.

The appropriate thickness for each surface may vary depending upon complexity of the surface. If the die surfaces are very complex, EDM might need to remove more material from surfaces. This can be achieved by coating the inside of a prototype with wax. The prototype can be copied onto the tool material by copy milling with high feed and depth of cut to generate a rough-machined die. This wax-coated prototype can be filled with wax to increase its strength so that it can act as a pattern in casting process. In the casting process, copper can make a positive prototype of the part to be used as an electrode in the EDM process to finish machine the rough-machined die.

Figure 5.12 shows a flow chart, indicating which process might be more suitable for a part, depending upon its size and number of surfaces. A small part with large number of surfaces can be made in several ways. The time required to write the NC program depends on the part. It is evident from Fig.11 that process #5 (the proposed Casting Prototype process) will outperform other processes in terms of total time, cost, surface finish and skilled labor.

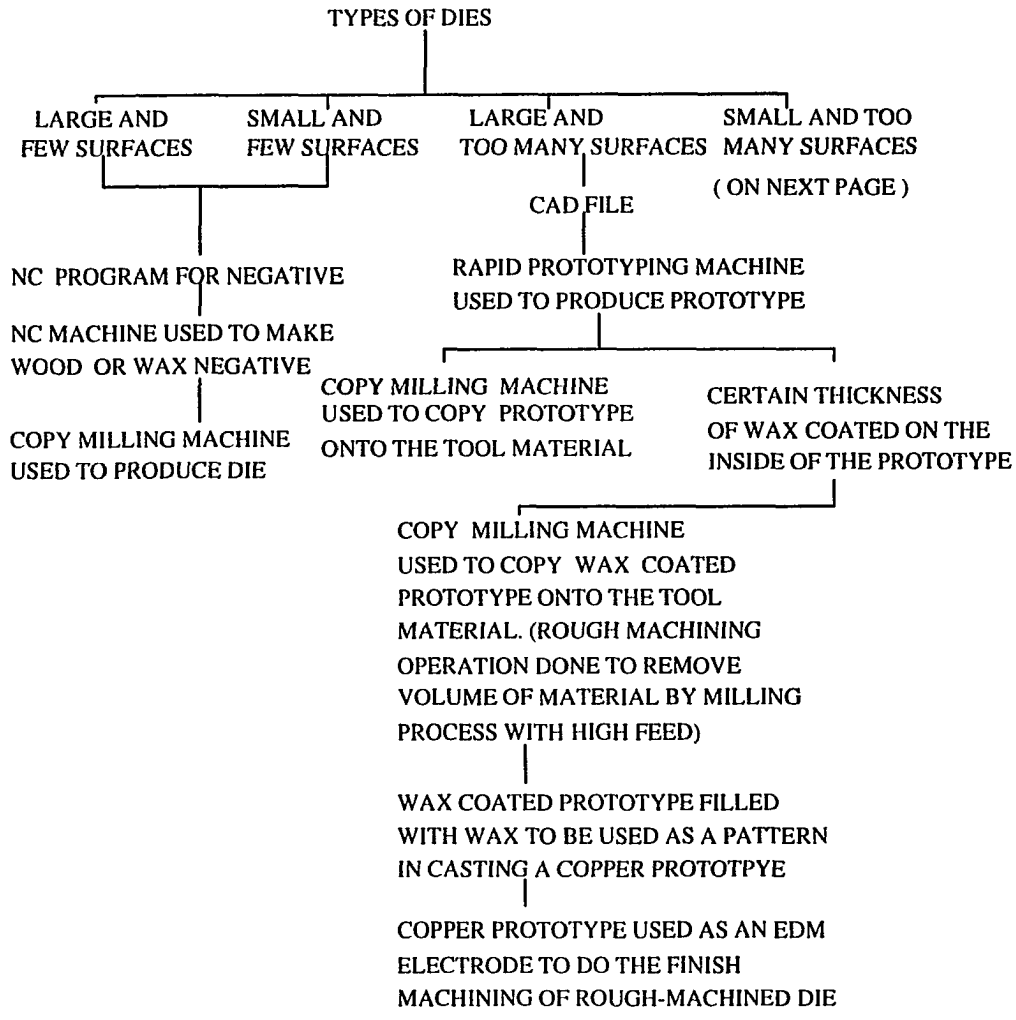

Figure 5.12: Flow Chart of Die Manufacturing Processes (continued on next page)

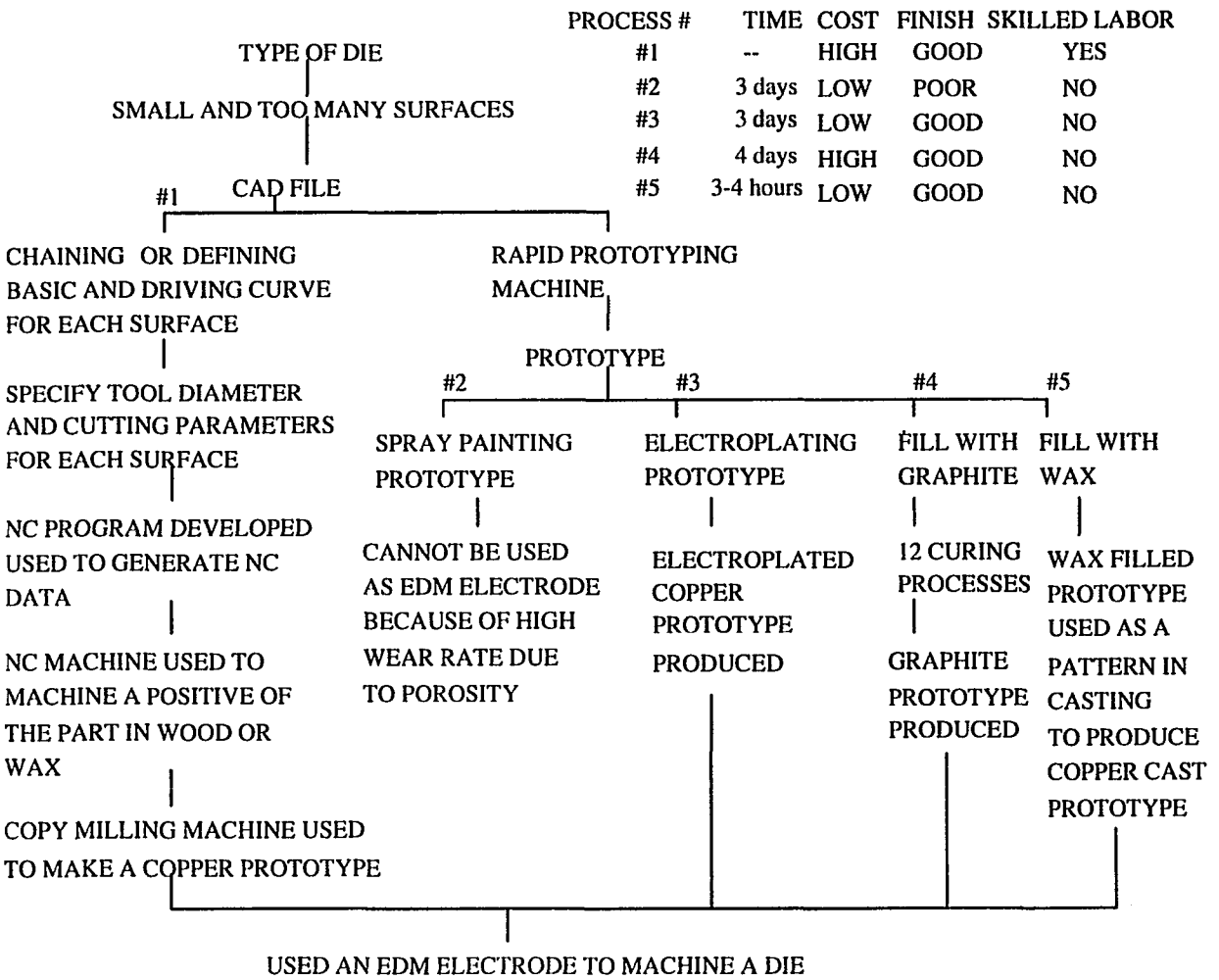

Figure 5.11: Figure 5.11 Continued

Conclusions

The example of making a master die by conventional methods in industry makes it evident that the process is time consuming, tedious and expensive. The casting technique would produce a surface finish similar to methods proposed earlier. The process is cheap, requiring hours rather than days to produce the electrode for EDM. The surface roughness of the prototype or EDM electrode made by casting might turn out to be poor, and this might affect the final die surface. To avoid this some finishing operation such as sand blasting can be used to improve the surface finish of the prototype or the EDM electrode.

The casting prototype process and EDM milling process have the additional advantage of using the copper prototype as an EDM electrode for re-machining a worn die.

References

1) Jensen, K.L., 1992, " Making Electrodes for EDM with Rapid Prototyping" pp. 295-301, Proceedings of the Third International Conference on Rapid Prototyping, June 7-10, 1992, Dayton, Ohio.

2) Barlow, J.W., 1992, "Metallic and Ceramic Structures from Selective Laser Sintering of Composite Powders", pp. 73-76, Proceedings of the Third International Conference on Rapid Prototyping, June 7-10, 1992, Dayton, Ohio.

3) Nakagawa,T., Inahura, M., Meng, Y., and Wei, J., 1992, "Applications of Laser Stereo-lithography to Casting and Computer Simulation" pp. 313-320, Proceedings of the Third International Conference on Rapid Prototyping, June 7-10,

1992, Dayton, Ohio.

4) Trappey, A. J. C. , Gupta Parag and Liu C.R. 1993 "Using Optimization Model to Control Workpiece Rigidity and Deformation in Workholding to Achieve Precision Machining" Published in "Operations Research in Production Planning and Control" A Springer Verlag publication edited by Fandel, Gulledge, and Jones. pp. 138-150.

Acknowledgments

The author would like to acknowledge the courtesy of Thai Engineering Products Co. Ltd., Bangkok, Thailand for providing the permission to publish work done in the tool and die section of the plant.

CHAPTER 6. DISCUSSION, RECOMMENDATIONS AND CONCLUSIONS

Discussion and Recommendations

In Chapter 2 concerning the analytical model the deflection of the tool was not considered. The tool deflection equation developed in chapter 4 can be incorporated in the non-linear analytical model developed in Chapter 2 to develop an analytical global tool-workpiece-fixture non-linear optimization model. This model can then provide the maximum global error. Obtaining the global error would require an optimization function that provides the total error due to tool deflection and workpiece deflection. The new optimization function would be a combination of the present optimization function and the tool deflection equation. However the exact relationship between tool deflection and workpiece deflection is not known that will provide the total error. This probably would require extensive experimentation to obtain a relationship.

Work performed in Chapters 3 and 4 is highly computationally intensive and required a large RAM. The initial idea was to model the workpiece, fixtures and the milling cutter together and use dynamic forces to visualize the maximum error in machining. However, the large RAM required for hyper-mesh generation in finite

element analysis left no choice but to divide the problem into two parts i.e (a) workpiece and fixture deflection along with friction and (b) cutter deflection. In future work with improvement in computational power and RAM availability, the problem could be solved as initially planned. This would provide insight into the relationship between tool deflection, workpiece deflection and maximum inaccuracy in the part machined. This would be a global finite element model.

A global finite element model would be too computationaly intensive as compared to the global analytical model whereas the global finite element model will be more accurate as compared to the analytical model. If a computer program is written which divides the workpiece into different sections, based on the fact that certain sections which are complex in geometry, will be solved by the global finite element model, the remaining simple sections would be solved by the analytical model. This would provide a reasonably accurate solution in a reasonable amount of computational time.

In future work, experiments can be performed on processes described in chapter 5. This would not only provide a better understanding of how to improve the process but may also provide marketing leads to develop a new process.

Conclusions

The goal of the thesis was to minimize the inaccuracy produced in parts due to end milling and develop new processes to reduce the cost and time taken to perform conventional CNC milling to produce dies for manufacturing parts. In Chapter 2 a non-linear analytical model was developed which can be used to determine optimal clamping forces for minimum workpiece deformation and it also ensures rigidity of

the workpiece and validity of Coulomb's law of friction. The model requires much less computational power. However, it is suitable for simple workpiece shapes only.

In Chapter 3 a finite element model as well as an algorithm was developed to determine the optimal clamping forces, and the deformation at any place on the workpiece or fixtures. It ensures the validity of Coulomb's law of friction under optimal clamping forces. It can be used for workpiece and fixturing elements having any possible complex shape. In this model flexible fixtures have been modeled for the first time and the method eliminates all the disadvantages which were encountered by previous models except that it requires a large amount of computational time. Approximately 2.5 hours were required for each load set on a DEC 5000 machine which implies that a total of 7.5 hours was required to solve the problem.

In Chapter 4 an equation was developed to determine the deflection of an end mill under a cutting force which was also verified by finite element analysis of an actual end mill. This equation should allow exact prediction of end-mill deflection with minimal computational time. The computed deflection under a given cutting force should help in choosing an appropriate end mill considering the accuracy desired and the nature of the job.

In Chapter 5 three new processes are proposed which can produce a die in less time and with lower cost as compared to conventional die manufacturing processes. These concepts should allow a new product to be brought to the market in a short time and at a lower cost. This research should help to produce accurate quality parts by using optimal clamping forces and appropriate end mills to machine parts or dies. The new processes developed will reduce the lead time and the cost required to bring a product to the market.